Diffusion Imaging with MR Tractography for Brain Tumor Surgery

Alberto Bizzi

Contents

A. Bizzi (✉)
Fondazione IRCCS Istituto Neurologico Carlo Besta,
Milan, Italy
e-mail: alberto.bizzi@istituto-besta.it

C. Stippich (ed.), *Clinical Functional MRI*, Medical Radiology Diagnostic Imaging,
https://doi.org/10.1007/978-3-030-83343-5_7

Abstract

In the last 20 years advances in Neurosurgery, Neuroradiology and Neuro-Oncology have dramatically changed management of brain tumors, especially of gliomas that are seated in eloquent areas and are carrying a higher risk for permanent postoperative neurological deficits.

This chapter aims to provide practical and clinically relevant information with a review of the current literature from glioma biology through MR diffusion basic principles, methodology and clinical application of MR tractography, so that the reader can get a throughout interdisciplinary impression of the state of the art.

In contrast to brain metastases and meningiomas, gliomas extensively infiltrate the extracellular space of the gray and white matter changing the anatomic and functional properties of the brain. MR diffusion imaging has great potentials to contribute to disclose the mechanisms of interaction between gliomas and the host tissue.

Diffusion tensor imaging (DTI) is the most established and validated clinical application of MR tractography and it is increasingly requested by neurosurgeons. More advanced diffusion MR acquisition schemes such as high-angular resolution diffusion imaging (HARDI) and more sophisticated tractography algorithms such as spherical deconvolution (SD) and Q-ball imaging (QBI) have been developed to overcome DTI limitations. The community is beginning to apply the advanced methods in presurgical mapping.

A detailed understanding of the relationship between eloquent white matter fascicles and infiltrating gliomas is mandatory to correctly planning a resection and interpret the functional neurophysiological responses recorded during intraoperative monitoring (IOM) with electromyography (EMG), motor evoked potential (MEP), and direct intraoperative electrical stimulation (IES). It should be emphasized that MR diffusion tractography provides anatomical, not functional information.

The neurosurgical community is increasingly recognizing the value of MR diffusion imaging with tractography in evaluating patients with gliomas. MR tractography is a great educational tool for neurosurgeons and neuroradiologists. Presurgical visualization of eloquent fascicles in the proximity of a mass has been associated with a higher probability of total resection in low and high grade gliomas. Postoperative MR tractography is increasingly used to correlate postoperative deficits with white matter anatomy, and guide rehabilitation strategies.

This chapter presents optimized clinical presurgical HARDI protocols and tractography methods for visualization of the major white matter tracts that are part of the motor, language and visuospatial attention systems. Practical examples of how to interpret MR tractography findings are given, illustrative cases with typical and atypical presurgical findings are presented. Complementary applications with functional MR imaging (fMRI) are highlighted. Finally, the clinical value and limitations of presurgical MR diffusion imaging are discussed.

Abbreviations

AC	Anterior commissure
ADC	Apparent diffusion coefficient
AF	Arcuate fasciculus
AG	Angular gyrus
ALA	5-Aminolevulinic acid
BA	Brodmann area
BOLD	Blood oxygenated level dependent
CC	Corpus callosum
CL	Linear anisotropy coefficient
CP	Planar anisotropy coefficient
CST	Corticospinal tract
DEC	Directionally encoded color
dlPFC	Dorsolateral prefrontal cortex
dODF	Diffusion orientation distribution function
DSI	Diffusion spectrum imaging
DTI	Diffusion tensor imaging
DWI	Diffusion weighted imaging
ECS	Extracellular space
EOR	Extent of resection
EPI	Echo planar imaging
FA	Fractional anisotropy
FAT	Frontal aslant tract
FEF	Frontal eye field
FLAIR	Fluid attenuated inversion recovery
fMRI	Functional magnetic resonance imaging
fODF	Fiber orientation diffusion function
FST	Frontal striatal tract
GBM	Glioblastoma multiforme
HARDI	High-angular resolution diffusion imaging
HGG	High grade glioma
IES	Intraoperative electrical stimulation
IFG	Inferior frontal gyrus
IFOF	Inferior frontal occipital fasciculus
ILF	Inferior longitudinal fasciculus
IOM	Intraoperative monitoring
IPL	Inferior parietal lobule
ITG	Inferior temporal gyrus
LGG	Low grade glioma
M1	Primary motor cortex
MD	Mean diffusivity
MEP	Notor evoked potential
MFG	Medial frontal gyrus
MLF	Medial longitudinal fasciculus
MRI	Magnetic resonance imaging
MTG	Medial temporal gyrus
ND	Neurite density
NODDI	Neurite orientation dispersion and density imaging
ODI	Orientation dispersion index
OR	Optic radiations
PMC	Premotor cortex
PMd	Premotor dorsal
PMv	Premotor ventral
PPC	Posterior parietal cortex
QBI	Q-ball imaging
ROI	Region of interest
S1	Primary somatosensory cortex
SC	Spherical anisotropy coefficient
SCF	Subcallosal fasciculus
SD	Spherical deconvolution
SFG	Superior frontal gyrus
SLF	Superior longitudinal fasciculus
SMA	Supplementary motor area
SMG	Supramarginal gyrus
SPL	Superior parietal lobule
STG	Superior temporal gyrus
T2WI	T2-weighted image
TPFIA	Temporo-parietal fiber intersection area
UF	Uncinate fasciculus
vlPFC	Ventrolateral prefrontal cortex
WHO	World Health Organization
WM	White matter

1 Introduction

In the last 25 years tremendous advancements in Neurosurgery, Neuroradiology and Neuro-Oncology have changed the management of brain tumors. Advancements in Neurosurgery include implementation of microscopic surgery, intraoperative monitoring (IOM) and imaging-guided methods in the operating theater (Keles and Berger 2004). Twenty-five years ago brain tumors infiltrating "eloquent areas" were considered "inoperable" by the majority of neurosurgeons. Implementation of modern surgical techniques

has widened the indications for brain tumor surgery to include lesions located in the proximity of the primary motor cortex and of the optic radiations, or infiltrating Broca and Wernicke areas of the language system. The aims of surgery in lower grade gliomas are maximal tumor resection according to "functional margins" and whenever possible to perform "supratotal resection" that extends beyond the areas with MR signal abnormalities. Achievement of these goals significantly increases overall survival by delaying malignant transformation of diffuse gliomas. The aim of surgery in glioblastoma multiforme (GBM) is to remove up to 95% of the enhancing and solid component of the tumor in order to delay recurrence of the tumor. In the last two decades refinement of intraoperative functional mapping methods has resulted in much more reliable identification of functional margins of the motor and language systems.

Advances in Neuroradiology, in particular in the field of functional MR imaging (fMRI) and MR diffusion tensor imaging (DTI) have changed the way surgeons evaluate patients before surgery. Advanced neuroimaging methods can now provide morphological and functional information about the alterations induced by the tumor on the hosting brain. This new information is quite important and relevant, especially when a diffuse infiltrating glioma is growing in an eloquent brain structure. It has been shown that presurgical mapping with fMRI and DTI may improve surgical targeting, guide surgical strategy and intraoperative assessments, reduce intraoperative time (Petrella et al. 2006). It is a fact that neurosurgeons are increasingly requesting fMRI and DTI as part of their routine presurgical evaluation. Functional maps are frequently used to discuss the aims of surgery with the patients and their family, before securing the consent to proceed.

Advances in Neuro-Oncology have been also quite impressive in the last decade. Substantial progresses have been made in the molecular classification of many brain tumors. Large-scale molecular profiling approaches have identified new mutations in gliomas which have allowed subclassification into distinct molecular subgroups with characteristic features of age, localization, and outcome (Sturm et al. 2012). Randomized clinical trials have demonstrated that molecular characterization allows identification of subgroups of gliomas that are associated with distinct prognosis and predicted treatment response (Stupp and Hegi 2013). The diagnostic importance of *isocitrate dehydrogenase* (IDH) mutational status in diffuse gliomas was first formally recognized within the updated fourth edition of the WHO Classification of Tumors of the Central nervous System in 2016 (Louis et al. 2016). The incorporation of IDH and other molecular biomarkers into an integrated diagnosis of gliomas provides a more reproducible and clinically meaningful classification of diffuse gliomas in adults (Brat et al. 2020; Eckel-Passow et al. 2015). Thus molecular analyses have become a must of the standard diagnostic workup in all patients with a brain tumor (Thomas et al. 2013). These advances in neuro-oncology emphasize the importance of tumor tissue sampling for molecular studies.

All together the above-mentioned advances have changed treatment strategies for this disease, especially so when the lesion is located in the proximity of eloquent structures. In the early nineties it was quite common to follow a "wait-and-see" strategy or performing a stereotactic needle biopsy, while today radical tumor exeresis has become the standard of care. These advances have paved the way to a *personalized treatment strategy* that is going to influence the outcome of brain tumors in the years to come (Weller et al. 2012).

2 Neuro-Oncology of Gliomas

2.1 Histology and Molecular Markers

Diffusely infiltrative gliomas are by far the most common type of primary brain neoplasms in adults and they are classified by genetics, tumor cell lineage and index of proliferative activity. The historical histopathological classification in

astrocytomas and oligodendrogliomas has become less important than the IDH-status. The IDH mutation is the earliest genomic event of tumorigenesis and it is almost always retained during tumor progression. In contrast to IDH-mutant gliomas, IDH-wildtype astrocytic tumors are distinct clinical and genetic entities with more aggressive clinical behavior and they have a poor prognosis (Louis et al. 2016; Brat et al. 2020). The age range of IDH-wildtype (sixth and seventh decades) is higher than that of IDH-mutant gliomas (third and fifth decades).

The term glioblastoma (GBM), corresponding to WHO grade 4, should be reserved for IDH-wildtype diffuse astrocytic gliomas that have genetic and histologic features predictive of a highly aggressive clinical behavior. Among brain neoplasms GBMs have the highest proliferative activity and they may grow very quickly; they usually become symptomatic within a few months. GBMs have a dismal prognosis with a median survival time of 14 months, despite radio and chemotherapy (Stupp et al. 2005).

On the contrary, IDH-mutant gliomas have genetic and histopathologic features predictive of a less aggressive clinical behavior with longer survival times (median 3–5 years) and they occur in younger adults. IDH-mutant gliomas are subdivided into two subgroups: the astrocytic phenotype with co-mutation in *TP53* and *ATRX*, and the oligodendrocytic phenotype with codeletion of 1p/19q chromosomes and *TERT* promoter mutation. These genetic abnormalities are mutually exclusive. *Diffuse astrocytomas* WHO-2 will ultimately progress to WHO-3 (*anaplastic astrocytomas*) and then to WHO-4. *IDH-mutant, codeleted* WHO-2 and WHO-3 *oligodendroglioma* respond well to chemotherapy and they are associated with a relatively longer survival time than IDH-mutant astrocytic tumors (Louis et al. 2007).

2.2 Pattern of Growth and Velocity of Expansion

One important property of gliomas is their skill to infiltrate extensively the extracellular space (ECS) in gray as well as in white matter (WM). Like "guerilla warriors" glioma cells abuse the host "supply" vessels rather than constructing their own for satisfying their oxygen and nutrients requirements (Claes et al. 2007). This property is found in IDH-mutant as well as in IDH-wildtype, implying that the invasive phenotype is acquired early in oncogenesis. Glioma cells have the capability to migrate and modulate the ECS. Glioma cells may follow different patterns of growth that depend on preexisting host tissue elements. This growth pattern has significant prognostic implications and it is a major factor in therapeutic failure. Different glioma subtypes may follow different patterns of infiltration that depend upon the "weapons and tools" used by the invading "guerilla cells" and by the interaction with the environmental factors of the host. Glioma cells of a particular subtype may be extremely successful to infiltrate along myelinated WM tracts (intrafascicular growth), whereas tumor cells of other subtypes may accumulate in the subpial, perivascular, or perineuronal space (Giese and Westphal 1996). Other subtypes preferentially infiltrate the gray matter's neuropil in specific anatomic regions such as the insular cortex or the supplementary motor area in the superior frontal gyrus (SFG) (Duffau and Capelle 2004). The most extreme example of diffuse infiltrative growth is represented by gliomas infiltrating multiple lobes, subcortical nuclei or other anatomic brain regions (Mawrin 2005).

Measuring the spontaneous velocity of diametric expansion is important to predict patient's overall survival. The velocity of diametric expansion is faster in GBMs than in LGG; the latter have a spontaneous velocity in the range of 2–8 mm/year with a mean of 5.8 mm/year (Pallud et al. 2013). While LGG may continue to grow and infiltrate brain tissue at a stable velocity, GBMs grow fast and usually dislocate or destroy adjacent WM fasciculi and gyri (Nimsky et al. 2005). We will see later how these differences in velocity of expansion may have important implications for the interpretation of functional and MR diffusion imaging data.

2.3 Aims of Brain Tumor Surgery

Is surgery still the best treatment option for patients with a new diagnosis of brain tumor, despite the high costs and the relative high morbidity risk? The role of surgery is crucial for determining the diagnosis controlling seizures and planning radio and chemotherapy. The infiltrative nature of diffuse gliomas and their frequent localization in so-called eloquent areas has historically limited the extent of resection (EOR) due to the high risk of causing permanent focal neurological deficits. The controversy about the value of surgery in patients with LGG and HGG has not yet been fully resolved. Stereotactic biopsy is associated with a substantial risk of inaccuracy and sampling error. Currently, indications for biopsy are very limited in gliomas. Furthermore, biopsy has no therapeutic impact. Despite the lack of phase III study, most recent data strongly argue in favor of achieving a maximal resection of the tumor. Accordingly, in the last two decades there has been a paradigm shift from a surgical approach that relied mainly on anatomical landmarks to one based on identification of eloquent brain structures. Observational and retrospective studies have provided indication that radical surgical resection may offer a survival advantage over stereotactic biopsy and subtotal resections. Different considerations apply to surgery in LGG and HGG.

In the past the "wait-and-see" approach in LGG was justified by the lack of prospective randomized controlled clinical trials providing Level I evidence that extensive surgical resection had an impact on the quality of life and overall patients' survival (Laws 2001; Laws et al. 2003). In the majority of clinical studies EOR was not objectively assessed on postoperative MRI scans. Only recently authors have begun to include systematic measurement of residual tumor measured on postoperative MRI scans. Clinical studies have demonstrated that EOR correlates with survival times. LGG patients with resection >90% will have significantly longer overall survival times (Smith et al. 2008). In addition, supratotal resection that extends beyond the areas of signal abnormalities will significantly increase time of progression-free survival (Yordanova et al. 2011).

Until a decade ago in patients with GBM it was an even more open question whether simple debulking was effective or whether the neurosurgeons should strive to achieve maximal cytoreduction. A randomized study demonstrated that elderly GBM patients treated with open craniotomy rather than stereotactic biopsy have longer overall survival times (171 vs. 85 days), but overall benefit of open surgery to patients seemed to be modest, since time of deterioration did not differ between the two treatment groups (Vuorinen et al. 2003). In the past more emphasis has been placed on the role of radio and chemotherapy than on surgery.

The issue of complete resection as a causal, not only prognostic factor for overall survival in patients with GBM has been readdressed in a randomized phase III 5-aminolevulinic acid (ALA) study. This study investigated 5-ALA-induced fluorescence as a tool for improving EOR and provided a very high fraction of patients with postoperative MR imaging data acquired within 72 h. Residual tumor measured in the postoperative MRI scan was defined as tissue with a volume of contrast enhancement greater than 0.175 cm^3. Of the 243 GBM patients included in the ALA study 121 (49%) had incomplete resection and 122 (50.2%) had complete resection: the median overall survival was 11.8 months in the former and 16.9 months in the latter group (Stummer et al. 2008). Long-term survivors (>24 months) were almost exclusively among patients of the complete resection group. It is known that neurosurgeons may be less aggressive during resections in the elderly and when the tumor is near critical areas. It was shown that the difference in survival remained stable and significant when patients were restratified according to age (>60 years) in two groups, corroborating a causal effect of EOR on survival independent of age. The difference in survival among the two groups remained stable also when patients were restratified in two groups of patients with or without tumors in eloquent locations. The EOR not only influences survival, but also the efficacy of adjuvant therapies. The ALA cohort study pro-

vided for the first time Level 2b evidence that in GBM as a single factor survival depends on complete resection of the enhancing tumor. This level of evidence is inferior to randomized studies (Level 1) yet superior to case-control studies (Level 3), case series (Level 4), or expert opinions (Level 5).

The same authors (Stummer et al. 2011) reported that extended resections performed using 5-ALA carry a greater risk of temporary impairment of neurological function; patients with a greater risk of developing permanent postoperative deficits were those with preoperative symptoms such as aphasia unresponsive to steroids. Infiltration and destruction of eloquent brain, rather than vasogenic edema, are likely responsible for these preoperative focal neurological deficits. This data emphasizes again the importance of identifying the anatomic boundaries of the lesion with presurgical MR tractography and ultimately the functional limits with subcortical intraoperative electrical stimulation (IES). The importance of EOR as a predictor of overall survival has been shown also in a series of 107 patients with recurrent GBM when gross total (>95% by volume) resection is achieved at recurrence, overall survival is maximized regardless of initial EOR, suggesting that patients with initial subtotal resection may benefit from additional surgery (Bloch et al. 2012).

Detection of functional boundaries during surgery should be achieved with the aid of intraoperative neurophysiology and supported by presurgical fMRI and MR diffusion tractography (Bello et al. 2010). When a temporary deficit is repeatedly elicited with direct subcortical IES in the proximity of the wall of the surgical cavity, the functional limits of the resection are reached and the resection in that part of the tumor should be stopped. Identification of the functional limits is critical especially in gliomas infiltrating the motor system, in particular when the tumor involves the corticospinal tract (CST) (Bello et al. 2014). There is very low possibility of function compensation in the CST network when fast (20 μm thick) fibers are damaged because the function cannot be transferred to a nearby or distant network (Robles et al. 2008). Other critical networks that if damaged are likely to produce permanent deficits are the inferior frontal-occipital fasciculus (IFOF), the arcuate fasciculus (AF) and the subcallosal fasciculus (SCF) for the language system and the optic radiations (OR) for the visuospatial system. Damage or resection of several other long-range fascicles is likely to induce severe transitory neurological deficits followed by near to complete recovery in the matter of few weeks or months.

Another important parameter to determine is preoperative estimation of the residual tumor volume. Mandonnet et al. computed a probabilistic atlas of glioma residues with preoperative MR imaging data that allowed a preoperative estimation of the expected EOR. The atlas enhances the anatomic regions where tumor cannot be resected. In their series of 65 patients with LGG the success rate of the presurgical classification for partial vs. subtotal resection was 82% (Mandonnet et al. 2007a). The residual volume was underestimated in 9 patients with partial resection, overestimated in 3 patients with subtotal resection. It is remarkable that the regions with the highest probability of residual tumors are essentially located in the WM. Regions with a probability of residual tumor greater than 70% include the CST, the IFOF and the AF. Other regions with high percentage of residual tumor were found in the posterior aspect of the corpus callosum and the anterior perforated substance. The last two anatomic structures are not considered functionally essential, however they are either difficult to access or contain lenticulostriate vessels. This study once again outlines the importance of identifying and safeguarding vital vascular and functional structures during tumor resection.

3 Magnetic Resonance Diffusion Imaging Methods

3.1 Conventional MR Imaging

Magnetic resonance imaging (MRI) is currently the method of choice for detecting brain tumors. MRI is very sensitive to detect alterations in

water content that are so common in brain tumors. Water accumulation alters the MR signal on T2- and T1-weighted MR images and it is one of the first macroscopic changes occurring very early in the natural history of the neoplasm. Water accumulation precedes other metabolic and physiologic changes such as elevation of choline, cerebral blood volume (CBV), glucose uptake and protein synthesis that are detected, respectively, by proton MR spectroscopy (H-MRS), perfusion MR imaging and positron emission tomography (PET). MRI accurately defines the size of the mass and its relationship with relevant anatomic landmarks. MRI identifies presence of blood products and/or abnormal vessels within the mass that are important for assessing tumor grade. MRI after intravenous contrast agent injection detects breakdown of the blood–brain barrier, a consistent sign of more aggressive behavior related to the presence of angiogenesis and immature vessels.

However, MRI has several limitations. Like in a guerilla war, visualization of the elusive invasive front may be problematic. MR imaging may significantly underestimate the extent of diffuse infiltrative glioma growth. Infiltrating glioma cells can be found at biopsy beyond the hyperintense area on T2/FLAIR images (Ganslandt et al. 2005). Discrimination of infiltrating tumor from vasogenic edema is often difficult. Radio and chemotherapy-induced changes may mimic tumor progression (pseudoprogression). Thus, evaluation of response to therapy may be problematic due to ambiguous and overlapping MR signal changes in pseudoprogression and recurrent tumor, pseudoresponse and true response.

Finally, one important limitation of conventional MRI at magnetic field strength of 1.5 and 3.0 T is that it is blind to orientation of WM pathways. At ultrahigh field strength (7.0 T and above) only the major WM tracts can be recognized on T2-weighted MR images; in addition susceptibility imaging is a very sensitive method able to detect the orientation of myelinated WM bundles (Duyn 2013; Sati et al. 2013).

3.2 Diffusion Tensor Imaging

MRI with diffusion-weighted sequences measures the effects of tissue microstructure on the random walks of water molecules (Brownian motion) in the brain. When molecules can diffuse equally in all directions diffusion is called *isotropic*, when molecules can diffuse only along a specific direction it is called *anisotropic*. Isotropic diffusion occurs if there are no barriers like in the cerebrospinal fluid or when the barriers are randomly oriented like in the gray matter. Anisotropic diffusion occurs when there are oriented barriers that favor movement of water along rather than across them. In tissues with an orderly oriented microstructure, such as the WM, diffusivity of water varies with orientation since water molecules are likely to encounter different obstacles and barriers according to the direction in which they move (Chenevert et al. 1990; Doran et al. 1990). In WM water diffuses fastest along the principal orientation of the bundles (parallel diffusivity), and slowest along the cross-sectional plane (radial diffusivity). In the WM the degree of anisotropy depends primarily on membrane density, mainly in the form of intact axonal membranes.

In 1994 Basser et al. showed that the classic ellipsoid tensor formalism could be deployed to measure anisotropy in the human body (Basser et al. 1994). The tensor not only describes the magnitude of the water diffusion, but also the degree and the principal directions of anisotropic diffusion. Mathematically the tensor describes the shape of the ellipsoid with three eigenvalues that represent the diffusivities along the three orthogonal axes and three eigenvectors that provide orientation. The three eigenvalues are numbered in decreasing order by magnitude ($\lambda 1 > \lambda 2 > \lambda 3$). DTI is currently the most robust and efficient method to analyze diffusion MR data. DTI has become so popular because it provides several unique insights into tissue microstructure. It quantifies mean diffusivity (MD) and diffusion anisotropy, which are useful indices of WM integrity; with the eigenvector ($\varepsilon 1$)

providing the orientation information that enables for tractography.

Multiple imaging parameters informative about tissue microstructure can be calculated from a single DTI acquisition. Fractional anisotropy (FA) measures the eccentricity of water molecules displacement. Anisotropy is found in other body tissues such as peripheral nerves, kidneys, skeletal and cardiac muscles; however neural bundles show the greatest degree of anisotropy, with parallel diffusion on the order of 2–10 times larger than perpendicular diffusion. In the healthy human brain the intravoxel orientation coherence of WM bundles is probably the most relevant factor affecting FA (Pierpaoli et al. 1996). FA is a scalar value that describes the degree of anisotropy of a diffusion process. FA ranges between zero and one and its values are displayed in gray scale maps. A value of zero means that diffusion is free or equally hindered in all directions ($\lambda 1 = \lambda 2 = \lambda 3$), the ellipsoid reduces to a sphere. A value of one means that diffusion occurs only along one direction and it is hindered or restricted along other directions ($\lambda 1 > 0$; $\lambda 2 = \lambda 3 = 0$); the ellipsoid reduces to a line. This means that the diffusion is confined to that direction alone.

FA is a scalar metric that measures the degree of anisotropy, but does not indicate the shape of the diffusion ellipsoid. Voxels with similar FA value may have different shapes (Alexander et al. 2000). When linear diffusivity prevails ($\lambda 1 \gg \lambda 2 = \lambda 3$) anisotropy has the shape of a cigar, when planar diffusivity prevails ($\lambda 1 = \lambda 2 \gg \lambda 3$) it has the shape of a Frisbee. While both linear and planar anisotropy coefficients (CL and CP) are responsible for increased FA, their relative values indicate the shape of the ellipsoid. CL specifically highlights the region of tubular tensors, whereas CP indicates regions of planar tensors. We will see later how anisotropy shape coefficients at the periphery of a mass may provide relevant information about the modality of growth of the lesion and how they may affect DTI tractography.

MD, parallel ($\lambda 1$), and radial diffusivity ($(\lambda 2 + \lambda 3)/2$) provide information about the integrity of WM bundles. These indices have become quite popular and they have been particularly used in the evaluation of neurological diseases such as multiple sclerosis, Alzheimer disease, other dementias, and psychiatric disorders.

The orientation of the largest eigenvalue can be color coded to provide directionally encoded color (DEC) maps. By convention, bundles oriented along the z axis (cranio-caudal) of the MR scanner are displayed in blue, those coursing in the x direction (right to left) in red and those coursing in the y direction (anterior to posterior) in green. DEC maps provide a simple and effective way to visualize orientation information contained in DTI and they clearly show the main projection (blue), commissural (red) and association (green) WM pathways (Pajevic and Pierpaoli 1999). On DEC maps it was possible to identify unambiguously the major projection, commissural and association pathways in the brain of 123 mammalian species (Assaf et al. 2020).

3.3 DTI Metrics and Brain Tumor Microstructure

How do the above parameters relate to changes in tissue microstructure? In imaging protocols for clinical research the spatial resolution of DTI is usually in the range of 2.0 × 2.0 × 2.0 mm. Despite the apparent low spatial resolution, DTI is used as a probe to investigate tissue microstructure and it is sensitive to molecular water displacements on the order of 5–10 μm. There are three main longitudinally oriented structures that could hinder water diffusion perpendicular to neural bundles: (1) microtubules and neurofilaments of the axonal cytoskeleton, (2) the axonal membrane (axolemma), and (3) the myelin sheath surrounding the axons. Additional confounders are fast axonal transport and streaming, and B_0 susceptibility. Multiple studies have shown that there are no major differences in diffusion measurements between myelinated and unmyelinated bundles, thus the axolemma is the primary determinant of anisotropic diffusion of

water. Therefore anisotropy should not be considered myelin specific. Notwithstanding, myelin can modulate the degree of anisotropy.

It is more intuitive to correlate changes in parallel and perpendicular diffusivities rather than changes in FA to WM pathological lesions. Injuries with collapse of the axolemma are likely to determine a decrease in parallel diffusivity. Myelin loss and axonal increased permeability to water will likely determine an increase in radial diffusivity, despite integrity of axonal membranes (Beaulieu et al. 1996).

Glioma cells migration and growth cause more complex microstructural changes in the brain tissue. Glioma cells remodel the extracellular matrix by destroying the surrounding tissue through secretion of matrix-degrading enzymes, such as the plasminogen activator and the family of matrix metalloproteinases. In the majority of tumor types widening of the ECS, changes in cellular size, destruction of axonal membranes, and a general disruption of the normal brain architecture are associated with accumulation of water in large amounts. Studies have shown a dramatic increase in the ECS volume of gliomas even during the early infiltration stage (Zamecnik 2005). These microstructural changes lead to higher water diffusivity (i.e., increased MD) and reduction in diffusion anisotropy (i.e., decreased FA), especially in the early avascular stage of growth that is typical of LGG. The above histopathological changes will likely be associated with minimal decrease in axial diffusivity and variable increase in radial diffusivity due to enlargement of the ECS and glioma cell infiltration. Overall the increased amount of water in the ECS appears to be the dominant factor leading to increased MD and decreased FA. However, the enlarged ECS is not filled with water alone. In LGG a dense network of glioma cell processes may hinder diffusion even of small molecules. In GBM the expansion of ECS is associated with the overproduction of aberrant glycoproteins (i.e., tenascin) in the extracellular matrix that not only stabilize the ECS volume, but also serve as a substrate for adhesion and subsequent migration of the tumor cells through the enlarged ECS. Tumor invasion in WM will likely interrupt thousands of axons thus decreasing tissue anisotropy.

Gliomas have a propensity for microscopic infiltration of WM bundles well beyond their macroscopic borders. Microscopic glioma cells infiltration extends outside of the area of T2-signal hyperintensity and it is typically undetectable by conventional MR imaging. In areas with T2-signal hyperintensity tumor infiltration may be indistinguishable from peritumoral vasogenic edema that has a similar propensity to diffuse along WM bundles. DTI has been the focus of extensive studies that have attempted to answer this relevant clinical question that has important therapy implications. Unfortunately, so far DTI results have been remarkably inconsistent on this topic. The degree of peritumoral edema may be highly variable among tumor types; the degree of glioma cell infiltration along WM bundles also may vary considerably, potentially influenced by multiple factors that are playing a key role in extracellular matrix alteration and in ECS volume expansion such as tumor location, biology and genetics. Early reports suggested that the infiltrating component might be discriminated from tumor-free perilesional vasogenic edema on DEC maps (Field et al. 2004), however this method was not considered reliable. Price et al. advocate using the isotropic (p) and anisotropic (q) components of the diffusion tensor instead of FA to characterize glioma microstructure. The authors demonstrated that it was possible to differentiate areas of solid, high cellular tumor from areas of tumor infiltration on the basis of the anisotropic component q, but not necessarily the latter from areas of perilesional vasogenic edema (Price et al. 2006).

Perhaps the partial failure of the classic DTI parameters (i.e., MD, FA, parallel and radial diffusivities) to reliably characterize the many types of microstructural changes occurring in gliomas should come as no surprise and raise a specificity issue. FA and the other diffusion imaging parameters are sensitive but not enough specific to

detect complex microstructural changes. Future research should focus into more advanced multi-compartmental models taking into accounts the many factors involved (Zhang et al. 2012; Papadogiorgaki et al. 2013).

3.4 MR Tractography

DTI fiber tracking or tractography is a natural extension of diffusion ellipsoid imaging (Conturo et al. 1999; Mori et al. 1999; Basser et al. 2000). It is the process of integrating voxel-wise tract orientations into a trajectory that connects remote brain regions. In WM regions (i.e., corpus callosum, CST, and OR) where the fascicles are compact and parallel the diffusion ellipsoid is prolate. The orientation of the principal eigenvector does not change much from one voxel to the next. We can use a mathematical procedure (algorithm) to generate a trajectory connecting consecutive coherently ordered ellipsoids within the brain, a muscle or another fibrous tissue. Starting from a "seed point" voxel trajectories are generated in all directions until "termination" criteria are satisfied. We can choose one seed point and form a tractogram with all streamlines going through that seed point, or delineate two ROIs and generate a tractogram with all streamlines connecting those two brain regions. The algorithm requires two important assumptions that are known as the FA and the angle thresholds. Trajectories cannot extend to voxels with FA values that are close to background noise, because the degree of uncertainty of the ellipsoid orientation would be too high, thus we use a FA threshold >0.15–0.20. Trajectories are interrupted when in consecutive voxels the angle formed by the intersection of their respective principal eigenvectors is smaller than a set angle (i.e., angle threshold <35°–45°), because it is assumed that the majority of WM fascicles do not U-turn. The algorithm aims to generate trajectories through the data field along which diffusion is least hindered. The trajectory or streamline is the basic stone of deterministic tractography and it cannot be divided into smaller units. It has no direct relationship with any biological structure (axon, bundle, or fascicle) even though it reproduces its macroscopic trajectory in 3D space.

Strategies for generating diffusion tractograms vary greatly among algorithms and they can be broadly classified into local or global, model based or model free, deterministic or probabilistic. Deterministic tractography methods are the most intuitive and they are based upon streamline algorithms where the local tract direction is defined by the major eigenvector of the diffusion tensor as described above (Conturo et al. 1999; Mori et al. 1999). Mathematically a streamline can be represented as a 3D-space curve, as described by Basser et al. (2000). One limitation of the deterministic method is that any errors in calculations of the streamlines will be compounded as the streamline progresses from the seed to the termination point. The accuracy and variance of the tract reconstruction are a function of the algorithm, the signal-to-noise ratio, the diffusion tensor eigenvalues, and the tract length.

Limitations of fiber tracking performed with the streamline approach motivated the development of probabilistic tracking algorithms (Jones 2008). The aim of probabilistic tractography is to develop a full representation of the uncertainty associated with any assumption that might be made. Given a model and the data, probabilistic tractography provides a voxel-based map of high and low confidence (values given in percentage) that the trajectory of least hindrance to diffusion will connect the seed with the target point. From a mathematical point of view, the assumptions and the comparisons that can be made in studies across individual subjects and groups are more complete and flexible with probabilistic than with streamline tractography. Notwithstanding, streamline tractography is easier to implement in clinical practice and its more intuitive approach has contributed to its popularity among neuroanatomists and neuroradiologists.

A DTI tractography atlas for virtual in vivo dissection of the principal human WM tracts using a deterministic approach is very useful and practical for beginners (Catani and Thiebaut de Schotten 2008). The greatest success of fiber tracking is its use for in vivo dissection of major WM fascicles in individual healthy and pathological human brains. Tractography is also of value for segmenting WM pathways and providing quantitative measurements for comparison across subjects or groups.

3.5 Limitations of DTI and MR Tractography

The tensor is the most robust diffusion model, however it has several limitations when it is applied to brain WM. DTI provides two types of new contrasts: diffusion anisotropy and fiber orientation, which carry rich anatomical information about WM complexity. However, when interpreting MR diffusion data it is very important to understand well the inherent limitations of each method: (1) MR diffusion measurements are very sensitive to noise, motion and brain pulsatility, therefore to scanning time; (2) diffusion anisotropy carries information at the microscopic cellular (protein filaments and microtubules, cell membranes, and myelin) and macroscopic (vessels, glial cell networks, and population of bundles with different orientation) level that is averaged over a relative large voxel volume. Partial volume effects may become a problem in WM regions with more than one bundle such as the paraventricular zones, where FA is low and the degree of uncertainty in the estimation of bundle orientation increases. (3) DTI does not measure any specific parameter for the intraaxonal restricted water pool. (4) The calculation of the tensor assumes that fiber structures are homogeneous within a voxel but this assumption is not true when there are two or more fiber populations: one orientation cannot represent accurately the orientations of two fiber populations! Two strategies have been proposed to reduce this problem: increase spatial image resolution by reducing the voxel size or extract information with higher angular resolution from each voxel and abandon the simple tensor model. (5) DTI-based tractography algorithms cannot determine if bundles are crossing or kissing. (6) Diffusion MR cannot differentiate the directionality of axons within bundles. (7) At the spatial resolution currently used in clinical MRI, diffusion cannot track streamlines thru the gray matter, thus it cannot track the trajectories of WM bundles to their cortical terminations.

One of the major limitations of the classic tensor model is that for each voxel it provides only a single fiber orientation: this is a major obstacle for tractography and connectivity studies. Using spherical deconvolution methods with a spatial resolution of $2 \times 2 \times 2$ mm^3 it has been estimated that the proportion of WM voxels containing more than one bundle (crossing fibers) is about 90% (Jeurissen et al. 2013). These findings suggest that the DTI model may be inadequate to measure the complexity of fiber trajectories in the WM.

In voxels with more than one fiber population the orientation measured with classic DTI is the average of the orientations of all bundles present in that voxel. As a result, the shape of the diffusion ellipsoid in voxels with crossing fibers may appear either prolate or oblate. A prolate (stretch out, linear) object has the shape of a spheroid generated by an ellipse rotating about its longer axis with the polar radius much greater than the equatorial radius ($\lambda 1 \gg \lambda 2 = \lambda 3$), while an oblate (flatten, planar) object has the shape of a spheroid generated by rotating an ellipse about its shorter axis with the equatorial radius much greater than the distance between the poles ($\lambda 1 = \lambda 2 \gg \lambda 3$). A geometric analysis of DTI measurements in the human brain using a three-phase tensor shape diagram demonstrated that there is a tensor shape hierarchy between different WM tracts in the order of commissural, deep projection and association WM tracts (Alexander et al. 2000). The CC and the CST show the greatest linear shape, while the AF and the subcortical WM tracts show

a significant planar component of their tensor measurements. The causes of planar diffusion in the brain are not perfectly understood. Bundles arranged in sheets could explain planar diffusion (Wedeen et al. 2012); however, a more likely origin is presence of crossing WM tracts within the large voxels typical of the DTI experiment. The linear shape of CC and CST may outline the compacted nature of the bundles in the central segment of those tracts, whereas the planar shape of the AF at the level of the centrum semiovale may reflect that most voxels contain AF and CC crossing fibers.

The shape of the diffusion ellipsoid of the voxels in the proximity of a focal lesion can be affected by mass effect. Especially in voxels near the borders of fast growing gliomas the ellipsoid can become oblate with undefined principal orientation. It is important to evaluate the shape of the ellipsoid when interpreting tractography results in the proximity of a mass, because it might provide a warning sign about false positive results. Oblate voxels are confusing for tractography because the difference between $\lambda 1$ and $\lambda 2$ is minimal and noise will cause the principal eigenvector to have random orientation in the plane: tracking might go either way in oblate voxels.

Detection of WM bundles within a tumor and surrounding areas of vasogenic edema may be also problematic. Intraoperative direct electrical stimulation has detected presence of functioning WM tracts within areas of T2-signal hyperintensity especially so in LGG. It is assumed that a significant number of electrically competent and signal conducting axons are preserved despite infiltration by glioma cells. Tumor infiltration alters MR diffusivity along WM bundles and it may distort their geometry. The increased free water content may artificially decrease FA, thus leading to false negative results if FA decreases below the FA threshold that is commonly used for tractography. It may be responsible for false positive results due to increasing degree of uncertainty in estimating the orientation of the principal eigenvector. DTI studies have shown interruption of streamlines inside the tumor or areas of vasogenic edema, especially when FA threshold was set at >0.15 (Bastin et al. 2002; Bizzi et al. 2012). This issue raises a sensitivity issue for MR tractography with a relative high rate of false negative results in areas of decreased FA, high diffusivity and T2-hyperintensity that are especially common in LGG. Other authors have validated with IES the tractography findings obtained with FA threshold (>0.10) through regions of tumor infiltration (Bello et al. 2008). An alternative approach is to use advanced diffusion multicompartmental models such as Neurite Orientation Dispersion and Density Imaging (NODDI) method (Zhang et al. 2012) that will be discussed in detail in the next section. NODDI is a practical high-angular resolution diffusion imaging (HARDI) method with two shells for estimating the microstructural complexity of dendrites and axons in vivo on clinical MRI scanners. NODDI allows separation of the restricted intraaxonal compartment from the isotropic and hindered compartments and provides estimates of two parameters that are more specific than FA: neurite density and orientation index.

3.6 Crossing Fibers and the Need for Advanced MR Diffusion Imaging Methods

It is important to understand well the limitations of MR tractography, especially when the method is applied in the interest of neurosurgical patients. Tractography can determine the trajectories of major WM fascicles but it cannot infer in which direction the signal is transmitted along each pathway. It cannot track streamlines to their cortical termination and it may fail at fiber crossing because the DTI model can recover only a single fiber orientation in each voxel. It is a user-dependent method based on a priori anatomic knowledge. It is also important to be aware that tractography does not provide functional information. IES is the only method able to test WM function and generate a subcortical functional

map that has proven to maximize tumor resection and minimize hazards.

The ambiguity in determining fiber orientation in a voxel containing more than one fascicle is related to the model applied with DTI, but it is not a limitation of diffusion MRI in general. DTI models the dispersion of water molecules using a Gaussian distribution, thus the assumption is that the scatter pattern during the diffusion time has an ellipsoid shape. Voxels contain hundreds of thousands of axons that are organized in bundles and fascicles that can have a wide range of complex configurations. The fibers within each voxel may be parallel, fanning, bending, and crossing at an acute or perpendicular angle. DTI is accurate to represent parallel fibers, but it cannot distinguish them from fanning and bending fibers, except for a lower FA value. In voxels with crossing fibers at an acute angle the principal orientation measured with DTI is misleading, as the mean fiber orientation that has a prolate shape does not correspond to the direction of any fiber. In voxels with orthogonal crossing fibers DTI fails to identify the two fascicles and its best approximation is an oblate ellipsoid that contains none of the useful directional information.

In the past decade there has been a lot of effort to move beyond DTI and solve the crossing fiber problem. Development of new models and algorithms that exploit more sophisticated imaging acquisition schemes such as HARDI has been addressed (Seunarine and Alexander 2009). The field is very complex and a detailed description of the many advanced methods goes beyond the purpose of this chapter.

Model-based approaches, such as the multi-tensor model, resolve fiber crossing by modeling distinct fiber populations separately. The model-based approaches assume that the voxel contains distinct populations of fibers and that diffusing molecules do not exchange between fiber populations. The multi-tensor model is a generalization of DTI that replaces the Gaussian model with a mixture of Gaussian densities. The "ball and stick" model assumes that water molecules belong to one of two populations: an isotropic component that does not interact with fibers and diffuses freely in the voxel and a restricted component that diffuses inside and immediately around axons (Behrens et al. 2003). The composite hindered and restricted model of diffusion (CHARMED) proposed by Assaf describes the restricted fiber population with a cylinder and the hindered population in extracellular space with an anisotropic Gaussian model (Assaf et al. 2004). The model-based methods do not naturally distinguish fanning and bending configurations from parallel fiber populations.

The aim of non-parametric methods is to estimate from diffusion MRI measurements the fiber orientation diffusion function (fODF) that provides more insight into the underlying fiber configuration. These methods do not rely solely on parametric models of diffusion, but try instead to reconstruct the fODF without placing modeling constraints on its form. Diffusion spectrum imaging (DSI) and Q-ball imaging reconstruct a function called the diffusion orientation distribution function (dODF). Spherical deconvolution (SD) methods recover a more direct estimate of the fODF.

DSI attempts to measure the scatter of diffusion directly and makes no assumptions about tissue microstructure or its shape (Wedeen et al. 2008). The acquisition requirements are the major limitations of DSI: standard protocols require long acquisition times with 500–1000 measurements at the expense of image resolution; stringent hardware with very strong gradients is required in order to apply very short pulses. The acquisition requirements in Q-ball imaging are more manageable than DSI. In its original work Tuch showed that Q-ball can resolve fiber crossing consistently using an acquisition scheme with 252 gradient directions at a $b = 4000$ s/mm^2 (Tuch 2004) although the approximation of the dODF introduces some blurring, which may reduce angular resolution and precision of peak directions.

The SD algorithm has the advantage of relatively short acquisition times, which are close to standard DTI clinical protocols, reduced computational times compared to some of the other methods, and the ability to resolve crossing fibers with a good angular resolution (Dell'Acqua et al. 2010). SD is based on the assumption that the

acquired diffusion signals from a single voxel can be modeled as a spherical convolution between the fiber orientation distribution (FOD) and the fiber response function that describes the common signal profile from the WM bundles contained in the voxel (Tournier et al. 2004). A major limitation of SD is its susceptibility to noise, which often results in spurious peaks in the recovered fODF. Acquisition requirements are compatible with clinical protocols: 64 directions with $b = 2000–3000$ s/mm^2 with a total scan time of 16 min. DTI and SD reconstructions can be obtained from the same dataset.

NODDI combines a three-compartmental tissue model with a two-shell HARDI protocol optimized for clinical feasibility. NODDI adopts a tissue model that distinguishes three types of microstructural environment: intracellular (restricted), extracellular space (hindered), and cerebrospinal fluid (isotropic) compartments (Zhang et al. 2012). Each environment affects water diffusion in a unique way and gives rise to a separate normalized MR signal. The intracellular compartment refers to the space bounded by the membrane of neurites and it is modeled as a set of sticks. NODDI provides measurements of several parameters, among which the two most innovative are neurite density and an index of orientation dispersion that defines variation of neurites orientation within each voxel. These parameters have great potential to provide relevant information for brain tumor tissue characterization and may be particularly efficient to track fibers in voxels with an increased amount of water such as those with vasogenic edema and glioma infiltration. Tractography can be performed using the SD algorithm, the NODDI or the DTI model from one HARDI acquisition scheme.

3.7 Clinically Feasible Brain Mapping Imaging Protocols and Pre-processing Requirements

It is mandatory to acquire diffusion data with relatively high spatial and angular resolution in order to perform a state of the art tractography study. High spatial resolution plays in favor of tractography because it reduces the gap in size between voxels and fascicles. High-angular resolution increases the discrimination of crossing fascicles at an acute angle. Unfortunately, improved spatial resolution always comes at the expense of longer acquisition times and lower signal-to-noise ratio. It is important to verify the capability of the MR unit in order to reach a good compromise between spatial resolution, signal-to-noise ratio and total acquisition scan time. In clinical practice the isovolumetric voxel size should be no larger than 1.5 mm when acquiring data with 1.5 T or even better with 3.0 T MR units. One common strategy to improve the angular resolution and the signal-to-noise ratio of the HARDI acquisition scheme is to acquire a dataset with 32 or 64 gradient directions and a b value in the range of 1500–3000 s/mm^2. MR units with strong gradients (high maximum amplitude and fast slew rate) are beneficial to keep the TE to a minimum value. Especially if fMRI is also acquired, scan time inferior to 20 min is recommended in order to keep the total time of the study session within 45 min.

DEC maps are very useful for preliminary interpretation of clinical studies in patients with disease, especially when used by experienced users. Low angular resolution DEC maps can be acquired with DTI acquisitions that use a minimum of 6 gradient directions and b value of 800 s/mm^2; however, the examiner should be aware that performing tractography with a low quality dataset may increase the likelihood of errors.

For NODDI acquisition scheme the following imaging parameters are recommended: two shells (b value of 700 and 2000 s/mm^2) with similar TR and TE, and respectively, 20 and 64 gradient directions will result in a total scan time of about 20 min.

Clinical MRI diffusion studies are performed by acquiring single-shot echo-planar images (EPI) with diffusion sensitizing gradients of different strengths and orientations that are applied for a relative long time in order to achieve the desired b value. EPI read-out is very sensitive to

static magnetic field (B_0) inhomogeneity that produces nonlinear geometric distortion primarily along the phase-encoding direction. Susceptibility artifacts are more pronounced at air–tissue interfaces and are most obvious in the orbitofrontal and mesial temporal regions, near the sphenoid sinus and the temporal petrous bone. In addition, patient bulk motion and additional image distortion induced by eddy currents, that do not cancel out when diffusion gradients are applied for a relative long time, cause additional artifacts on DWI. Analysis of diffusion imaging studies requires correction for patient motion and for susceptibility and eddy current artifacts. The many acquired DWIs have to be spatially aligned to avoid systematic errors in the parametric maps computed from misaligned DWI (Rohde et al. 2004). Several software are available for correcting DWI artifacts and confounds (Jenkinson et al. 2012; Leemans et al. 2009; Pierpaoli et al. 2010). Their use for pre-processing of DWI is strongly recommended in order to obtain reliable DTI measurements.

Since March 2012 the American Society of Functional Neuroradiology (ASFNR) has released and updated a document with ASFNR Guidelines for Clinical Application of Diffusion Tensor Imaging that is available on its website (https://www.asfnr.org/clinical-standards).

4 Functional Systems of the Brain and the Connectome

Current view is that the brain is hierarchically organized in terms of anatomical structure and function. The brain is a highly integrated system and for teaching purposes it may be divided into three distinct systems that function as a whole: the sensory, the motor, and the associative systems.

The sensory systems are in charge of processing special somatic sensations coming from the outside world: visual, auditory, tactile, and vestibular systems. Other sensory systems are specialized in processing visceral input: the olfactory, gustatory, and limbic systems. They are organized in primary sensory and unimodal cortical areas that continuously exchange information. Most sensory information is routed to the cerebral cortex via the thalamus. Only olfactory information passes through the olfactory bulb to the olfactory cortex in the uncus, bypassing the thalamus. The sensory systems converge to so-called multimodal areas that are located in the associative cortices of the parietal, temporal, and frontal lobes.

The motor system is responsible for purposeful movement; it plans for action, coordinates and executes the motor programs. The primary motor cortex (M1) plans and executes movements in association with other motor areas including the PMd, PMv, SMA, PPC, and several subcortical brain regions. The PPC plays an important role in generating planned movements by modulating the input received from the three sensory subsystems that localize the body and external objects in space. The PPC modulates planned movements, spatial reasoning, and visuospatial attention. The dlPFC is in charge of executive functions, including working memory, cognitive flexibility, and abstract reasoning. The dlPFC integrates sensory and mnemonic information and the regulation of intellectual function and action. Cognitive flexibility is the ability to switch between thinking about two different concepts and to think about multiple concepts simultaneously.

The associative system integrates current states with past tense states to predict proper responses based on a set of stimuli. The many association areas are located in the prefrontal, parietal, and temporal regions of both cerebral hemispheres; they permit perception and form a cohesive view of the external world. The association areas relate the information to past experiences, before the brain makes a decision and generates a motor response. The association areas are organized as distributed networks, and each network connects areas distributed across widely spaced regions of the cortex.

Network science does quantitative analysis of different aspects of connectivity that are peculiar of a complex system (Sporns 2014). Virtually all complex systems form networks of interacting

parts composed of multiple and redundant neural circuits that process and transfer the information either serially or in parallel. A network is made of a group of elementary macro (or micro) components that are closely connected and work as a unit. At the macroscale level nodes and pathways are the basic components of the network. At the microscale level the components are neurons, dendrites, axons, and synapses. Understanding such complex systems will require knowledge of the ways in which these components interact and the emergent properties of their interactions.

The visuospatial, motor, and language systems are of great interest for presurgical mapping because they are in charge of functions that are essential for human life. These systems may share similar elementary components; however, their networks display peculiar different and organized patterns. Each network of a functional system is dedicated to a specific sensory, motor or cognitive modality and it includes several specialized nodes that have different roles in processing information. The *primary sensory cortex* is the brain area containing neurons that receive most of their information directly from the thalamus. The distance from the body sensory receptors at the periphery defines secondary and tertiary cortical sensory areas. These are unimodal and multimodal association areas that play an important role in integration and modulation of the input signals reaching the cortex, and in planning of motor actions. Secondary motor areas located in the SMA and in the PMv and PMd cortices compute programs of movement that are conveyed to the *primary motor cortex*, where are located the cortical pyramidal motor neurons that project directly to the spinal cord.

The organization of functional systems follows several principles. The information conveyed within each network is processed and transformed at every node level. Information may be amplified, attenuated, integrated with information conveyed from other nodes of the same system. There are two main groups of neurons at each stage of the information processing: projecting neurons and local interneurons. The projecting neurons convey the information to the next node stage in the system. Each brain region may contain nodes of multiple functional systems. Axons leaving the node of a functional system are bundled together in a fascicle that projects to the next node. Bundles belonging to different networks and systems can course temporarily within the same fascicle. Short and long bundles may enter and exit at various locations along the course of a fascicle. All the nodes of the sensory and motor systems have a somatotopic organization that is repeated throughout the network. In this way an orderly neural map of information is retained at each successive level of processing in the brain. Visual, auditory, somatosensory, and motor maps are built at different stages of their respective networks.

Most functional systems are hierarchically organized. In the primary visual cortex an individual neuron may fire only when it receives the signal input from a very specific outside stimulus. Following the same principle multiple neurons in the primary visual cortex converge on individual cells in the association cortical areas. At very advanced stages of information processing, individual cortical neurons are responsive to highly complex information.

In the following sections the functional organization of the three functional systems that are more clinically relevant for presurgical mapping are addressed.

4.1 The Motor System

The task of the motor system is to maintain performance of basic functions such as balance, posture, locomotion, reaching, and communication through speech and gesture by moving body parts, limbs, and eyes. The motor system produces movement by translating neural signals into contractile force in muscles. The agility and dexterity of an athlete or of a piano player reflect the capabilities of his motor system to plan, coordinate, and execute motor programs that have been learnt and practiced many times until they can be executed automatically for the most part.

According to modern theories the motor system acts as a distributed network. The neurons of origin of the network are located in at least five

distinct cortical areas of each hemisphere: M1, PMv, PMd, prefrontal, and parietal areas. According to their targets the descending fibers are divided into four groups: the ventromedial and dorsolateral brainstem pathways, the corticobulbar, and the CSTs (Lemon 2008). It is important to emphasize that the CST originates from cortical areas that have different functions: M1, PM, SMA, the cingulate motor area, the primary somatosensory cortex (S1), the posterior parietal cortex, and the parietal operculum. M1 contains the greatest density of neurons giving rise to CST and corticobulbar tract. The human CST consists of about one million axons, of which about 49% originate in M1, 19% in the SMA, 21% in the parietal lobe (S1 and posterior parietal cortex), 7% in the PMd, and 4% PMv (Fig. 1). The axonal projections of the cortical motor neurons converge in the corona radiata, a fan-like array of descending and ascending fibers connecting the cortex with thalamus, basal nuclei,

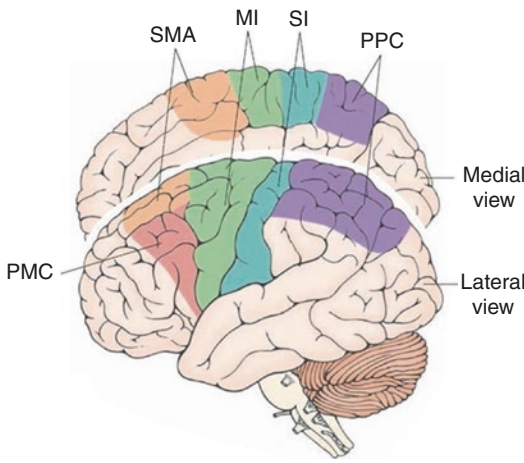

Fig. 1 The corticospinal tract arises from M1, S1, SMA, PMd, and PMv. Approximately 49% of the one million axons arises from M1, 21% from S1. The remaining 30% of the fibers originate from the PMC, the region immediately rostral to the precentral gyrus: 19% arises from SMA, 7% from PMd, and 4% from PMv. The descending axonal projections converge in the corona radiata, then enter the internal capsule maintaining a somatotopic distribution: corticobulbar fibers are located within the genu, corticospinal fiber in the middle third of the posterior limb of the internal capsule with the face-hand-foot represented in the anterior-posterior direction. The PPC does not contribute to the CST but modulates its activity. (Modified from http://what-when-how.com)

and spinal cord. More ventrally the descending tracts enter the internal capsule maintaining a somatotopic distribution: fibers originating from PMv, PMd, and SMA and prefrontal fibers originating from the frontal eye field areas course in the anterior third of the posterior limb, whereas the fibers originating in M1 course in the intermediate third. In the midbrain the fibers of the corticobulbar tract and CST become even more compact and enter the cerebral peduncles. At this level the frontal projections are located medially while tracts originating in the parietal, temporal, and occipital lobes are located more laterally in this order. In the pons the tracts course between the transverse pontine fibers, before beginning to cross to the contralateral side in the decussation of the pyramids at the level of the medulla oblongata. This contingent of the CST continues its course in the lateral columns of the spine. However, about 10% of the fibers of the CST continue their journey to the spine in the ipsilateral anterior columns and will cross side only when they reach their target. The CST terminates widely within the spinal gray matter, presumably reflecting control of nociceptive, somatosensory, reflex, autonomic, and somatic motor functions. These peculiar features explain why a single neuroanatomical pathway can mediate multiple functions (Lemon and Griffiths 2005).

There are striking differences across species in the organization of the descending pathways, and in particular of the CST. Some higher primates have unique direct projections to spinal motor neurons that bypass part of the integrative mechanisms of the spinal cord in order to generate motor output. Tracing studies with retrograde transneuronal transport of rabies virus from single muscles in rhesus monkeys have identified cortico-motoneuronal cells located in the caudal region of M1 that is buried in the central sulcus. This area is the lowest threshold site within M1. These cortico-motoneuronal cells make monosynaptic connections with motoneurons in the spine (Rathelot and Strick 2009). The cortical territories occupied by cortico-motoneuronal cells for different muscles overlap extensively within this region of M1. The findings of these tracing studies are against a focal representation

of single muscles in M1. The axons originating in dorsal M1 may have connections with other muscles in addition to the one it was injected with the rabies virus. Thus, the overlap and intermingling among the different populations of neurons may be the neural substrate to create a wide variety of muscle synergies (Rathelot and Strick 2006) and may indeed represent a resource for neuroplasticity. The extent of CST projections from cortico-motoneurons in this newly recognized M1 area correlates with index of dexterity, skilled use of hands and digits across species. Recent studies suggest that the monosynaptic cortico-motoneuronal system is related to voluntary control of relatively independent finger movements. Preservation of the axons originating from M1 monosynaptic neurons is mandatory in order to maintain highly skilled movements in patients with a brain tumor infiltrating the CST or growing in its proximity.

The CST also carries M1 axons that form synapses with interneurons in the spinal cord. This *indirect pathway* is coursing more rostral and it is important for coordinating larger groups of muscles in behaviors such as reaching and walking. The motor information provided by the cortico-motoneuronal system via the CST is significantly modulated by information originated in secondary cortical motor areas. In the macaque it has been shown that electrical stimulation of the PMv could produce powerful stimulation of the M1 outputs to the spine. This neuronal circuit may represent an important parallel route through which a secondary motor area could exert its motor effects (Cerri et al. 2003). In addition, the output of M1 is modulated by neurons located in other motor regions located in the thalamus, basal nuclei, and cerebellum. The activity of these subcortical structures is also very important for the execution of smooth movements.

Mapping of the CST in the operating room is not a trivial procedure. Subcortical direct IES of the CST with the 60 Hz bipolar probe evokes the unnatural and synchronous stimulation of many fascicles and may well exert mixed excitatory and inhibitory effects on target neurons. On the contrary, subcortical direct IES with the monopolar probe is capable to discriminate the different components of the CST that is so important for brain surgery (Bello et al. 2014).

In summary, in the motor system neuronal information is processed in a variety of discrete networks that are simultaneously active. In the particular case of the CST the signal carrying motor information is conducted along fibers that are originating in different parts of the neuronal network and are converging into the CST that eventually carry them to a common target in the brainstem or in the spinal cord.

For the many different functions it carries, the CST is probably the most complex and important pathway of the entire human brain. For sure it is the most important and eloquent structure that must be safeguarded in brain surgery. Lesions along the CST cause a pyramidal disconnection syndrome with neurological signs that vary according to lesion location and the interval from time of onset. Motor deficits can range from hemiparesis to hemiplegia. Lesions cause a breakdown in fine sensorimotor control of the extremities, implying a deterioration not only in motor function, but also in the capacity to interrogate correctly the sensory feedback from the limb (Lemon and Griffiths 2005). Implicit in modern concepts of a distributed motor network is that neurological signs resulting from lesions to a descending pathway cannot be interpreted any longer as simply being due to the removal of the lesioned pathway. Soon after an acute injury of the CST, activity-dependent, fast neuroplastic changes occur and the clinical outcome must be interpreted as the consequence of compensatory changes of the motor network as a whole, including the response of uninjured fibers.

4.2 The Language System

Language is a native, uniquely human trait that we learn without any formal teaching or training. As humans we use language automatically to communicate, however language is not the only mean we use for communication. People learn to use a highly structured stream of sounds or signs. In contrast, non-human primates and many other animals from bees to whales are able to commu-

nicate with sounds and signs, but they are unable to combine words to construct larger utterances. Despite intense training, the ability of binding words to build a linguistic sequence does not exist in other primates. Language emerges spontaneously in all children of the human species and it has a universal design that is based on two components: *words* and *grammar*. A word is an arbitrary association between a sound and a meaning. Grammar has three subsystems: *morphology* defines the rules for combining words and affixes in larger words; *syntax* consists of rules for combining an inventory of words into phrases and sentences; *phonology* consists of rules combining sounds into a consistent pattern that is characteristic of a specific language. In particular, syntax is a specific cognitive system of rules and operations that distinguishes language from other means of communication.

The relationship of specific brain regions with the language system has been more difficult to localize than for the motor and sensory systems. Interest in the structures responsible for the human ability to process speech and language dates back at least to the time of the Greek philosophers. Historically, it was the German neuroanatomist Franz Joseph Gall (1758–1828) who pioneered the study of the localization of mental functions in the brain. Gall suggested that language was located in the left frontal lobe. However, in 1861 the French neurologist Paul Broca began to explore the brain anatomy of language with the invention of the "lesion method." During an autopsy Broca located the stroke lesion in the left inferior frontal gyrus. In 1874 the German Carl Wernicke described the clinical case of a few patients with a deficit in language comprehension. All patients with comprehensive aphasia had lesions in the posterior half of the left superior temporal gyrus. Joseph Jules Dejerine and his wife Augusta made also important contribution to the field of aphasia research. They understood the importance of the association fibers that formed an intricate network that connected the cortical language centers, including Broca and Wernicke areas, and the visual image center in the angular gyrus. The concept of an interconnected *language zone* separated the Dejerines from the doctrine of the French neurologist Jean-Martin Charcot (1825–1893), who postulated the existence of largely autonomous centers for different language modes (Miraillé 1896).

Knowledge about the neural basis of language processing accelerated 100 years later with the advent of neurophysiology first and more recently of advanced brain imaging methods (Price 2010; Friederici 2011). In the last two decades the classic theory of language localization proposed by Wernicke and Geschwind has been intensely revised thanks to the large amount of imaging data collected with neurophysiology (event-related potential, magnetoencephalography, and IES) and neuroimaging (fMRI and DTI). In the seventies of the twentieth century it was found that neurological patients with Broca aphasia following stroke not only had deficits in language production but they also showed problems in language comprehension when confronted with grammatically complex constructions. Patients with Wernicke aphasia not only had deficits in comprehending the meaning of utterances, but they also had problems in word selection during speech production. These observations led to the theory that Broca's area subserves grammatical processes during both speech production and comprehension. Similarly, the revised language theory suggested that Wernicke's area supports lexical-semantic processes (Caramazza and Zurif 1976). We predict that in the years to come neurosurgical patients will provide a new important source of data, especially now that mapping of brain function before and during removal of a focal brain lesion is recommended according to state of the art medical practice guidelines.

In particular, three important discoveries were made. First, it was confirmed that language is strongly lateralized to the left cerebral hemisphere. This finding was also confirmed with fMRI that showed that language is lateralized to the left in about 96% of right-handed subjects (Pujol et al. 1999). Only 4% of right-handed individuals show a symmetric blood oxygenated level dependent (BOLD) response during a language task. The BOLD response is also lateralized to the left in about 76% of left-handers; it is

symmetric in 14% of them, whereas it is lateralized to the right side in the remaining 10%. More recently, the asymmetry of the language network has been demonstrated also with deterministic DTI tractography: the direct AF segment connecting Broca with Wernicke territories is found only on the left side in 62% of right-handed healthy subjects; it is bilateral but left lateralized in 20% and symmetric only in 17.5% of subjects (Catani et al. 2007). The second discovery was that three different aphasic syndromes were associated with damage to three specific brain structures: (1) *Broca aphasia* with damage to pars opercularis of the inferior frontal gyrus; (2) *Wernicke aphasia* with damage to the posterior part of the superior temporal gyrus; (3) *conduction aphasia* with damage to the AF that was thought to be a unidirectional pathway carrying information from Wernicke to Broca area. The third important discovery was that both Wernicke and Broca areas were presumed to interact with heteromodal high-order associative areas in the frontal, parietal, and temporal lobes.

In the first anatomic classic model of language proposed by Wernicke in 1874 there were two cortical centers: Broca area was dedicated to speech production and Wernicke area to auditory comprehension. Wernicke thought that the two centers were indirectly connected by fibers passing through the external capsule and relaying in the insula. It was Dejerine that proposed that the AF was connecting directly the two centers. The classic model was later modified by Geschwind in 1970 who emphasized the importance of a third cortical center located in the angular gyrus (Geschwind 1970).

Recent studies in patients with stroke, head injury, and neurodegenerative diseases (i.e., Alzheimer and frontal temporal dementia) have uncovered other cortical and subcortical regions that belong to the language network. Patients with damage to the left temporal pole (Brodmann area, BA38) may have difficulty to retrieve names of unique places and persons, but can retrieve names of common things. With damage to the mid-portion of the left MTG (BA20 and 21) patients have difficulty to recall both unique and common names, without any associated grammatical and phonemic deficit. Damage to the posterior part of the left inferior temporal gyrus (BA37) instead causes a deficit in recalling words of tools and utensils. The precentral gyrus of the left insula is another language-related area that was not included in the classic models. Patients with stroke lesions in the anterior insula show articulatory planning deficits: a difficulty in pronouncing phonemes in their proper order (Dronkers 1996). Other two areas that were recently considered part the language network are located in the mesial surface of the frontal lobe. The SMA in the left SFG and the left anterior cingulate cortex (BA24) play an important role in the initiation and maintenance of speech. Damage to these areas, especially after surgery is often associated with akinesia and mutism leading patients to fail to communicate by words, gestures, or facial expression. These patients usually recover within a few days (Krainik et al. 2003).

Aphasias are classified in to three major syndromes and few sub syndromes. In *Broca aphasia* the damaged network is involved in both the assembly of phonemes into words and the assembly of words into sentences. The network is thought to be concerned with relational aspects of language, which include the grammatical structure of sentences and the proper use of verbs. The cortical areas damaged in Broca aphasia are frontal BA44, 45, 46, 47, parietal areas BA39 and 40 and the insula. In *Wernicke aphasia* the damaged network is involved in generating speech sounds and in associating the sounds with concepts. Wernicke area is no longer considered the center of auditory comprehension as it was conceived in the Wernicke–Geschwind model (Geschwind 1970). Aphasic patients with lesions in the posterior third of the STG and MTG (BA 22) often shift the order of individual sounds and make frequent phonemic paraphasias. These patients also make semantic paraphasias that are errors in selecting words with substitution of one full word with another that has a meaning relation. In *conduction aphasia* the damaged network is required to assemble phonemes into words and coordinate speech articulation. Patients with conduction aphasia cannot repeat

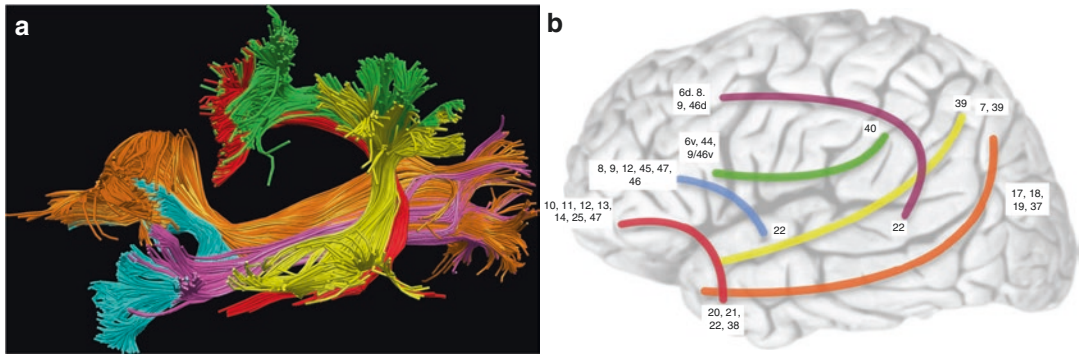

Fig. 2 (**a**) Modern theories about language have recognized that there is a lot of network redundancy in the system. Several models have been proposed, with some differences in connectivity, but all models acknowledge the importance of a dual-stream system with dorsal and ventral networks. The models that are heavily influenced by in humans DTI and post-mortem blunt fiber dissection methods suggest as many as five pathways relevant for language: the direct segment of the AF (red), the posterior segment of the AF (yellow), and the third segment of the SLF-III (green) are part of the dorsal pathway; the inferior fronto-occipital fasciculus (IFOF, orange), UF (cyan), and ILF (magenta) are part of the ventral pathway. The MLF is notably absent in this model. (**b**) Models that are heavily influenced by autoradiographic tract-tracing studies in the macaque monkey suggest as many as six dissociable fiber tracts. The autoradiography data also suggest the existence of a MLF (yellow), but dispute the existence of an IFOF. The extreme capsule (blue), UF (red), MLF and ILF (orange) are part of the ventral pathway connecting the inferior part of the frontal lobe with the temporal, parietal, and occipital lobes. The AF (violet) and SLF-III (green) are part of the dorsal pathway. Numbers refer to the corresponding Brodmann's areas for putative terminations and connections. (Modified from Dick AS et al. - Brain 2012: 135; 3529–3550)

sentences word for word, cannot easily name pictures and objects, they make phonemic paraphasias, but can produce intelligible speech and comprehend simple sentences. Related lesions involve the STG, SMG and AG, the insula and the adjacent WM. Until recently there was not much evidence in the literature that a simple disconnection of the AF alone could cause conduction aphasia, as it was originally suggested by Monakow and later by the Dejerines (Dejerine and Dejerine-Klumpke 1895). Only recently Bizzi and colleagues showed with DTI tractography that preoperative mild conduction aphasia in glioma patients is strictly associated with involvement of the AF (Bizzi et al. 2012).

The large amount of neuroimaging data becoming available is providing new opportunities for testing innovative models of the language network (Fig. 2). In 2004 Hickock and Poeppel outlined a dual-stream model of speech processing with a *dorsal stream* mapping acoustic speech signals to the articulatory subnetworks in the IFG and a *ventral stream* processing signals for comprehension. The model assumed a widely distributed network with a strongly left-lateralized dorsal pathway and a largely bilateral organized ventral pathway (Hickok and Poeppel 2007). The dorsal stream will connect cortical nodes of the articulatory subnetwork located in the left dominant posterior IFG (pars opercularis and triangularis), ventrolateral premotor cortex, and anterior insula with the sensorimotor interface nodes localized in the posterior STG and AG. The ventral stream will connect a combinatorial subnetwork located in the anterior MTG and inferior temporal sulcus (ITS) with a lexical interface node located in the posterior MTG and ITS and with the articulatory subnetwork already described.

In 2012 Friederici proposed a functional anatomical model of the language network that was focused on different processing steps from auditory perception to comprehension (Friederici 2012). One novelty of this model was that particular attention was dedicated to definition of the structural connections between the cortical nodes of the network. In this model of sentence comprehension several hubs or nodes are connected via the dorsal and ventral pathways. Transformation of sounds in words and phrases occurs within

50–80 ms after acoustic and phonological analysis taking place in the middle portion of the STG. Once the phonological word form is identified, its syntactic and semantic information are retrieved in the anterior STG/STS. This subnetwork operates in the anterior temporal lobe as comprehension moves from phonemes to words and phrases. Lexical-semantic integration occurs in the MTG. Information transfer within this temporal subnetwork is likely provided by short-range bundles within the IFOF.

A second language subnetwork elaborates syntactic and semantic data and requires nodal processors in the anterior (BA47 and 45 for semantic processing) and in the posterior (BA44 for syntactic processing) IFG. Information transfer between the anterior temporal and IFG is assumed to be supported by ventral pathways: semantic information is conveyed via the IFOF connecting the pars orbitalis and triangularis (BA47 and 45) with the temporal and occipital cortices; syntactic information is conveyed via the UF connecting pars opercularis (BA44) with the anterior temporal cortex (Anwander et al. 2007). Patients with lesions involving the ventral language stream have been reported to have semantic and syntactic comprehension deficits (Tyler et al. 2011). A third subnetwork of the model proposed by Friederici is in charge of integrating semantic/syntactic processing at a hierarchical level in order to achieve sentence comprehension. Thus, elaborated information is bidirectional exchanged between the IFG, the posterior MTG (BA22 for semantic processing) and the AG (BA39 for syntactic processing). The connection from the IFG to the AG likely occurs via the direct or indirect route of the AF, whereas it is still under debate whether the connection to the MTG occurs via the ventral (IFOF) or the dorsal (AF) pathway.

The contribution of the dorsal and ventral WM pathways connecting the frontal and temporal speech regions is central to understanding how the cortical areas interact to produce a seamless language system. One emerging concept is that the AF is involved primarily in phonology, articulation, and syntax and the IFOF is mainly implicated in semantics. While authors vary in their claims concerning the extent of functional specialization, all authors argue for some degree of functional differentiation. The authors of a recent study performed in 24 patients with chronic stroke in the left hemisphere suggested that segregation of function for the dorsal and ventral pathways is limited to the phonological and semantic tasks (Rolheiser et al. 2011). On the other hand, morphology and syntax require a synergy between the AF and the IFOF rather than a segregated system. In this DTI study both dorsal and ventral bundles were associated with syntactic performance in both comprehension and production tasks. Comprehending syntax utilizes equally both the AF and IFOF, while syntactic production is predominantly permitted via the AF. By defining the WM architecture as a synergy, the overall determinant of task performance is not dictated by which WM tract is involved, but by how prefrontal and posterior temporal cortical speech regions use and integrate a constant flow of very complex linguistic information.

4.3 The Visuospatial Attention System

What you see is determined by what you attend to. Visuospatial attention is a complex dynamic process that involves filtering relevant information from our spatial environment. We simultaneously attend to and look at objects in a visual scene by means of saccadic eye movements that rapidly bring the fovea onto stimuli of interest. The processing of visual stimuli appearing in the attended spatial location will be enhanced, while stimuli appearing in other parts of the visual field will be suppressed. Visuospatial attention is necessary for selecting and inhibiting visual information over space, because the environment is overloaded with far more perceptual stimuli that our brain can effectively process. Visuospatial attention allows people to select, modulate, and sustain focus on the information that is most relevant to their own behavioral goals. The selected item may enter visual working memory and/or become the target of a movement.

There are multiple forms of attention to external and internal stimuli (Chun et al. 2011). External attention refers to the selection and modulation of sensory information: visual, auditory, olfactory, tactile, and gustatory. Each of these attention systems selects locations in space, or modality-specific output. The visual attention system is by far the most developed in humans while in other animals the auditory or the olfactory attention systems may be in charge of guiding the behavior of the animals in response to environmental stimuli. Internal attention refers to the selection, modulation, and maintenance of internally generated information, such as task rules, responses, long-term memory, or working memory. Visuospatial attention also interacts with other attention processes.

The concept of spatial selective attention refers operationally to the advantage in speed and accuracy of processing for objects lying in attended regions of space as compared to objects located in non-attended regions (Posner 1980). When several events compete for limited processing and comprehending capacity and control of behavior, attention selection may resolve the competition.

fMRI studies in humans have shown that the anatomical structures which are activated during the performance of attention-related functions are located in the parietal and frontal lobes and form multiple functional parietofrontal networks (Corbetta and Shulman 2002). The posterior parietal cortex (PPC) and the frontal eye field/dorsolateral prefrontal cortex are nodes of a dorsal attention network that is active during the orientation period. The temporo-parietal junction and the ventrolateral prefrontal cortex are nodes of a ventral attention network that is active when subjects have to respond to targets presented in unexpected locations. The ventral network is in charge of detecting unexpected but behaviorally relevant events and is responsible for maintaining attention on goals or task demands that are a top-down process. Physiological studies have found that the activity of the frontal and parietal nodes is coordinated during execution of a visual attention task but show distinctive dynamics. In the parietal cortex bottom-up signals appear first and are characterized by an increase of fronto-parietal coherence in the gamma band (25–100 Hz), whereas in the PFC top-down signals emerge first and tend to synchronize in the beta band (12–30 Hz) (Buschman and Miller 2007).

In the monkey brain the activity of neurons dedicated to visuospatial attention has been recorded simultaneously in the parietal and frontal cortices. Axonal tracing studies have shown that parietal and prefrontal neurons are directly and extensively interconnected through a system of fascicles running longitudinally in the centrum semiovale, dorsally to the AF and laterally to the CST. Three distinct parietofrontal long-range segments of the SLF that had been previously described in the rhesus monkey (Petrides and Pandya 1984) have been recently demonstrated also in the human brain using MR tractography with the SD algorithm (Thiebaut de Schotten. 2011a, b).

The dorsal and first segment of the SLF (SLF-I) connects BA5 and 7 in the PPC including the dorsal bank of the intraparietal sulcus with BA8 and 9 in the SFG; the SLF-II connects BA39 and 40 in the inferior parietal lobule (IPL) including the ventral bank of the intraparietal sulcus with BA8 and 9 in the MFG; the ventrally located SLF-III segment connects the AG (BA40) with the BA44, 45 and 47 in the IFG. The SLF-I connects the cortical nodes of the dorsal attention network activated during the voluntary orienting of spatial attention toward visual targets, while the SLF-III overlaps with the ventral network that is activated during the automatic capture of spatial attention by visual targets and damaged in people with visuospatial neglect (Fig. 3). The middle SLF-II segment connects the parietal nodes of the ventral network with the prefrontal nodes of the dorsal network and it may represent a direct communication between the two networks. The SLF-II may act as a modulator for the dorsal network, redirecting goal-directed attention mediated by the SLF-I to events identified as salient by the SLF-III, as suggested by Corbetta in the fMRI study cited above (Corbetta and Shulman 2002).

The parietofrontal network is bilaterally represented with some degree of asymmetry variable among the three segments. By measuring the vol-

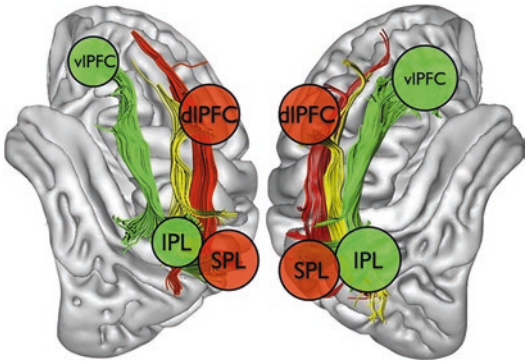

Fig. 3 A schematic representation of the parietofrontal visuospatial attentional networks based on fMRI (Corbetta and Shulman 2002) and MR tractography data (Thiebaut de Schotten et al. 2011a, b). The major cortical nodes are located in the vlPFC and dlPFC, IPL, and SPL. The three segments SLF-I (red), SLF-II (yellow), and SLF-III (green) are believed to connect the parietal and frontal nodes of the dorsal with the ventral attention networks. (Figure as originally published in (Ciaraffa et al. 2012))

umes of the tracts reconstructed with tractography in 20 healthy subjects Thiebaut de Schotten et al. found that the SLF-I is symmetrically represented in the two hemispheres, the SLF-III is right lateralized and the SLF-II shows a trend of right lateralization, but with substantial inter-individual differences that are correlated to behavioral signs of right hemisphere specialization (Thiebaut de Schotten et al. 2011a).

An acute stroke damaging the fronto-parietal network will affect the ability to process visuospatial information and it usually will manifest with neglect. In most of the patients the deficits are transitory and become apparent only with clinical tests that elicit hemispatial neglect. Patients with visual neglect fail to pay attention to objects presented on the side of space contralateral to a brain lesion. While it is undisputed that right lesions provoke more severe and durable signs of neglect than strokes in the left hemisphere, identification of eloquent anatomic structures that, if injured, will cause visual neglect has fostered an intense debate in recent years.

Visual neglect has been associated with right hemisphere lesions in gray matter structures (parietal, frontal, or temporal cortices), in the basal nuclei or in the thalami. More recently, visual neglect has been associated with isolated WM injury that was possible to assign to specific fronto-parietal WM tracts with the aid of tractography. In a 55 -years-old man with transient visual neglect tractography was essential to

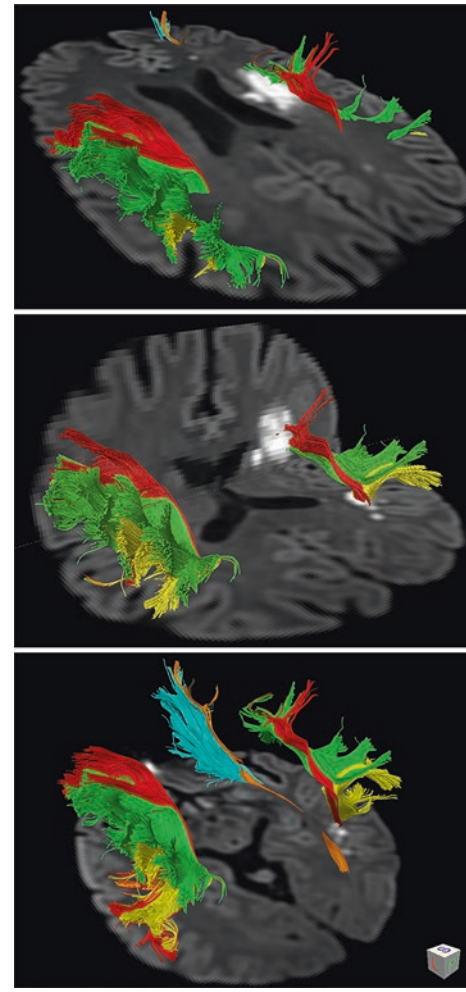

Fig. 4 Fifty-five years-old right-handed male presenting with acute onset of severe left visual neglect and left hemiparesis. MR DWI showed small multiple acute ischemic infarcts in the right cerebral WM and no evidence of infarcts in GM. DTI tractography was instrumental to accurately localize one infarct to the SLF-III (green) that is a component of the large-scale networks controlling visuospatial attention. Another infarct was localized in the stem of the AF (AF-direct in red, AF-posterior segment in yellow); the IFOF (orange) and UF (cyan) were not involved. This case report supports the hypothesis that neglect may result from disruption of a distributed attention network (Ciaraffa et al. 2012)

determine that a small acute ischemic WM infarct involved the SLF-III (Fig. 4) (Ciaraffa et al. 2012).

Signs of transient neglect were evoked also in two neurosurgical patients during resection of right hemisphere LGG while they were asked to bisect 20-cm horizontal lines. Patients deviated rightward upon subcortical direct IES of the SMG and of the posterior STG, but made no mistakes when the FEF and the anterior part of the STG were stimulated. However, in one patient it was the stimulation of the SLF-II underneath the IPL that evoked the strongest deviation rightward (Thiebaut de Schotten et al. 2005). The importance of SLF-II damage was replicated with IES in other six neurosurgical patients with right hemisphere gliomas (Vallar et al. 2014) and it is further supported by studies in right hemisphere stroke patients with chronic unilateral neglect, where maximum lesion overlap was along the trajectory of the SLF (Doricchi and Tomaiuolo 2003; Thiebaut de Schotten et al. 2008). The use of a DTI-based atlas of the human brain allowed a detailed analysis of WM lesion involvement in another study in 38 patients with chronic neglect. Results revealed that damage to the SLF-II (and to the SLF-III with lesser significance) was the best predictor of chronic persistence of left visuospatial neglect (Thiebaut de Schotten et al. 2014). Taken together these tractography studies support the importance of parietofrontal disconnection in the pathogenesis of neglect and they outline the important contribution of tractography studies in assigning lesion location to specific WM tracts.

4.4 The Connectome

The human nervous system is an assembly of an average of 86 billion of projecting neurons and local interneurons (Azevedo et al. 2009), wired together by countless, slender axons, and dendrites to form a very dense wiring diagram. Recently this diagram has been renamed "*the connectome.*" This term, like *genome*, implies completeness. A connectome is not made by few or even many connections. It is all the connections of an individual brain. The connectome of a human being is unique; it has many similarities and many differences with the connectome of other individuals. Unlike the genome, which is relatively fixed from the moment of conception, the connectome changes throughout life. Neurons adjust and rewire their connections by strengthening or weakening them, by creating and eliminating synapses.

More than 100 years ago, Ramon y Cajal predicted that one of the main factors guiding the evolution of the brain was a trade-off between rapid information transfer and the cost of wiring (Ramon y Cajal 1995). The costs of building and running a bigger brain network are metabolically more expensive, but are also quite rigorously controlled to be as low as possible for any given function (Bullmore and Sporns 2012). The results of a recent study with diffusion MRI in 123 species of mammals confirmed that the connectome and the wiring cost are conserved across mammals (Assaf et al. 2020). This conservation principle holds for all mammals, independent of brain size, suggesting a selective evolutionary pressure in favor of efficient connectivity and wiring costs. This conservation principle applies not only to inter- but also to intraspecies variations of the connectome. How is global connectivity maintained despite the large diversity in brain size and shape across mammals? The results of Assaf and colleagues' study found that species with fewer (commissural) interhemispheric connections have more efficient intrahemispheric connectivity. The results suggested that intrahemispheric connectivity compensates for poorer interhemispheric connectivity, maintaining the overall connectivity. The conservation principle may play a role also during ontogeny of the connectome. A recent study showed that patients with agenesis of the corpus callosum have stronger intrahemispheric connections (Owen et al. 2013). Agenesis of the corpus callosum is one of the most common human brain malformations and it can be considered a prototypical human disorder of axon guidance, one in which fibers that would normally have crossed the midline as part of the corpus callosum instead form *Probst bundles*, large white matter tracts

that course anterior-posterior parallel to the interhemispheric fissure within each cerebral hemisphere.

Neuroanatomical localization is critical to understanding the brain. The Human Connectome Project (HCP) began in 2010 with the goal to develop improved neuroimaging methods and to acquire a data set of unprecedented size and quality for mapping the normal human macroscale connectome. Better maps of the brain's areas and their connections may also improve our ability to understand and treat neurological and psychiatric disorders (Glasser et al. 2016). In the last two decades, comprehensive connectivity maps or connectomes have been generated with functional and diffusion MR imaging data, electroencephalography (EEG) and magneto-electroencephalography (MEG) acquired in healthy human subjects and other organisms. These brain graphs have revealed topological principles of brain network organization. There is now strong evidence that human brain networks have *small-world properties* of high clustering and high global efficiency, a modular community structure and heavy-tailed degree distributions that indicate a number of highly connected nodes or hubs (Achard and Bullmore 2007).

Virtually all systems require the integration of distributed neural activity. Network analysis of human brain systems has consistently identified regions called "hubs" that are critically important for enabling efficient neuronal signaling and communication (Van den Heuvel and Sporns 2013). Hub nodes mediate many of long-range connections between brain modules, and are efficiently interconnected to form a "rich club" (Van den Heuvel and Sporns 2011). The high level of centrality of brain hubs also renders them points of vulnerability that are susceptible to disconnection and dysfunction in brain disorders. It has been shown that in many neurological diseases focal lesions are concentrated in the highly connected hubs of the human connectome (Crossley et al. 2014), also known as the "*anatomical rich club*" (Van den Heuvel and Sporns 2011). Lesions may be concentrated in hubs purely because of their greater topological value. Some diseases might affect brain regions with uniform probability but lead to symptoms when the lesion happened to damage a hub. Regarding presurgical mapping for brain tumor surgery it is important to describe the relationship of the tumor with critical hubs and long-range connections because these are crucial components of eloquent systems.

5 Mapping WM Tracts for Brain Surgery

5.1 Brain Tumor Semeiotic of FA and Directionally Encoded Color Maps

Diffusion imaging with DEC maps and MR tractography is increasingly requested by neurosurgeons because its clinical relevance has been proven. In the motor system DTI has become more popular than functional MRI because it is capable of identifying CST trajectories. MR tractography nicely illustrates the dorsal and ventral language pathways. When a mass dislocates the OR tractography provides necessary information in order to plan the surgical approach to the lesion. DEC maps are immediately available at the console and they can be very practical and useful to determine the relationship of a mass with adjacent tracts. Expert users can identify the course of the main fascicles already on DEC maps. Notwithstanding, it is fiber tracking that best illustrate the trajectory of a tract in 3D and its relationship with the tumor.

On DEC maps and with tractography it is possible to determine whether the main WM tracts are *normal*, *dislocated*, *abnormal,* or *interrupted* (Jellison et al. 2004). In the first section we have already pointed out that diffuse infiltrating slow-growing gliomas behave biologically differently from fast expanding GBMs. LGG rarely dislocate WM tracts. LGG infiltrate bundles that remain functional as it was demonstrated by IES. On the contrary HGG, metastases, and meningiomas have the tendency to displace or destroy bundles. Knowledge of this difference in

behavior is important preoperatively in order to identify the trajectory of eloquent WM tracts in relationship to the tumor.

It is quite common to observe a tract *dislocated* by a mass becoming more visible on FA and DEC maps because it is compressed and thus more compact with elevated FA. For instance, the CST dislocated by a mass can show paradoxical increased FA value and maintain a blue hue regardless of whether it is shifted (Fig. 5). Gliomas growing in the temporal and occipital lobes are likely to displace the OR in the opposite direction from their point of origin. Presurgical MR tractography will show the trajectory of the OR with exquisite detail and it will be useful to neurosurgeons in planning the point of entry for the corticotomy (Fig. 6). Gliomas infiltrating the perisylvian cortex are likely to displace dorsally the direct segment of the AF. The position of the AF stem or isthmus in the deep temporal occipital WM is easy to recognize and it is a practical landmark on axial DEC maps. The AF stem is color coded in blue and it is frequently dislocated posteriorly by aggressive tumors. Gliomas tend to dislocate the AF stem posteriorly and the frontal arm of the direct AF segment dorsally. A slow-growing tumor growing in the IFG nearby Broca area is likely to dislocate the frontal arm of the direct AF posteriorly without interrupting its major trajectories. Patients with LGG infiltrating Broca area are unlikely to have speech deficits (Plaza et al. 2009). A mass originating in the ventral precentral gyrus may dislocate the AF medially. More aggressive gliomas originating in ventrolateral precentral cortex (BA6) may initially dislocate the AF medially, then as they expand they may interrupt its trajectories causing conduction aphasia (Bizzi et al. 2012).

Intraoperative DTI has been used to show shifting of the CST tract during tumor resection. In a series of 27 patients with glioma the authors used DEC maps to find that dislocation of the CST may occur either inward or outward. The authors underscored that intraoperative updating of the DTI results is important (Nimsky et al. 2005). A WM tract that is compressed by a mass may turn out to be easier to track especially when FA is increased. This phenomenon is likely due to decreased radial diffusivity with minor changes in axial diffusivity. Tracts that are usually more difficult to visualize such as the OR and the contingent of CST fibers projecting to M1 of the face/mouth area may be enhanced when they are compressed by a large mass (Fig. 7).

A WM tract is considered *abnormal* on DEC maps when it is coursing throughout an area of T2-signal hyperintensity, with altered FA and MD but it shows native orientation (color hue). Despite early reports suggesting that DEC maps might separate diffuse infiltrating gliomas from tumor-free vasogenic edema (Jellison et al. 2004), this differentiation is not reliable. The expansion of the ECS deployed by infiltrating glioma cells and the increased water content secondary to vasogenic edema may likely appear with similar and overlapping DTI abnormalities.

LGGs have a predilection to infiltrate associative unimodal and multimodal cortices in the insula, temporal pole, orbitofrontal, and SFG (Duffau and Capelle 2004). Insular gliomas easily infiltrate adjacent IFOF fibers coursing in the ventral floor of the extreme capsule and the UF in the temporal pole. Cancer cells may grow around and move along WM fascicles and infiltrate adjacent frontal and temporal lobes: a swollen temporal stem is a hint that the glioma cells are using the WM tracts as infrastructures to infiltrate additional territory. On axial DEC maps the trajectories of the IFOF in the temporal stem and the extreme capsule is coded in green. Only rarely LGGs may dislocate the IFOF and the UF. On the contrary, GBMs originating in the anterior aspect of the left temporal lobe are more likely to dislocate or interrupt rather than infiltrate the IFOF. MR tractography identifies the trajectories of the IFOF and UF when they are dislocated. Unfortunately, heavy tumor infiltration or vasogenic edema may result in significant MD increase with FA drop. In this scenario MR tractography fails to detect residual bundles because FA decreases below the threshold and the eigenvector may become undetermined. The possibility of false negative findings should be raised in the radiology report to the neurosurgeon. It is important to keep in mind that MR tractography does not provide functional information and that

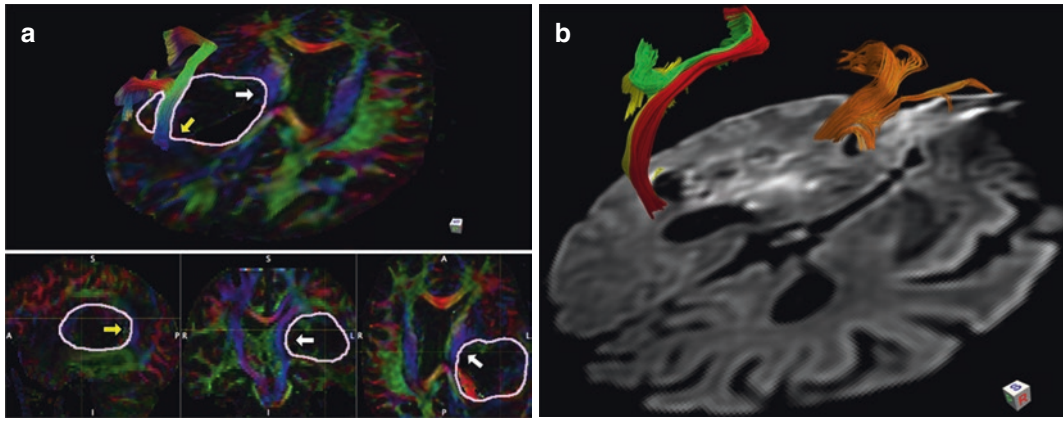

Fig. 5 (**a**) Sixty-five years-old right-handed female with recent onset of severe comprehensive aphasia. MRI showed a large enhancing mass deep seated in the left posterior temporal lobe. DEC maps with tractography showed that the mass dislocated anteriorly and medially the left CST (white arrows) and posteriorly the left AF (yellow arrow). In the upper box MR tractography of the direct segment of the AF with DEC streamlines. In the lower boxes form the left side are sagittal, coronal and axial DEC maps with the margins of the mass outlined. A GBM WHO-IV was removed at surgery. (**b**) DTI tractography of the three segments of the AF (direct in red, anterior in green, posterior in yellow) displayed in 3D over DWI in the axial plane is confirming that the GBM dislocated the AF posteriorly

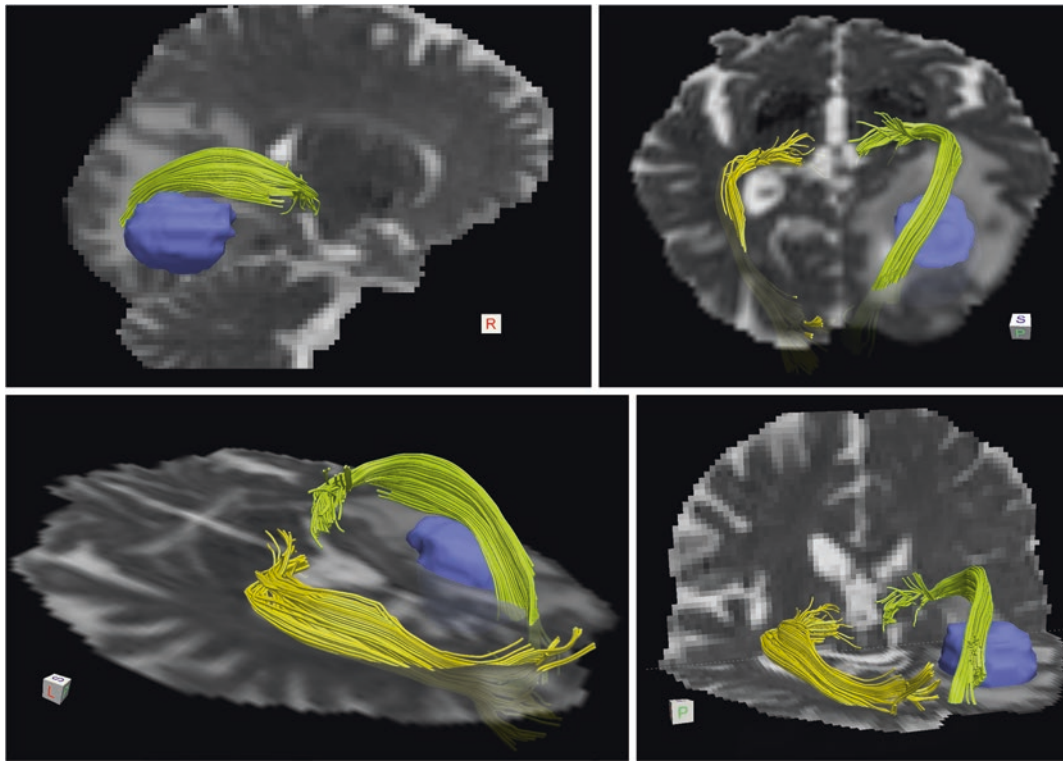

Fig. 6 Seventy-six years-old male with GBM WHO-IV surrounded by abundant perilesional vasogenic edema in the right occipital lobe displacing the OR dorsally. Note the asymmetry with the right OR (light green) displaced dorsally relative to the left OR (yellow) on multiple T2-weighted MR images with overlaid streamline tractography performed with spherical deconvolution. The mass is colored in blue

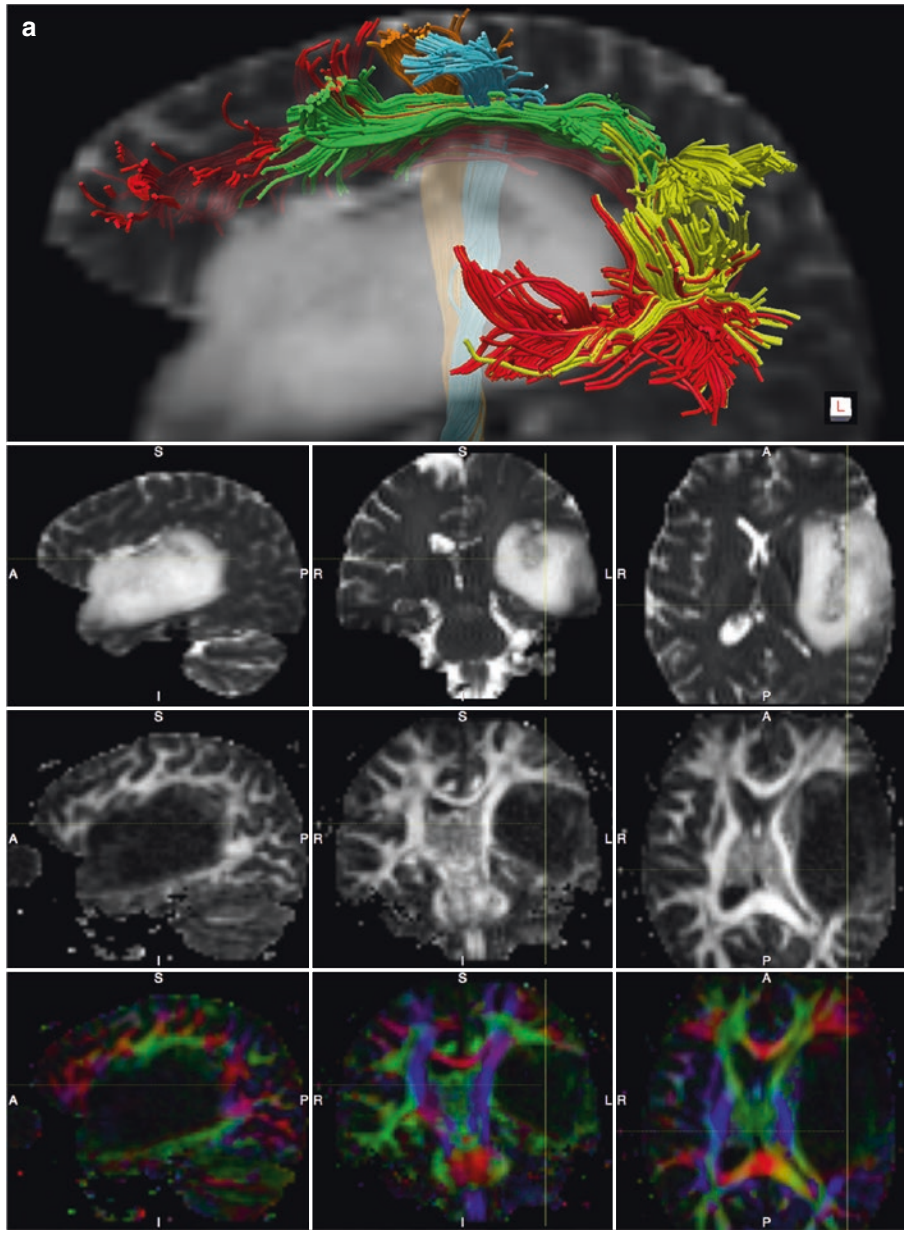

Fig. 7 (**a**) Thirty-six years-old male with astrocytoma WHO-II. The three segments of the left AF (direct segment in red, posterior segment in yellow, and SLF-III in green) and two components of the CST projecting respectively to M1 (yellow) and S1 (cyan) in the area of the face/mouth are displayed over a sagittal T2-weighted MRI (upper row). Note in sagittal, coronal, and axial T2-weighted MRI (second row), FA maps (third row) and DEC maps (bottom row) that the large mass is infiltrating the left insula and the whole temporal lobe and it is displacing the CST medially and the AF dorsally. Presurgical tractography was useful to show that eloquent fascicles (AF and CST) were outside of the mass, thus a complete resection could be attempted after detection of the functional limits with IES mapping. Diffusion data were acquired with HARDI (64 gradient directions, $b = 2000$, $2 \times 2 \times 2$ mm^3) and tractography was performed with spherical deconvolution algorithm. (**b**) Tractograms of the CST and AF are displayed over a coronal T2-weighted MRI (left panel). The severe mass effect paradoxically enhanced detection of the CST fibers projecting to the face/mouth area. This contingent of fibers is usually poorly visualized with normal anatomy due to crossing fibers, even with spherical deconvolution algorithm. Lateral view of the tractograms from below showing CST streamlines crossing the AF (right panel)

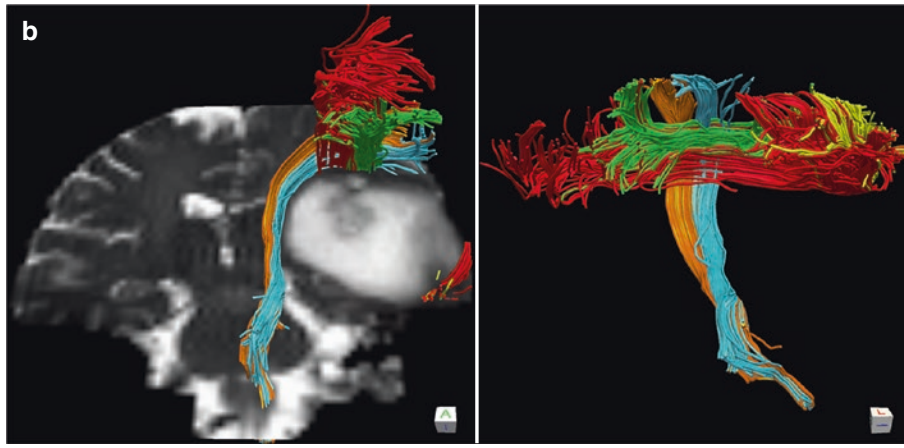

Fig. 7 (continued)

IES is the only method that is reliable in testing WM function and to detecting presence of functional bundles inside a tumor.

A WM tract is considered *interrupted* when the FA value drops below the FA threshold used for tractography and its trajectories are lost in the area of the tumor. From a biophysical perspective, this scenario occurs when diffusion becomes isotropic inside the tumor or the main orientation of anisotropy is not coherent anymore with the native orientation of the tract of interest. A threshold of FA > 0.2 is usually recommended for tractography in healthy tissue; however, it has been shown that lowering the threshold to FA > 0.1 can help to identify residual trajectories inside a tumor (Bello et al. 2008) with the trade-off of raising the chance of false positive results. From a neuro-oncological perspective, interruption of a tract may be due to three conditions: tissue destruction, heavy glioma cell infiltration, or vasogenic edema. In the first condition tractography would provide a true negative result, in the second a result that requires validation with IES or histopathological examination of the surgical specimen, while in the case of vasogenic edema would provide a false negative result. It has been shown that vasogenic edema may be associated with false negative results that should not be confused with bundle destruction (Bizzi et al. 2012; Ducreux et al. 2006). We have already mentioned that the use of advanced diffusion imaging methods that use multicompartmental models such as NODDI (Zhang et al. 2012) has potential to better address this critical issue.

The appearance of a ring of increased anisotropy at the periphery of the mass is another controversial condition that has been described in brain tumors. The cause for high FA values at the interface between the mass and the surrounding brain tissue is not well understood. Few studies have investigated tensor shape indices in the periphery of focal lesions. Significantly higher CL values have been reported near the enhancing ring of GBM rather than of metastasis (Wang et al. 2009). The authors of another study suggested that CL and CP can distinguish true from pseudo WM trajectories inside an abscess cavity (Kumar et al. 2008). CL and CP mean values measured within the abscess cavity were significantly different compared with those of WM tracts; however, FA, MD, and CS values overlapped. High CP with low CL inside an abscess cavity indicates that the shape of the diffusion tensor is predominantly planar, whereas it is linear in WM tracts. These geometrical DTI indices may be used for differentiating true from pseudo WM tracts inside the abscess cavity and in general at the periphery of a tumor. The finding of high FA and CP inside a tumor should be considered non-specific, while high FA and CL may indicate the possibility of residual WM tracts within a glioma. Elevated FA and CL at the periphery of a mass should suggest the proximity

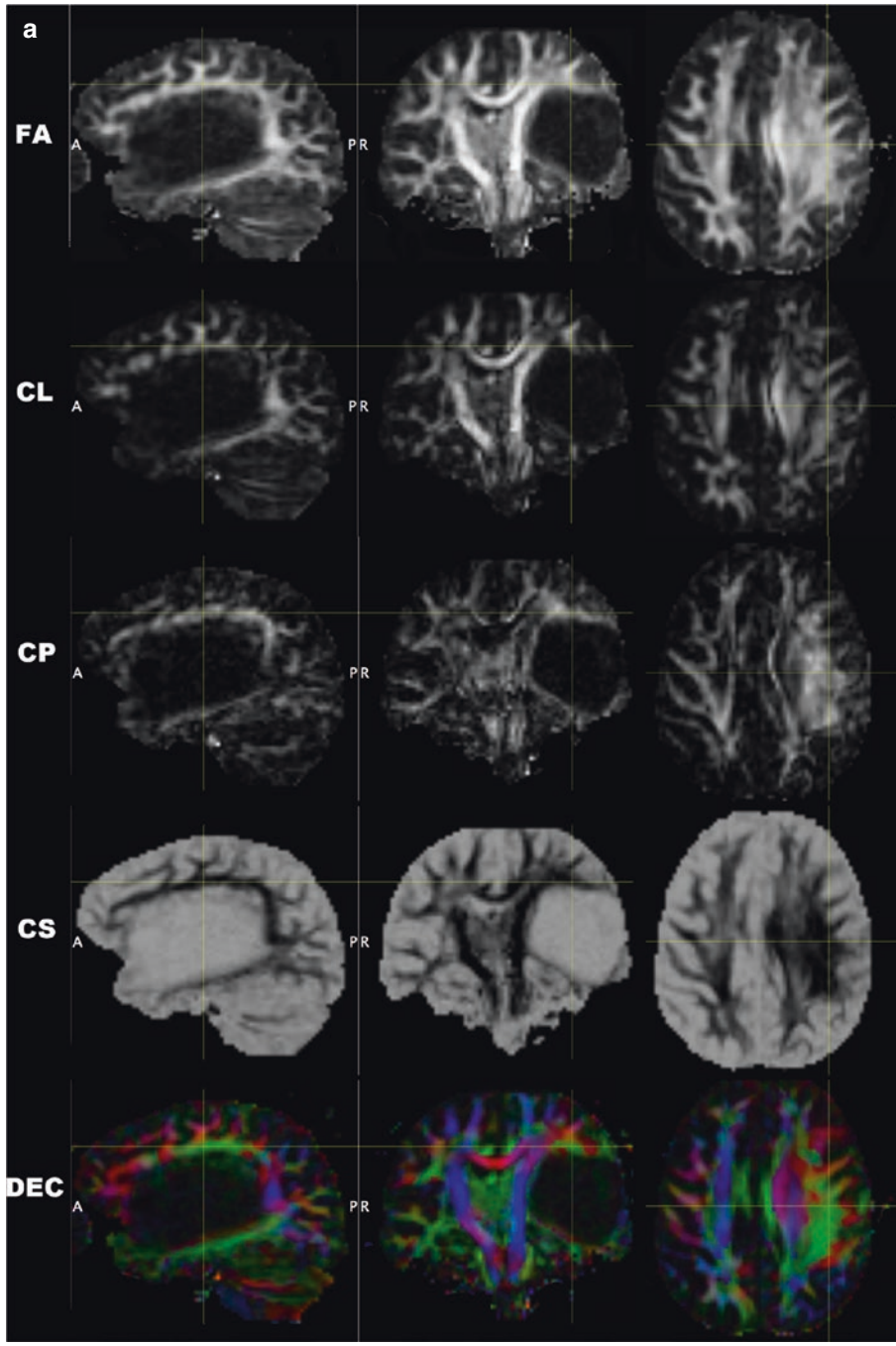

Fig. 8 (**a**) Parametric maps available from DTI dataset of the same case illustrated in Fig. 7: fractional anisotropy (FA), linear, planar, and spherical anisotropy shape coefficients (CL, CP, CS) and direction encoded color (DEC) maps. A large mass such as this astrocytoma may disrupt the architecture of the WM around it. When CL is high (bright) there is usually one dominant tract such as the CST in the medial boundary of the lesion in this case. When CP is high there may be two crossing fibers such as the AF and the CST in the dorsal boundary. CL and CP maps are often more informative than FA alone. (**b**) Parametric maps available from NODDI dataset of the same case illustrated in Fig. 7: neurite density (ND) and orientation dispersion index (odi). The very low ND value within the mass is suggesting that unlikely there should be residual fibers within the tumor; odi is elevated within the mass showing a paucity of oriented sticks (fascicles)

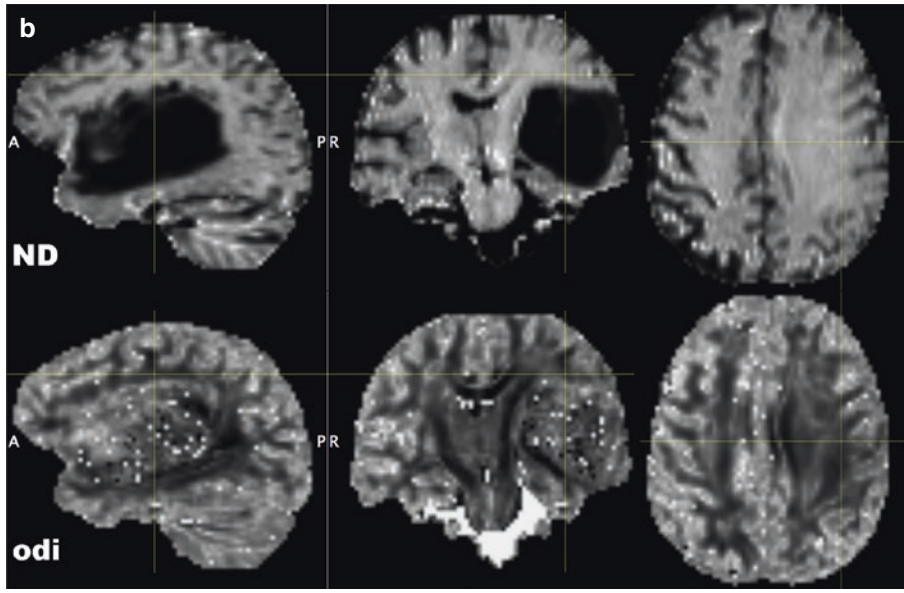

Fig. 8 (continued)

of a compacted WM tract that can be identified with the aid of DEC maps (Fig. 8a). Finding of elevated CP around the periphery of a mass, especially if associated with elevated MD, should raise suspicion for pseudo WM tracts. In this last scenario elevated planar diffusivity might be an epiphenomenon of mass effect at the interface between the tumor and the brain tissue, especially when there is accumulation of water in the ECS (i.e., vasogenic edema). NODDI measures innovative parameters such as neurite density and orientation dispersion index that may also help to characterize tumor infiltration and vasogenic edema within and around a mass (Fig. 8b).

5.2 Mapping Strategies with MR Tractography

The main aims of mapping WM structures in neuro-oncology are (1) presurgical planning; (2) intraoperative guidance during direct subcortical IES and tumor resection; (3) postoperative evaluation after tumor resection.

The advantage of using tractography for presurgical mapping is to show in 3D-space the relationship of the trajectory of the fascicles of interest with a focal lesion and other anatomical landmarks. The neurosurgeon will select the best route to reach the lesion without damaging eloquent tracts, and will choose which tract to test with IES in the operating room. Among neurosurgeons there is consensus that the CST, AF, IFOF, UF, and OR are the most clinically relevant fascicles for presurgical mapping.

The general principle of tractography is to use the orientation information provided by the tensor, the fODF, or the dODF. The most commonly used directional assignment corresponds to the major eigenvector of the diffusion tensor. Starting from one or more "seed" ROI and propagating the trajectories according to the tractography algorithm until the tracts are terminated generates a streamlined tractogram. Specific geometrical and anatomical constraints are used to extract the trajectories that meet specific connection criteria. Geometrical constraints (FA threshold) are used to terminate tracking in voxels with very low FA and undetermined fiber orientation or to avoid unrealistic trajectories with very sharp turns (angle threshold). Rules based on Boolean logic (i.e., true or false) can be applied to select ("IN") or exclude ("OUT") specific streamlines or pathways.

It is tradition since the early days of deterministic tractography to filter out spurious streamlines that are known to represent artifacts from a priori knowledge. Spurious tracts represent false positive streamlines that are mainly due to errors to estimate tract orientation with diffusion imaging in the presence of crossing, bending, and fanning fibers. The number of spurious tracts is variable, it changes with WM fascicles and it depends on the quality and spatial resolution of the HARDI dataset. The number of spurious tracts is usually small in the proximity of a LGG, whereas it may increase significantly in the hemisphere ipsilateral to a HGG, especially when the mass is aggressively growing and disarranges WM architecture.

It is important to use a precise and correct terminology when describing imaging findings in a radiology report. Diffusion MR tractography provides anatomical (structural) information that has no functional content. *Fasciculus* and *bundle* are anatomic terms: a multitude of axons or fibers form bundles of different diameters; several bundles form a fasciculus. The words *streamline* and *trajectory* should be used when describing results in MR tractography studies. The words *pathway* and *stream* are used mainly in functional imaging studies depicting information flow.

5.3 Motor System

5.3.1 Corticospinal Tract

The CST is the most eloquent of all WM structures and damage to the CST leads to permanent motor and speech deficits. Mapping of the CST is requested when a lesion is located in the paracentral region, SMA, PMd, PMv, and in the proximity of its course at the level of the thalamus, basal nuclei, or brainstem. The CST carries axons organized in bundles projecting from the M1 (49%), post-central and PPC (21%), SMA-proper (19%), PMd (7%), PMv (4%). IES of the CST is best performed with the high-frequency monopolar probe rather than with the low-frequency 60 Hz bipolar probe (Bello et al. 2014). It is mandatory to identify all components of the CST in order to avoid postoperative motor deficits (Fig. 9). The typical course of the CST and the somatotopic organization of its fascicles is important to know in order to predict potential deficits during removal of a lesion. In M1 the tongue and face areas are located ventrally and laterally to the hand area, the leg and foot are located dorsally and medially in the paracentral lobule. After leaving the cortex the CST curves slightly backwards, then it bends forward before entering the posterior limb of the internal capsule. Along this way the somatotopic fibers twist about 90° counter-clockwise so that the tongue and face bundles descend anteriorly and the foot and leg bundles posteriorly. At the level of the internal capsule the hand bundles occupy the mid portion of the CST.

Tracking of the CST should be performed with a two ROIs approach using streamline or probabilistic tractography. Delineation of the seed ROI is usually performed on b_0 (i.e., T2WI) or FA maps in multiple axial slices in the precentral and post-central gyri, posterior third of the SFG (i.e., SMA) and MFG (i.e., PMd and PMv). The ROI should include the subcortical WM since fiber tracking does not reach the cortical layers. The ROI in M1 should extend from the mouth to the foot area. Delineation of the target ROI should be done at the level of the pons in the ipsilateral tractus pyramidalis (blue on DEC maps) that is anterior to the pontocerebellar fibers (red on DEC maps) and lemniscus medialis (blue on DEC maps). Some authors prefer to delineate the target ROI in the ipsilateral cerebral peduncle of the midbrain or in the posterior limb of the internal capsule. After connecting the two ROIs the tractogram should be inspected for a priori anatomic consistency.

Spurious streamlines should be removed with "out-ROI" filters with the aim to show the backbone of a "clean tractogram." Spurious tracts to the contralateral CST are frequently found along the trajectories of the CC and of the pontocerebellar peduncles. Spurious tracts are due to artifacts of fiber tracking in voxels with crossing

fibers. The number of spurious tracts is variable and depends on the quality and spatial resolution of the HARDI dataset, however some spurious tracts should always be expected in the above regions. Out-ROIs are usually needed in the mid-sagittal plane and in the middle cerebellar peduncles.

Tracking the backbone of the CST from the hand knob area (omega sign) in M1 to the pons is relatively easy. Unfortunately streamline DTI tractography usually fails to reconstruct streamlines originating in the tongue, face, leg, and foot areas due to the presence of crossing fibers with the CC and the SLF at the level of the centrum semiovale (Mandelli et al. 2014). Implementation of HARDI acquisition scheme with more advanced algorithms such as SD (Dell'Acqua et al. 2013), multi-tensor (Yamada et al. 2007),

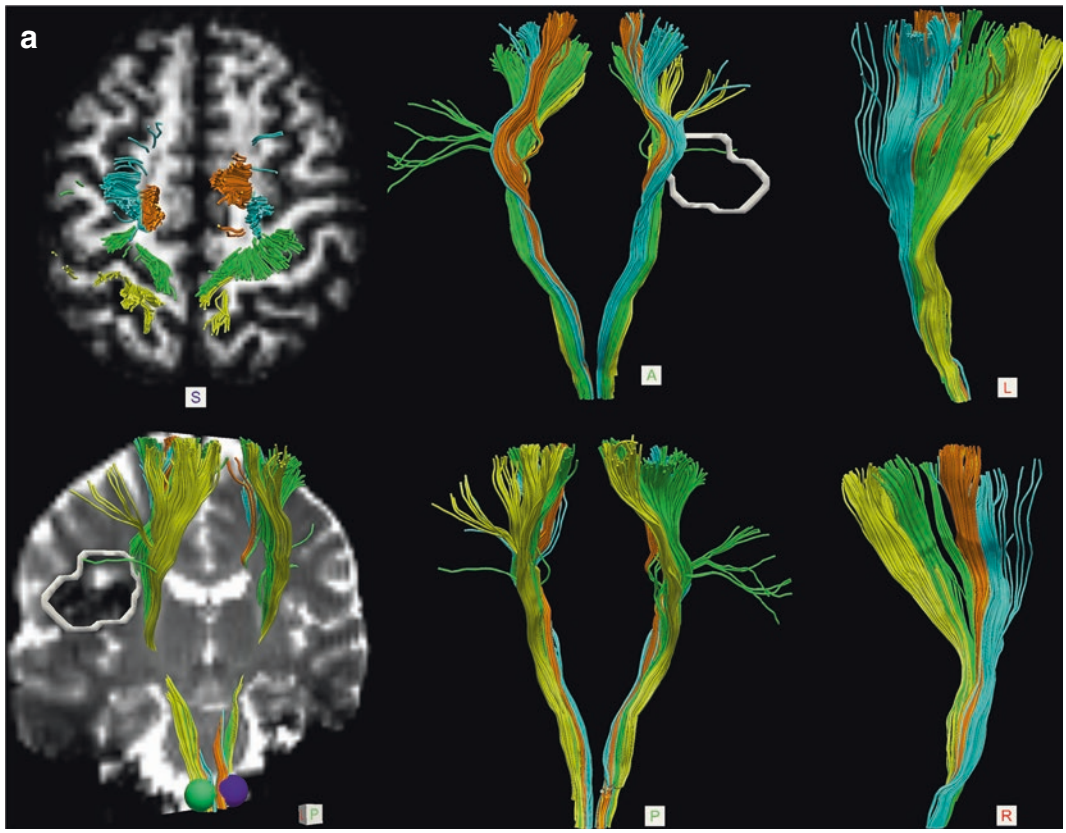

Fig. 9 (**a**) Thirty-one years-old male with cavernous angioma (white circle) seated in the deep WM below the left SMG. The medial margin of the focal lesion is abutting the left CST. Diffusion data were acquired with HARDI (64 gradient directions, $b = 2000$, $2 \times 2 \times 2$ mm^3) and tractography was performed with spherical deconvolution algorithm. Tractography of the CST components originating from M1 (green), SMA (orange), PM dorsal (cyan), and S1 (yellow). The components of both corticospinal tracts (CST) are displayed over axial FA map at the level of the central sulcus (upper row, left panel) and coronal T2-weighted MRI (lower row, left panel); anterior and posterior views of both CST in the middle panels; lateral and medial view of the left CST on the right panels. (**b**) Tractography showing that the components of the left CST projecting to M1 (green) and S1 (yellow) are adjacent to the medial margin of the cavernous angioma. Intraoperative view (left upper corner) showing direct subcortical electrostimulation of the floor of the surgical cavity with the monopolar probe: a current of 8 mA evoked MEP responses of the right hand and leg confirming that the CST was very close to the angioma

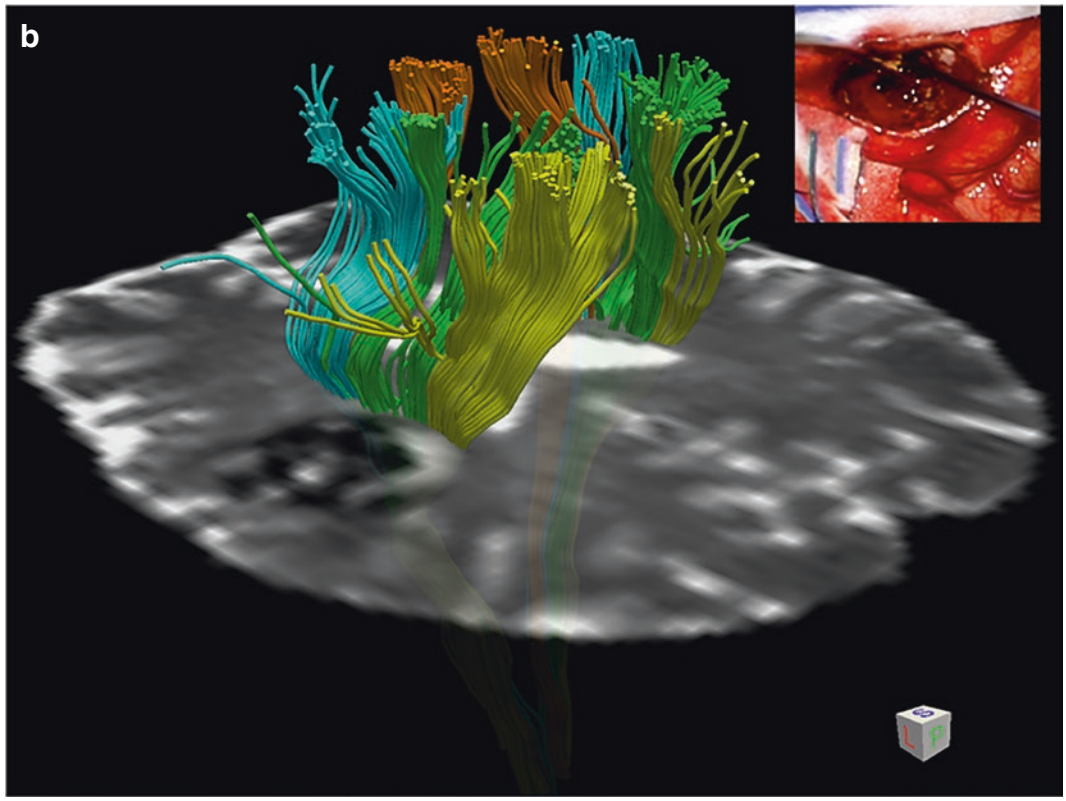

Fig. 9 (continued)

Q-ball, and probabilistic tractography (Bucci et al. 2013) allows depiction of additional trajectories that are originating from the face, tongue, and foot regions of M1.

5.3.2 SMA Connectivity

The SMA is at the center of a rich network of WM connections with motor, language and limbic structures. The connectivity of the SMA is of particular interest for brain tumor surgery since it is one of the favorite areas infiltrated by LGG (Duffau and Capelle 2004). The "SMA syndrome" characterized by transient contralateral akinesia and mutism with a usually complete recovery in 6–12 months can follow surgery in this area. Immediate severe postoperative deficits can be quite stressful for the patient. Knowledge of the connections of the SMA can provide new insights on the genesis of the SMA syndrome; assessment of the extension of infiltrating tumors can assist the neurosurgeon in predicting the postoperative course of patients.

The SMA is located in the medial posterior third of the SFG and it is functionally and connectively divided into two parts by a virtual line arising from the AC and perpendicular to the AC-PC line. The SMA-proper and pre-SMA play a different role with regard to motor function. The SMA-proper is more directly related to the execution of movement, while the pre-SMA is involved in planning and preparation of higher motor control. Differences in connectivity of the two regions provide an anatomical basis for explaining these functional aspects. The SMA-proper is a component of the CST network and it sends fibers through the corona radiata and the

internal capsule to the spinal cord, while the pre-SMA has no direct connection with the cord. The SMA-proper is thought to play a role in the direct execution of movement due to this corticospinal projection. Neuroradiologists should pay particular attention to track also streamlines projecting from the SMA-proper to the spine when mapping the CST.

In a post-mortem dissection and tractography study Vergani et al. identified five main types of connections: (1) short U-fibers in the depth of the precentral sulcus, directly connecting the SMA-proper with M1, especially at the level of the hand region; (2) U-fibers connecting SMA with the cingulate gyrus; (3) an intralobar frontal tract connecting the SMA with pars opercularis BA44 and BA6 (this fascicles has been named by Catani the "frontal aslant tract" (Catani et al. 2012)); (4) fibers connecting the SMA with the striatum; (5) SMA callosal fibers connecting homologous areas (Vergani et al. 2014). Both the SMA-proper and the pre-SMA have direct connections with the head and body of the caudate nucleus. The presence of striatal connections has been demonstrated in a DTI study by Lehericy et al. (2004). This cortico-striatal connection is part of a wider network that reverberates back to the cortex through the thalamus. It is believed that this cortico-basal nuclei-thalamo-cortical network may be implicated in different aspects of motor control, including initiation, sequencing, and modulation of voluntary movements. A predominance of striatal fibers on the left side in right-handed individuals provides evidence for this pathway to play an important role in language.

5.4 Language System

Mapping of the language system is requested when a lesion is located in the perisylvian region of the dominant hemisphere: insula, dorsal aspect of the frontal, temporal, and parietal lobes and in the adjacent WM pathways. Modern theories about language have recognized that there is a lot of network redundancy in the system. The implications of a dual-stream system with dorsal and ventral networks cannot be overemphasized. The AF is the main component of the dorsal network that is considered critical in syntactic analysis and modulation of acoustic speech signal to the articulatory loop located in the ventrolateral part of the frontal lobe. The IFOF, UF, and inferior longitudinal fasciculus (ILF) are the main fascicles of a ventral perisylvian network that is considered critical for lexical and semantic processing occurring in the anterior temporal lobe. The ventral network is involved in processing sound into meaning and comprehension. However, there are other aspects of language that may rely on a more extended language network with additional fascicles like the middle longitudinal fasciculus (MLF) connecting the STG with the IPL, the frontal aslant tract (FAT), and the subcallosal fascicle connecting language sites with the SMA.

5.4.1 The Dorsal Pathway: Arcuate Fasciculus

The AF is an essential component of the language system connecting regions devoted to formal aspects of language in temporal-parietal areas with regions involved in intentional and social communication in prefrontal areas (Catani and Bambini 2014). According to Catani the AF has three main cortical projections in the ventrolateral prefrontal (Broca), IPL (Geschwind), and posterior third of the temporal (Wernicke) lobe (Catani et al. 2005): (1) a direct (long segment) pathway connecting Broca with Wernicke territories, (2) an anterior segment connecting Broca with the IPL; (3) a posterior segment connecting Geschwind territory with the posterior third of the MTG. The three nodes are used in tractography as seed points to track the trajectories of the three segments that form the AF. Macroscopically the direct segment has two arms that converge in a stem (isthmus) that is located in the deep WM of the posterior temporal lobe. The fronto-parietal arm courses lateral to the corona radiata in the centrum semiovale, then it bends ventrally; the temporal arm of the AF courses along a cranio-

caudal axis lateral to other long-range fascicles that are coursing in the deep WM underneath the AG and STG: they are the MLF, IFOF, and OR. The fronto-parietal and temporal arms of the AF-direct converge to form a stem (blue on DEC maps) that is an important landmark for tractography. The anterior and posterior AF segments are lateral to the direct segment; on DEC maps the streamlines of the anterior segment are green, those of the posterior segment are predominantly blue and green.

Tracking of the three segments of the AF should be performed with a two ROIs approach using streamline or probabilistic tractography with delineation of three seed ROIs on sagittal slices in the posterior IFG including BA6 and PMd (Broca territory), posterior third of MTG (Wernicke territory), and IPL (BA39/40, Geschwind territory). DEC and FA maps are quite useful in delineating seed and target ROIs. The ROI in the IPL and in the posterior IFG should include only a small layer of subcortical WM, while ROI delineation in the MTG should include the deep WM and in particular the AF stem.

The three tractograms should be inspected for a priori anatomical consistency after connecting each pair of ROIs. Spurious streamlines should be removed with "out-ROI" filters with the aim to illustrate the backbone of a "clean tractogram." Spurious tracts are often found overlapping with the trajectories of the CC and IFOF, due to fiber-tracking artifacts in voxels with crossing fibers. A statistical significant leftward asymmetry has been reported for the volume and number of streamlines of the direct segment of the AF. Furthermore, left lateralization has been shown in males, while a bilateral distribution has been shown in females. Individuals with more symmetric distribution performed better at remembering words using semantic association. These findings suggest that the degree of lateralization of the long segment of the AF is heterogeneous in the normal population and, paradoxically bilateral representation, not extreme lateralization might ultimately be advantageous for specific cognitive functions (Catani et al. 2007). In addition, it was shown in a longitudinal DTI study that the volume of the direct segment of the AF in the right hemisphere is an important predictive factor for recovery of language after stroke in the left dominant hemisphere (Forkel et al. 2014a).

In the past the terms AF and SLF have been used as synonyms, but we agree with Catani that the equivalence of terms is anatomically incorrect despite some overlap between the fascicles. The term SLF should refer to a group of three longitudinal tracts connecting the dorsolateral cortex of the frontal and parietal lobes. The third segment of the SLF (SLF-III) overlaps with the anterior segment of the AF, while SLF-I and SLF-II are not components of the language network. The posterior segment of the AF runs along the cranio-caudal axis and it connects the AG with the posterior third of the MTG. It should not be confused with the MLF that runs longitudinally along the anterior-posterior axis of the SFG.

5.4.2 The Ventral Pathway: IFOF, UF, and ILF

The *IFOF* is a long association fascicle connecting the frontal with the temporal, parietal, and occipital lobes (Catani et al. 2002). The IFOF carries visual information from occipital areas to the temporal lobe and it is likely to play an important role in visual object recognition, and in linking object representation to their lexical labels (Catani and Mesulam 2008). Macroscopically the IFOF has two arms that converge in the temporal stem: the frontal arm projects to the IFG, MFG, dorsolateral prefrontal cortex, orbitofrontal cortex, and frontal pole; the temporo-parieto-occipital arm provides short-range bundles to the anterior temporal and insular cortex, long-range bundles to the posterior STG and MTG, and to the parietal and occipital cortex. Anatomically the IFOF can be subdivided into three segments: frontal, intermediate temporal, and parieto-occipital. Anatomic dissection of 14 post-mortem

human cerebral hemispheres using the Klingler method has identified two components of the IFOF: a dorsal component connecting the frontal areas with the superior parietal lobule and posterior portion of the superior and middle occipital gyri and a ventral component connecting the frontal areas with the ventral part of the temporal lobe (fusiform gyrus, temporo-occipital sulcus, and inferior temporal gyrus) and with the inferior occipital gyrus (Martino et al. 2011). IFOF terminations have been demonstrated with post-mortem dissections within the SPL, superior, middle, and inferior occipital gyri (Martino et al. 2010). The ventral fibers of the IFOF partially overlap with the OR projecting into the superior and inferior banks of the calcarine sulcus. Caversazi et al. used Q-ball residual-bootstrap to reconstruct the IFOF using one single ROI delineated in the extreme capsule and thresholds of FA > 0.15 and <60° angle (Caverzasi et al. 2014). The authors were able to duplicate the above reported post-mortem findings. In comparison with classic DTI-based tractograms more extended projections of the anterior arm of the IFOF were found with Q-ball imaging in the lateral and medial orbitofrontal gyri, pars orbitalis and triangularis, rostral portion of the MFG, and even in the SFG. More extended projections of the posterior arm of the IFOF were found to project to the lingula, pericalcarine and lateral occipital cortices, cuneus, and caudal portion of the fusiform gyrus. Trajectories of the dorsal component were found to project to the AG and SPL. The anatomy of the IFOF projections to the occipital lobe was consistent among the 20 healthy subjects with greater than 75% overlap along its entire course.

At the level of the temporal stem the IFOF occupies the posterior and dorsal two-thirds of the stem and the streamlines can easily be distinguished from those of the UF coursing in the anteroventral and lateral part of the stem. As the IFOF exits the temporal stem it runs in the ventral part of both the external and extreme capsules, encasing the inferior part of the claustrum (Ebeling and von Cramon 1992). The extreme capsule should not be considered a tract but a gross anatomy-defined WM structure. The intermediate segment of the IFOF runs in the roof of the temporal horn, superior and lateral to the OR. Within the posterior temporal region the IFOF trajectories run lateral to the tapetum and medial to the MLF, AF-direct, and posterior segment of the AF.

In the macaque monkey the IFOF is less developed than in humans, as monkeys lack the MTG and their IFOF connects primarily to posterior occipital areas (Forkel et al. 2014b; Schmahmann et al. 2007; Thiebaut de Schotten et al. 2012). In the monkeys the IFOF overlaps to some extent with the extreme capsule and this explains why it has been reported with that name in the literature (Petrides and Pandya 1988; Schmahmann and Pandya 2006). Other authors have adopted the monkey anatomic terminology also for human studies and refer to the extreme capsule as the direct connection between the prefrontal areas and the MTG (Saur et al. 2008, 2010).

Tracking of the IFOF is performed with a two ROIs approach using streamline or probabilistic tractography with delineation of the seed ROI in the temporal stem (green on DEC maps) and the target ROI in the deep WM of the occipital lobe at the level of the calcarine fissure. The seed ROI is delineated in multiple axial slices, whereas the target ROI in one coronal slice is perpendicular to the IFOF trajectories. The tractogram should be inspected for a priori anatomical consistency after connecting the two ROIs. In the human brain the IFOF is an easy tract to reconstruct with tractography because it runs longitudinally in the anterior-posterior direction and it is the dominant tract along most of its course. Spurious streamlines should be removed with "out-ROI" filters. Brain tumors expanding in the temporal or parietal lobe are likely to dislocate its trajectories or even to disrupt its course by increasing the number of spurious streamlines. A statistical significant rightward asymmetry has been reported for

the volume and number of streamlines of the IFOF (Thiebaut de Schotten et al. 2011b).

The role of the IFOF in semantic processing is supported by IES mapping studies showing with high reproducibility that stimulation of the fascicle throughout its course from the frontal to the occipital lobe evokes semantic paraphasias (Duffau et al. 2008a). The anterior (frontal) arm of the IFOF should be detected with IES and represents the functional boundary in glioma infiltrating the pars opercularis of the IFG, the PMv or PMd areas of the dominant hemisphere. The intermediate and temporo-occipital segments of the IFOF represent the functional boundary in gliomas infiltrating the insula and the deep temporal lobe.

The *UF* is a hook-shaped bundle connecting the frontal lobe with the anterior temporal lobe. Macroscopically the UF has two arms that converge in the temporal stem: the frontal (dorsal) and the temporal (ventral) arms. From the stem the UF fans out into the frontal and temporal lobes. At the level of the temporal stem and in the proximity of the anteroventral portion of the extreme and external capsules the UF and IFOF look like very compacted bundles with the UF located ventral and anterior to the IFOF. In the frontal lobe the UF bundles project to the lateral and medial orbitofrontal cortex; in the temporal lobe the bundles project to the pole, amygdala, anterior part of the hippocampus, anterior third of STG and MTG (Martino et al. 2011).

The UF is part of the limbic system and it is likely involved in emotion and memory. It also plays a role in lexical retrieval, semantic associations, and specific aspects of naming. In a series of 44 patients who underwent awake surgery for removal of a left frontal or temporal glioma, removal of the UF in 18 patients resulted in long-term deficit of famous face naming, but not of picture naming of objects (Papagno et al. 2010, 2016). Patients were able to retrieve biographical information about people they could not name. Proper name impairment is a post-semantic deficit that requires damage of a functional network that has several nodes connected by the UF: the orbitofrontal cortex involved in face-encoding, the ventromedial prefrontal cortex involved in the processing of emotions and the temporal pole involved in naming famous faces (Gorno-Tempini et al. 1998).

Tracking of the UF is performed with a two ROIs approach using streamline or probabilistic tractography with delineation of the seed ROI in the temporal stem and the target ROI in the anterior WM of the temporal lobe at the level of the anterior commissure. The seed ROI is delineated in multiple axial slices, whereas the target ROI in one coronal slice is perpendicular to the UF trajectories. The tractogram should be inspected for a priori anatomical consistency after connecting the two ROIs. The UF is an easy tract to reconstruct with tractography despite its bending and fanning trajectory because it does not cross other compact tracts. Spurious streamlines are scarce and they can be removed with "out-ROI" filters. The UF is symmetrical fascicles without significant differences in tract volume between the two hemispheres.

The *ILF* is a ventral associative bundle with long- and short-range fibers connecting the temporal and occipital lobes. The long bundles course medially to the short fibers and connect visual areas to the temporal pole, amygdala, and hippocampus. The ILF trajectories are coursing ventrally and laterally to the IFOF in the deep WM of the temporal and occipital lobes. The streamlines are green on DEC maps, but without tractography they are difficult to distinguish from the other fascicles running in the temporo-parietal fiber intersection area (TPFIA). Short-range fibers of the ILF connect the fusiform gyrus with the posterior part of the inferior occipital gyrus. Long-range fibers run medially to short-range fibers from the anterior temporal lobe to the ventrolateral occipital cortex; they course horizontally along the ventrolateral wall of the temporal and occipital horns with a posterior and lateral orientation. The ILF runs ventrally and laterally to the IFOF and OR for most of its course; the

ILF partially overlaps and crosses the IFOF and OR at the level of the TPFIA.

Tracking of the ILF is performed with a two ROIs approach using streamline or probabilistic tractography with delineation of the seed ROI in the occipital WM and the target ROI in the anterior WM of the temporal lobe at the level of the anterior commissure. Both ROIs are delineated in one coronal slice perpendicular to the ILF trajectories. The tractogram should be inspected for a priori anatomical consistency after connecting the two ROIs. Spurious streamlines can be removed with "out-ROI" filters. The ILF are symmetric fascicles without significant differences in tract volume between the two hemispheres.

The ILF is involved in face and visual object recognition, reading, visual memory, and in linking object representations to their lexical labels (Catani and Mesulam 2008). IES of the ILF systematically impaired reading ability at the level of the posterior surgical area. The ILF is involved in both the direct and indirect transfer of information between extrastriatal visual and anterior temporal areas involved in memory and limbic functions (Mandonnet et al. 2009). Moreover, it has been suggested that the ILF together with the UF provides an indirect pathway between the occipital and frontal language areas supporting semantic and lexical processing. The ILF, MLF, and UF are components of anterior temporal networks involved in selecting verbal labels for objects in a posterior-anterior progression of word comprehension, from generic to specific levels of precision. Overall the anterior temporal network enables mapping sound to meaning (Hickok and Poeppel 2007; Catani and Bambini 2014).

5.4.3 Frontal Aslant Tract and Subcallosal Fasciculus

The FAT is a recently described bilateral frontal intralobar fascicle connecting the anterior part of SMA-proper and the pre-SMA with the pars opercularis (BA44) of the IFG. Some fiber projections reach also the adjacent BA6. The FAT is the only intralobar tract connecting two non-adjacent gyri in the frontal lobe and it has been named "aslant" because of its peculiar oblique orientation in the coronal plane. It has been dissected with streamline tractography using the FACT algorithm (Oishi et al. 2008; Lawes et al. 2008) and with probabilistic tractography (Ford et al. 2010), however it is best visualized with the SD algorithm (Catani et al. 2012). It is one of few (previously unknown) tracts that have been first described with MR tractography (Oishi et al. 2008), then validated with post-mortem dissection studies (Lawes et al. 2008).

A significant leftward asymmetry in track volume in right-handed healthy subjects has been reported (Catani et al. 2012), suggesting a role in language connections. In one of our patients with oligoastrocytoma WHO-II seated in the lobar WM of the left frontal lobe we confirmed the relationship of this tract with language deficits. The presurgical MR tractography study showed that the FAT was adjacent to the medial and ventral margins of the mass, the CST was adjacent to the posterior margin, while the AF was relatively remote from it (Fig. 10). The mass was resected and the patient experienced severe mutism after surgery. Speech initiation deficits lasted longer than expected for a SMA syndrome and approximately 12 months after surgery the patient continued to have delayed reaction time to initiate speech. The postoperative MR tractography study confirmed preservation of the AF and SMA and suggested that the focal neurological deficit was associated with resection of the FAT. The authors of another MR tractography study in 35 patients with primary progressive aphasia showed that fractional anisotropy values of the FAT correlated with deficits in verbal fluency and suggested that this fascicle was part of the speech network (Catani et al. 2013).

Tracking of the FAT is performed with a two ROIs approach using streamline or probabilistic tractography with delineation of the seed ROIs in pars opercularis (BA44) and of the target ROI in

the pre-SMA and anterior SMA-proper in multiple axial slices. Placement of spherical ROIs with Trackvis software (http://trackvis.org/) is handily used to explore the frontal region for intralobar streamlines before dissecting the frontal tracts.

The SCF was first described in 1887 by Theodor Meynert who used the term "corona radiata of the caudate nucleus" (Meynert 1887) and later in 1893 by Muratoff (Forkel et al. 2014b). The *SCF* has been described in humans and monkeys. In the monkey Yakovlev and Locke described the SCF as a projection tract connecting the cingulum to the caudate nucleus (Yakovlev and Locke 1961). Moreover, the fronto-striatal fibers also have strong reciprocal connections with BA24 of the cingulate gyrus and the pre-SMA. For this reason the SCF is also named the fronto-striatal tract (FST). In a study of stroke patients using computerized tomography more severe limitation in spontaneous speech was associated with lesions in the most rostral and medial portion of the FST plus the periventricular WM near the body of the lateral

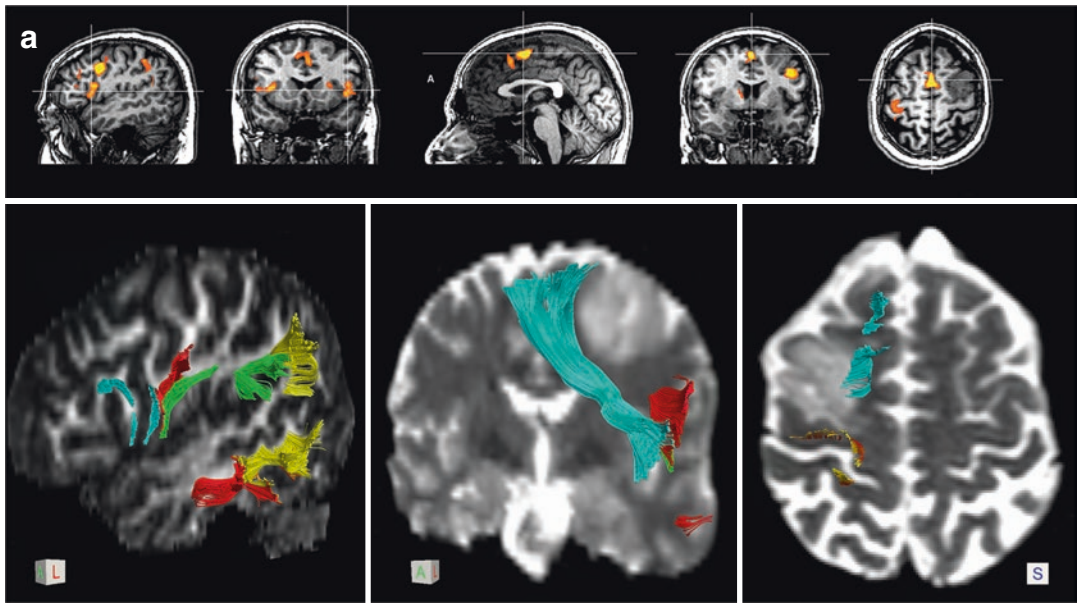

Fig. 10 (**a**) Twenty-nine years-old male with a mass infiltrating the lobar WM and the left MFG. Functional MRI with the verb generation task (upper row, from left to right) is showing BOLD response in left pars opercularis and PMv (sagittal and coronal images), in the pre-SMA and SMA-proper (sagittal image), SMA-proper and PMd (coronal image) and SMA-proper (axial image). Activation areas can be used to assist delineation of ROI for tractography in selected cases. In the left panel of the lower row the projections of the FAT (cyan) in pars opercularis and PMv, projections of the AF-direct (red) in PMv and posterior MTG, projections of the SLF-III (green) in PMv and SMG, projections of the posterior segment of the AF (yellow) in AG and MTG are overlaid on a sagittal FA map. The FAT is the medial and ventral limit of resection of the mass as illustrated in the coronal T2WI (mid panel). The relationship of the mass with the FAT and CST (red-orange scalar) that are, respectively, the medial and posterior margin of the mass is illustrated in the axial T2WI (right panel). (**b**) A left lateral oblique view of the main tracts evaluated in this case is displayed over sagittal and axial FA map. Note how big the FAT is in this case, probably enhanced by interruption of the crossing SLF due to presence of the tumor. Intraoperative monitoring with subcortical IES was not performed in this case and the patient immediately after surgery presented with severe mutism that lasted for a few weeks. Speech initiation deficits lasted longer than expected for a SMA syndrome and approximately 12 months after surgery the patient continued to have delayed reaction time to initiate speech. An oligoastrocitoma WHO-II was removed at surgery. The postoperative tractography study (not shown) confirmed that the severe SMA syndrome was associated with resection of the FAT despite preservation of the AF and SMA. Diffusion data were acquired with HARDI (64 gradient directions, $b = 1000$, $2 \times 2 \times 2$ mm^3) and tractography was performed with DTI interpolated streamline algorithm (thresholds FA > 0.15; angle <45°)

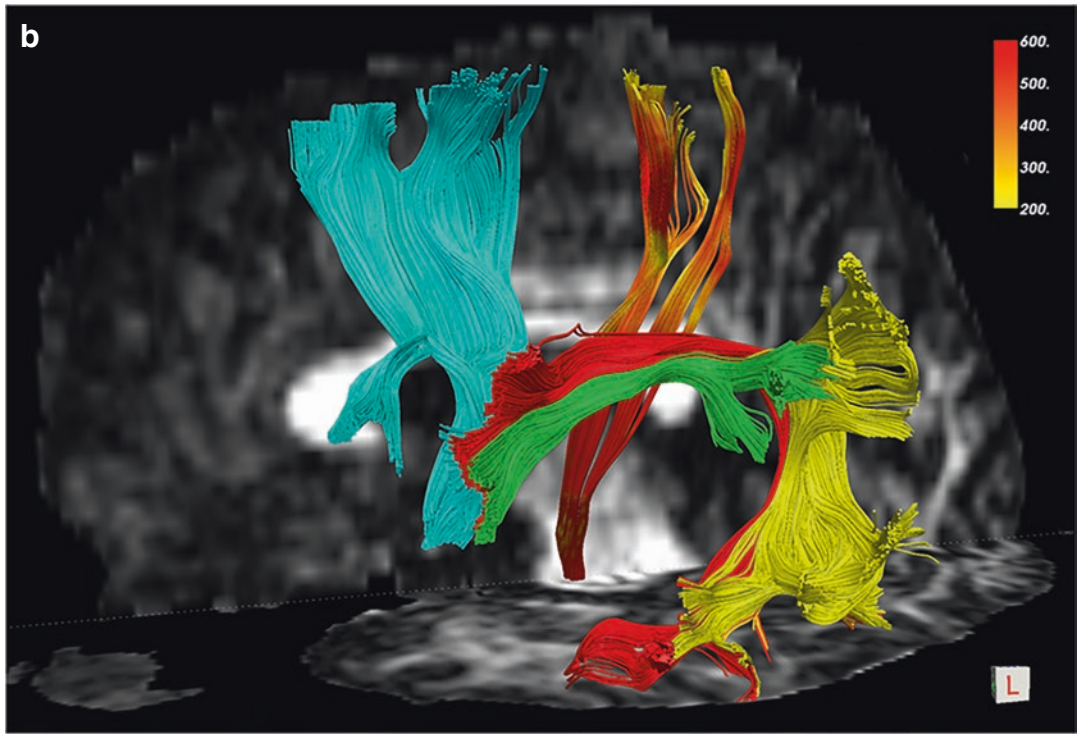

Fig. 10 (continued)

ventricle (Naeser et al. 1989). It is assumed that the FST may play an important role in the development of the intention to act and in the preparation for speech movement, both the initiation and limbic aspects of speech.

The SCF courses within the periventricular zone of the anterior horn of the lateral ventricle, medially to the superior fronto-occipital fasciculus, an association pathway connecting the frontal with the occipital cortex. The two fascicles should be clearly distinguished despite their anatomic proximity in the periventricular zone. To add to the confusion, occasionally the SCF and the superior fronto-occipital fasciculus have been used synonymously in the literature, despite they have clearly different anatomic and physiologic properties.

In a tractography study of 8 healthy subjects Léhericy et al. dissected fronto-strial projections and provided the first demonstration that frontal posterior and anterior premotor areas projections to the striatum are organized in distinct circuits along the caudal-rostral axis (Lehéricy et al. 2004). Fiber tracking of the FST is performed with the two ROI approach: a seed subcortical ROI is delineated in the caudate head and a target ROI in the pre-SMA. The trajectories of the FST ascend around the lateral wall of the frontal horn of the lateral ventricle, and then intermingle with ipsilateral FAT trajectories originating from the pars opercularis before entering into the pre-SMA. Subcortical IES of the FST evokes delayed speech initiation (Vassal et al. 2013).

5.4.4 Which Fascicles Are Eloquent for Speech?

Determination of which brain regions and fascicles are functionally eloquent for language and should be safeguarded during surgery remains an important and debated issue. The aim of IOM is to map the networks underlying different but interactive language processes that will define the functional limits of the resection. Several language tasks are available and selection of which

task to administer to the patient depends on the location of the lesion, presurgical imaging mapping and neuropsychological results, handedness, job, and hobbies of the patient (see Table 1).

In gliomas infiltrating the perisylvian region within the dominant hemisphere mapping of the cortical sites on the brain surface begins with identification of the motor strip, PMv, and posterior IFG (Broca area). The PMv (BA6) can be identified asking the patient to count while the neurosurgeon stimulates the surface of the cortex with a low-frequency bipolar probe. When the current depolarizes neurons in the PMv of a patient who is counting or during spontaneous speech, he/she will have a speech arrest (Duffau 2005), even if stimulated in the non-dominant hemisphere (Duffau et al. 2008b). Common and important language tasks are picture naming, reading, comprehension, syntax and language switching from one language to another.

After completing corticotomy, resection of the tumor continues only after all functional limits with eloquent subcortical pathways have been identified and disconnected from the tumor. With gliomas growing in the anterior frontal lobe the FAT and the SCF are found, respectively, laterally and medially. With gliomas growing in the suprasylvian region within the frontal or parietal opercula the SLF-III, AF-direct and CST are encountered in this order. The AF-direct is the deep limit of the resection also in superficial gliomas infiltrating the MTG and STG. The IFOF and OR are the deep limits in gliomas seating deep to the IPL and posterior temporal region. At the level of the ventral temporo-occipital junction the posterior part of the ILF should be identified because it is part of the reading network.

Which of the above fascicles if damaged may relate to permanent language deficits? In a large series of 115 patients with LGG infiltrating language areas Duffau et al. showed that tumor resection by safeguarding functional boundaries avoids permanent postoperative language deficits (Duffau et al. 2008a, b). The AF has been associated with language for a very long time; however, its role together with that of the UF, MLF, and ILF in maintaining the integrity of the network has been questioned by the neurosurgeons. The AF is a long-range fascicle and a few neurosurgeons suggest that IES of only a focal part of it may evoke phonemic paraphasia. The eloquent part of the AF should be safeguarded, whereas other parts may be removed with the tumor. The eloquent part can only be identified with subcortical direct IES due to a great variability among patients. Stimulation of the AF-direct segment induces transient phonemic paraphasia and repetition errors that are signs of conduction aphasia. Stimulation of the AF can also disrupt syntax (Vidorreta et al. 2011) or a wide network involved in language switching from native to secondary languages, a skill that is important to safeguard in bilingual patients (Bello et al. 2006; Gatignol et al. 2009). Stimulation of the SLF-III induces speech apraxia (Maldonado et al. 2011a) and it may be involved with verbal working memory (Maldonado et al. 2011b), while stimulation of the FAT and SCF induces speech initiation.

We have seen previously how important is direct subcortical IES of the IFOF in preserving semantic processes of language. The IFOF is the medial functional limit in gliomas located in the frontal operculum, insula and temporal lobe of the dominant hemisphere. On the contrary to what applies for the left AF, subcortical IES of the left IFOF throughout its course induces semantic paraphasia (Duffau et al. 2005; Bello et al. 2007).

The UF can be removed without permanent deficits if the IFOF is preserved: in Duffau's large series IES of the left UF did not evoke language deficits (Duffau et al. 2008a, b). However, short and long-lasting deficits in famous face naming in a series of patients with UF resection after removal of left frontal or temporal gliomas have been reported (Papagno et al. 2010, 2016).

In the literature there are conflicting findings about the role of the left ILF in language and semantics. Direct subcortical IES of the left ILF does not particularly impair spoken language generally, especially for picture-naming performances. IES of the left ILF did not induce language errors in 12 patients with LGG in the temporal lobe (Mandonnet et al. 2007b). However, the posterior part of the ILF should be

Table 1 For each System the main fascicles are listed with their cortical terminations. For each fasciculus are indicated the MEP electrode position or the task administered to the patient, the recorded incorrect responses and the neurological deficits occuring when the fasciculus of interest is preserved (transient deficit) or damaged (permanent deficit)

System	Fasciculus	Cortical terminations	IES/task	Response	Preserved	Damaged
Motor	CST	M1, PMv, PMd, SMA	Face, arm, tibialis	MEP or movement disorders (dystonic movement or movement arrest)	Transient motor deficits	Permanent motor deficits
Language	Lt AF	PMd, PMv, MTG	Picture naming	Phonemic paraphasia, anomia	Transient deficits	Conduction aphasia
	Lt IFOF	IFG, OFC, temporal, parietal, occipital	Picture naming	Semantic and verbal paraphasia, anomia	Transient aphasia	Semantic and verbal paraphasia, anomia
	Lt UF	OFC, T-pole	Picture naming, famous face naming	Anomia	Transient deficits	Long-term proper name recall
	Lt ILF	T-pole-occipital and visual word form area	Categorial, reading	Pure anomia, reading disorder	Transient categorial errors	Permanent alexia
	Lt FAT	SMA, BA44	Complex serial articulation	Perseveration, slurring	Speech initiation	Permanent delayed reaction time, deficit of syntax production
	Lt SLF-III	PMd, PMv, SMG and posterior STG	Picture naming, numbering	Number errors, articulatory deficits	Transient deficits	Permanent deficits
Vision	OR	LGN, V1	Alternate picture naming	Missed or "positive" responses (as phosphenes or visual illusion)	Quadrantoanopsia or even hemianopsia	Quadrantoanopsia or even hemianopsia
Visuospatial attention	Rt SLF-II	MFG, AG	Bisection line	Bisection error	Hemispatial neglect	Hemispatial neglect

safeguarded and preserved in gliomas located near the ventral temporo-occipital junction, because the ILF may play a crucial role in reading. In a single glioma patient, direct cortical IES near the visual word form area led to visual paraphasias that were also elicited by subcortical IES of the ILF in the anterior wall of the surgical cavity (Mandonnet et al. 2009). More recently, Duffau and colleagues showed that disruption of the anterior-to-middle segment of the ILF with IES during awake surgery systematically induced pure anomia during a picture-naming task in five patients with LGG in the ITG and posterior temporal lobe, but not in the other six patients with LGG infiltrating the anterior temporal lobe (Herbet et al. 2019). The authors concluded that their results showed that the information conveyed by the ILF is likely rerouted to alternative pathways such as the IFOF when glioma is damaging the anterior temporal cortex. These results also proved that the ILF plays a role in lexical retrieval in normal circumstances. These conclusions are further supported by the case report of a glioma patient who developed a long-lasting anomic aphasia after a presurgically planned interruption of the ILF.

In a series of eight patients with glioma in the left dominant STG subcortical IES of the anterior part of the MLF did not elicited language deficits and the patients did not developed any postoperative permanent language deficit (De Witt Hamer et al. 2011). Thus, the MLF may participate, but is not essential for language processing. Taken together the above studies in patients harboring gliomas seated in the dominant temporal lobe suggest that resections of the UF, ILF, and MLF may cause permanent aphasia in special circumstances when their function cannot be compensated by the IFOF.

Cortical direct IES of the SMA and pre-SMA produces both vocalization and arrest of speech (Penfield and Rasmussen 1950). Patients with lesions of the SMA may present various degrees of speech impairment from a total inability to initiate speech to deficits in phonologic fluency. It has been hypothesized that the SMA through the FAT may facilitate speech initiation. Very recently in a series of 19 patients with WHO-II gliomas infiltrating the SMA, pars opercularis, and/or the caudate nucleus inhibition of speech has been evoked not only by cortical IES of the BA6, pars opercularis or SMA, but also by direct subcortical IES of the left FAT (Kinoshita et al. 2014). Furthermore, the authors found a significant correlation between the severity of postoperative transitory speech initiation deficits and the distance of the FAT from the wall of the resection cavity. In the same study IES of the FST generated negative motor responses suggesting that the FST may be part of the "negative motor network" and may participate in the modulation of motor function including bimanual coordination. Despite the fact that the authors found a relationship between speech initiation postoperative deficits and the left FAT but not the left FST, the average distance between tumor resection and left FST showed a positive correlation with verbal phonemic and semantic fluency scores in the immediate postoperative period and plead in favor of the involvement of the left FST and caudate in speech control. All together these studies emphasize how much valuable is the anatomic information provided by pre- and postoperative tractography studies as a way to integrate IES mapping.

In conclusion, the IFOF, AF-direct, and AF-posterior language fascicles should be identified with presurgical tractography and IES performed in awake patients every time a mass is seated in the perisylvian region of the dominant hemisphere in order to identify the subcortical functional limits of the resection. At present the majority of neurosurgeons performing awake surgery would agree that the IFOF is the most essential of all language-related fascicles, followed by the AF and ILF. Damage to the IFOF is very likely to cause permanent language deficits. A resection very close to the UF, SLF-III, FAT, and SCF is likely to induce transitory speech disorders that may recover in a few weeks or months. We predict that the role of diffusion imaging with tractography in the routine evalua-

tion of pre- and postoperative glioma patients will soon become standard of care in neuro-oncology.

5.5 Visuospatial System: OR

The retinogeniculate fibers originate from neurons in the retina and project to the lateral geniculate nucleus. The OR, also called the geniculostriate fibers, are a large bundle of myelinated fibers that originate from relay neurons in the layers of the lateral geniculate nucleus and project to the ipsilateral primary visual area. The OR are part of the ventral part of the posterior thalamic radiations and can be divided into two main components: the dorsal fibers carrying visual information from the lower quadrants of the contralateral visual hemifield and projecting to the cortex of the cuneus into the superior bank of the calcarine fissure; the ventral fibers carrying visual information from the upper quadrant of the contralateral hemifield and projecting to the cortex of the lingual gyrus into the inferior bank of the calcarine fissure. The dorsal fibers originate from the dorsomedial portion of both lateral geniculate nuclei and arch directly caudally to pass through the retrolenticular limb of the internal capsule before projecting to the cuneus. On the contrary, the ventral fibers originate from the ventrolateral portion of the lateral geniculate nucleus and arch rostral, passing into the WM of the anterior temporal lobes to form a broad U-turn (loop of Meyer) before passing caudally and projecting to the lingula. Damage to the dorsal fibers results in a loss of vision in the contralateral inferior visual field. Damage to the Meyer loop in the anterior temporal lobe or to any other segment of the ventral contingent results in contralateral superior quadrantanopia. Lesions of the OR may result in quadrantanopia or may involve only a portion of a quadrant of the visual field. The closer a lesion is to the primary visual cortex the more congruous the visual field loss of one eye can be superimposed to the other eye. The more anterior a lesion is in the OR, the more likely it is that the visual deficit will be incongruous in the two eyes.

Tracking of the OR is performed with a two ROIs approach using streamline or probabilistic tractography with delineation of the seed ROI in the lateral geniculate nucleus and of the target ROI in the ipsilateral WM of the occipital lobe at the level of the calcarine fissure. The seed ROI is delineated in the lateral portion of the thalamus in multiple axial slices or using a sphere; the target ROI is delineated in one coronal slice perpendicular to the OR. The OR course together with the IFOF for most of their course (Fig. 6): the dorsal fibers of the OR overlap with the IFOF, as well as the upper two-thirds of the ventral fibers projecting to the inferior bank of the calcarine cortex. Only in the proximity of the more posterior part of the sagittal stratum the OR and IFOF diverge to reach their respective cortical terminations. The tractogram should be inspected for a priori anatomical consistency after connecting the two ROIs. Spurious streamlines can be removed with "out-ROI" filters. The OR are symmetric bundles without significant differences in tract volume between the two hemispheres.

During awake surgery the OR can be identified with IES administering a picture-naming task that displays simultaneously two objects in opposite quadrants. When the surgeon stimulates the dorsal bundles of the OR the patient will fail to name the object in the contralateral inferior hemifield, when he stimulates the ventral bundles the patient will fail to name the object in the contralateral superior hemifield.

5.5.1 Superior Longitudinal Fasciculus

Lesion studies in patients and more recent functional imaging studies in healthy human subjects have provided evidence that visuospatial attention relies on a bilateral fronto-parietal network, with right hemisphere dominance in most, but not all individuals. Synchronous activity of neurons in the frontal and parietal cortices during visual search has been demonstrated using multiple electrodes in monkeys, and scalp EEG in

young and elderly human subjects, suggesting that a bilateral fronto-parietal network may play an important role in top-down and bottom-up control mechanisms. Axonal tracing studies in the monkey have demonstrated that frontal and parietal neurons are connected through three separate fascicles coursing longitudinally in the dorsolateral WM of the centrum semiovale (Schmahmann and Pandya 2006). The three segments of the SLF, a major intrahemispheric association fiber pathway that connects the parieto-temporal association areas with the frontal lobe and vice versa, compose the network. In the classical description of Dejerine the AF was also considered part of the SLF; however, studies in monkeys showed that the SLF and AF are two separate entities. The trajectories of three separate segments of the SLF have been demonstrated also in the human brain with post-mortem dissections (Ludwig and Klingler 1956) and more recently with DTI (Makris et al. 2005) and SD (Thiebaut de Schotten et al. 2012) tractography. Overall, the anatomy of the SLF is highly conserved between humans and monkeys.

The *SLF-I* is the most dorsal component and connects the dorsolateral part of the superior parietal lobule and precuneus with the anterior dorsal part of the SFG. The *SLF-II* is the major component of the SLF and it connects the AG and anterior bank of the intraparietal sulcus with the PMd at the junction of the SFG and MFG. Its trajectories are contiguous with the anterior portion of the AF coursing above the Sylvian fissure and insula. The *SLF-III* is the ventral component of the SLF and it connects the IPL (Geschwind territory) with the ventral premotor and prefrontal areas (Broca territory).

Tracking of each of the three segments is performed with a two ROIs approach using streamline or probabilistic tractography. The seed ROI is delineated in a coronal slice at the level of the posterior commissure in the subcortical WM of the SPL and IPL. Three target ROIs are delineated on a coronal slice at the level of the anterior commissure in the dorsal subcortical WM of the superior, middle, and inferior/precentral frontal gyri. An additional ROI should be delineated in the temporal WM to filter out the trajectories of the AF-direct segment that course for some time intermingled with the SLF-II. After connecting the seed ROI in the parietal WM with each target ROI in the frontal WM the tractograms should be inspected for a priori anatomic consistency. Spurious streamlines should be removed with "out-ROI" filters. The SLF-III is an easy tract to reconstruct with DTI tractography in the human brain. Reconstruction of the SLF-I and SLF-II with DTI may be inconsistent because these tracts course along the AF and intersect crossing fibers of the CST and CC. Using the SD algorithm often improves the tracking. A statistical significant rightward asymmetry has been reported for the track volume of the SLF-III; no significant differences were found for the SLF-I and SLF-II (Thiebaut de Schotten et al. 2011a).

Brain tumors expanding in the frontal and parietal lobes may dislocate or interrupt the trajectories of multiple fascicles, including the SLF, FAT, and SCF. The branches of the SLF are only occasionally searched for with IES during surgery, despite the important role they play in the motor and the visuospatial systems. The authors of a recent intraoperative study showed that the SLF-II and the SLF-III together with the AF-direct and the PMv are part of a network involved in motor awareness of voluntary actions (Fornia et al. 2020). Intraoperative IES applied on PMv dramatically altered the patients' motor awareness, making them unconscious of the motor arrest. Another study shed light on a key aspect of cognitive control during the Stroop test: the management of conflicting incoming information to achieve a goal, termed "interference control." The SCF that is connecting the IFG with the striatum was found the key component of cognitive control in the right hemisphere (Puglisi et al. 2019). This latter study suggested that preserving cortico-striatal rather than cortico-cortical connections (i.e., SLF-II, SLF-III, FAT, and IFOF) may be critical for maintaining cognitive control abilities in the surgery of right frontal lobe tumors.

5.6 The Temporo-Parietal Fiber Intersection Area

The TPFIA is a critical neural crossroad with great implications for surgery; it is traversed by seven WM fascicles that connect some of the most eloquent areas in the human brain located in the IPL and posterior temporal lobes. Lesion studies have reported major language deficits such as aphasia (Fridriksson et al. 2010), alexia, agraphia, hemianopia and neglect (Müller-Oehring et al. 2003) in patients with a lesion located in the IPL or in the posterior temporal lobe. In the past clinicians have interpreted neurological deficits of higher cognitive function as a consequence of lesions in associative cortex, neglecting the importance of the WM pathways coursing underneath. Since most focal lesions also affect the subcortical and deep WM, potential damage to adjacent pathways should also be investigated since it may cause a disconnection syndrome (Catani and Ffytche 2005). Recently, unexpectedly high postoperative deficit rates were reported in patients with parietal gliomas. In a series of 119 parietal gliomas Sanai et al. reported a 8.4% permanent language deficit (Sanai et al. 2012), which is fivefold greater compared with the previously reported experience of the UCSF group with gliomas located within language areas (1.6%) (Sanai et al. 2008). The 6.7% rate of permanent visual deficits was also higher than expected in this series. An even higher rate of long-term mild language deficits (42.9%) was reported in a series of 14 consecutive patients with glioma involving the IPL who were operated with cortical and subcortical IES mapping (Maldonado et al. 2011a). This rate is 21-fold greater compared with the 1.7% rate of the overall experience of the same Montpellier group with LGG located within eloquent areas (Duffau et al. 2008a, b). Both studies underscore the importance of the WM pathways coursing underneath the IPL and the posterior temporal lobe that, if damaged, will have consequences far more serious than in other brain cortical and subcortical locations.

Martino et al. elucidated the complex organization and the surgical importance of the TPFIA using post-mortem cortex-sparing fiber dissection and streamline MR tractography (Martino et al. 2013). The TPFIA is seated in the WM underneath the AG, posterior MTG, and ITG and may extend underneath the posterior part of the SMG and STG. The authors described seven long-range WM fascicles passing through the TPFIA. In this section we will discuss the anatomic relationship among the seven tracts and the MLF in detail since the AF, ILF, IFOF, and OR have been already described in other sections.

Starting the virtual or post-mortem dissections from the lateral brain surface at the level of the temporo-parietal junction, the posterior segment of the AF is the most superficial bundle. This fascicle runs vertically and connects the AG with the posterior MTG and ITG. These association fibers had originally been discovered by Wernicke in monkey brains and in the past had been called "Wernicke perpendicular fasciculus." This fascicle is clinically relevant and should be preserved from surgical damage whenever possible. Lesions to the AF-posterior have been associated with preangular alexia without agraphia (Greenblatt 1973). In this peculiar syndrome, patients are unable to read but can still write or text short messages. The closer a lesion is located to the IPL, the more likely it is accompanied by agraphia, whereas the closer a lesion is to the IFG, the more likely it will involve disorders of face or color identification. The anterior aspect of this fascicle may be part of a brain network processing the age of faces (Homola et al. 2012). Bartsch and colleagues have reported four brain tumor patients in which surgical access through the TPFIA has led to alexia without agraphia due to damage of the AF-posterior (Bartsch et al. 2013). Such disconnection syndrome may be transient, but the associated deficit may also persist and turn out to be quite disabling.

Medial and slightly anterior to the posterior segment runs the direct segment of the AF that connects Broca with Wernicke territories. In the TPFIA the bundles of the AF-direct run vertically. Next there is the MLF that is medial to the stem of the AF-direct and lateral to the IFOF.

The *MLF* is a longitudinal fascicle that is coursing with an antero-posterior orientation in

the WM of the STG, parallel to the other longitudinal fascicles (SLF and ILF). At the posterior end of the STG the fibers bend dorsally and course in the posterior portion of the corona radiata until they project into the AG. The MLF connects the upper part of the temporal pole and the entire SFG with the AG (Makris and Pandya 2009; Makris et al. 2009). The MLF should not be confused with the posterior segment of the AF, because it is deeper located and it has a longitudinal rather than a vertical orientation. It has been suggested that the MLF has a role in language and attention (Makris and Pandya 2009; Menjot de Champfleur et al. 2013). However, Duffau et al. have evaluated eight patients with glioma infiltrating the STG using IES and have established that damage to the MLF does not cause long-term deficits, thus Duffau concluded that the MLF is not essential for language. No interference with picture naming was observed by IES of the MLF and no new permanent language deficits were detected with the Boston Diagnostic Aphasia Examination after extensive resection of gliomas that included large parts of the MLF. In the same IES study the IFOF was identified in all patients by eliciting semantic paraphasia, thus it can be easily distinguished from the MLF (De Witt Hamer et al. 2011).

The MLF crosses in the upper half of the TPFIA and it is more difficult to reconstruct than the AF with DTI streamline tractography; SD helps to some degree to depict the MLF. The seed ROIs should be delineated on coronal FA/DEC maps in the WM of the anterior part of the SFG at the level of the AC; the target ROIs should be delineated in the WM of the AG at the level of the splenium of the CC (Makris et al. 2009).

In the inferior half of the TPFIA runs the ILF, laterally to the IFOF and ventrally to the MLF. The ILF runs underneath the inferior temporal and lateral occipital gyri and connects the inferior part of the temporal pole with the ITG, the middle and inferior occipital gyri, and the ventral surfaces of the temporal and occipital lobes. Medial to the ILF there is the IFOF, then the OR. Their streamlines are difficult to separate with MR tractography because they are parallel and course together. On axial and coronal DEC maps they appear green along their entire course and they are seated in between two vertically oriented fascicles (blue on color maps): the AF stem on the lateral side, the tapetum on the medial side. The OR fibers are intermingled with those of the IFOF running in the most medial and ventral part of the TPFIA (Fig. 11). The tapetum is the most medial WM structure and consists of

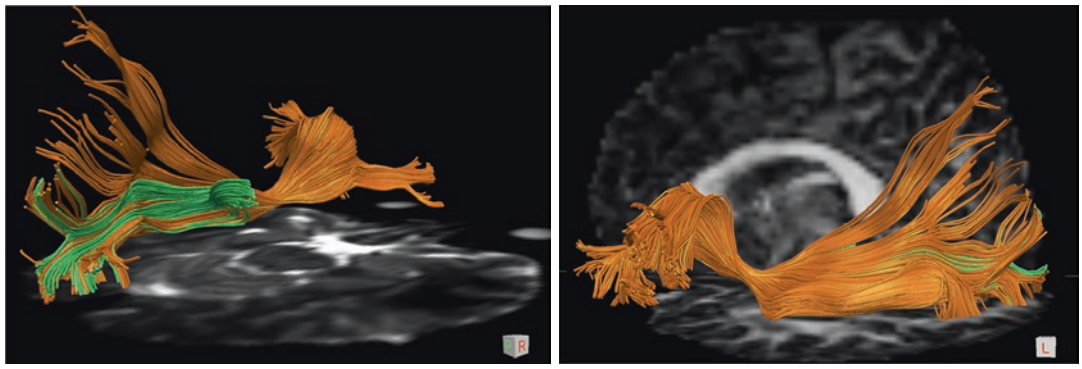

Fig. 11 Medial (upper panel) and lateral (lower panel) views of the left IFOF (orange) and OR (green) displayed over FA map and T2-weighted MRI, respectively. The OR streamlines are intermingled with those of the posterior third of the IFOF and both course along the most medial and ventral part of the temporo-parietal fiber intersection area (TPFIA). The IFOF and the OR are the most eloquent fascicles intersecting in the TPFIA. They course along the lateral wall of the occipital horn of the lateral ventricles and they are difficult to separate with MR tractography. Diffusion data were acquired with HARDI (64 gradient directions, $b = 2000$, $2 \times 2 \times 2$ mm^3) and tractography was performed with DTI interpolated streamline algorithm (thresholds FA > 0.1; angle <35°)

interhemispheric fibers that form the roof and lateral wall of the atrium, temporal, and occipital horns of the lateral ventricles. The tapetum connects both temporal lobes through the posterior part of the corpus callosum.

In summary, the seven tracts can be identified on axial and coronal DEC maps. Three of these tracts have a cranio-caudal orientation and their streamlines are directionally colored in blue; they are the posterior and direct segments of the AF laterally and the tapetum medially. Four tracts with anterior-posterior orientation course in between; the IFOF and the OR course throughout the entire TPFIA, while the MLF and ILF run laterally to the IFOF, respectively, in the upper and lower half of the TPFIA. It is necessary to use MR tractography to distinguish the trajectories of the five antero-posterior oriented tracts.

In the past the transcortical approach through the TPFIA was considered the most direct trajectory from the brain surface to reach a tumor in the posterior hippocampus, temporal, and occipital horns or atrium of the lateral ventricle. Recent postoperative data have shown that the TPFIA is one of the most vulnerable parts of the human brain; therefore knowledge of this important crossroad is now mandatory for surgical planning before a safe resection of deep-seated tumors. When a glioma infiltrating the AG and posterior third of the MTG and ITG extends 2–3 cm into the deep WM it will likely displace, infiltrate, or interrupt the fascicles coursing in the TPFIA. A detailed MR tractography study of the TPFIA should be performed to better understand the relationship between the mass and the seven fascicles. In our practice we have seen several patients with gliomas originating within the TPFIA. We were surprised to note that in a few patients the tumor was causing only mild preoperative neurological deficits. MR tractography was instrumental to explain this unexpected clinical finding. In pauci symptomatic patients the tracts could be reconstructed in their integrity suggesting that the mass was displacing rather than interrupting the tracts. We have seen also rapidly growing gliomas dislocating tracts in the TPFIA (Figs. 12 and 13). Visualization of eloquent tracts in the proximity of a glioma may have a positive predictive value for postoperative outcome, because it suggests that the fascicle is partially spared by the tumor and that an extended resection can be attempted.

It has been shown that MR tractography can reliably reproduce and strengthen the knowledge gathered from intraoperative and post-mortem dissection studies thus having a significant impact on patient management particularly so in cases when the surgical risk should be carefully balanced with the benefits of an extensive resection. Planning a surgical approach anterior or posterior to the TPFIA may preserve the direct and posterior segments of the AF, while in other cases a longitudinal surgical incision may be indicated to safeguard the IFOF, OR, MLF, and ILF that are running in the anterior-posterior orientation (Martino et al. 2013). Moreover, IES should be strongly considered for safe resection of deep-seated tumors, especially in the dominant hemisphere.

5.7 Integration with fMRI

We have seen how tracking of streamlines in the vicinity or within neoplasm is complicated by tumor infiltration, vasogenic edema, mass effect leading to tissue deformation and loss of anatomical landmarks. These changes deform the architecture of the WM and in several cases the use of a priori anatomical approaches for ROI delineation yields unsatisfactory tractography results. Selection of seed and target ROIs based on the results of fMRI has been proposed. Preliminary studies suggested that fMRI-based seed selection may allow for more specific and comprehensive fiber tracking (Schonberg et al. 2006; Smits et al. 2007). The combination and co-registration of clinically feasible fMRI and DTI datasets may help the tractographer to define seed ROIs which are relevant to track the pathway of interest. Schonberg et al. showed that it was feasible and easier to identify the seed and target points, respectively, of the CST and AF with the aid of fMRI maps of finger tapping and speech.

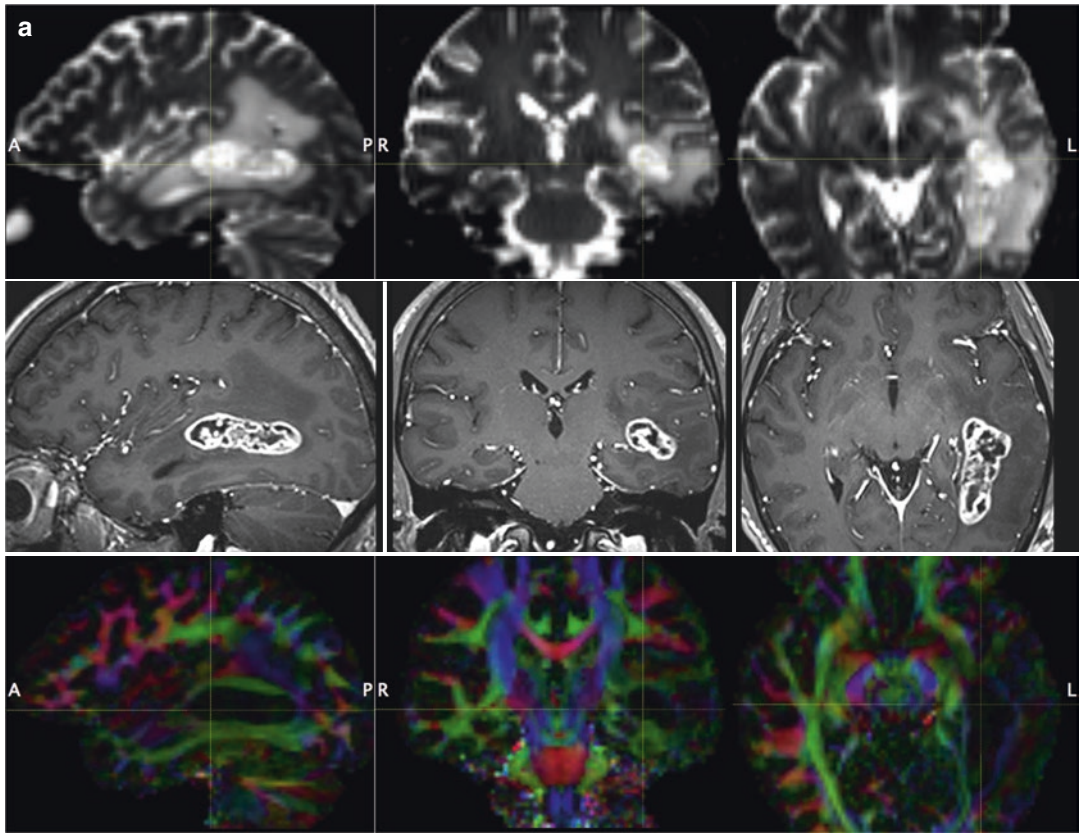

Fig. 12 (**a**) Fifty years-old male with an enhancing mass seated in the deep left temporo-occipital WM. There is extensive perilesional vasogenic edema that is bright on T2WI, hypointense on T1WI and low on FA maps. A GBM WHO-IV was removed at surgery. DEC maps show decreased hue (FA) and dislocation of several green (associative) tracts in the temporo-parietal fiber intersection area (TPFIA). T2WI upper row, T1WI post-gadolinium middle row, DEC maps lower row. (**b**) Tractography is showing that all fascicles in the TPFIA can be virtually dissected: the mass is dislocating the AF-direct (red) and AF-posterior (yellow) laterally, the IFOF (orange) medially. The AF-direct is the lateral functional boundary, whereas the IFOF is the medial boundary. The functional limits of the resection were confirmed in the operating room with direct subcortical IES. In this case the information provided by tractography is by far superior to that provided by DEC maps. Medial view (left column) showing the relationship of the AF, SLF-III (green), and IFOF with the mass. Anterior view (bottom row, left column) showing the mass splaying the AF-direct from the IFOF. Left lateral view (right column) showing dissection of four of the seven fascicles that form the TPFIA. Diffusion data were acquired with HARDI (64 gradient directions, $b = 2000$, $2 \times 2 \times 2$ mm^3) and tractography was performed with DTI interpolated streamline algorithm (thresholds FA > 0.1; angle <35°)

According to the author's remarks tracking of both fascicles was more accurate than with delineation of a priori anatomical seed points.

The initial enthusiasm about performing tractography in a semi-automated fashion by co-registering and combining the two methods has deflated since the early-published papers. So far, nothing can beat an experienced neuroradiologist in identifying the key anatomic landmarks especially when the anatomy of a network is distorted, displaced, or partially interrupted by a mass. The results of streamline tractography using a priori ROI delineation are quite consistent when using the same acquisition scheme, post-processing, and fiber-tracking routine.

In our practice we routinely acquire fMRI and HARDI during the same study session when we are asked to mapping the language system. We are

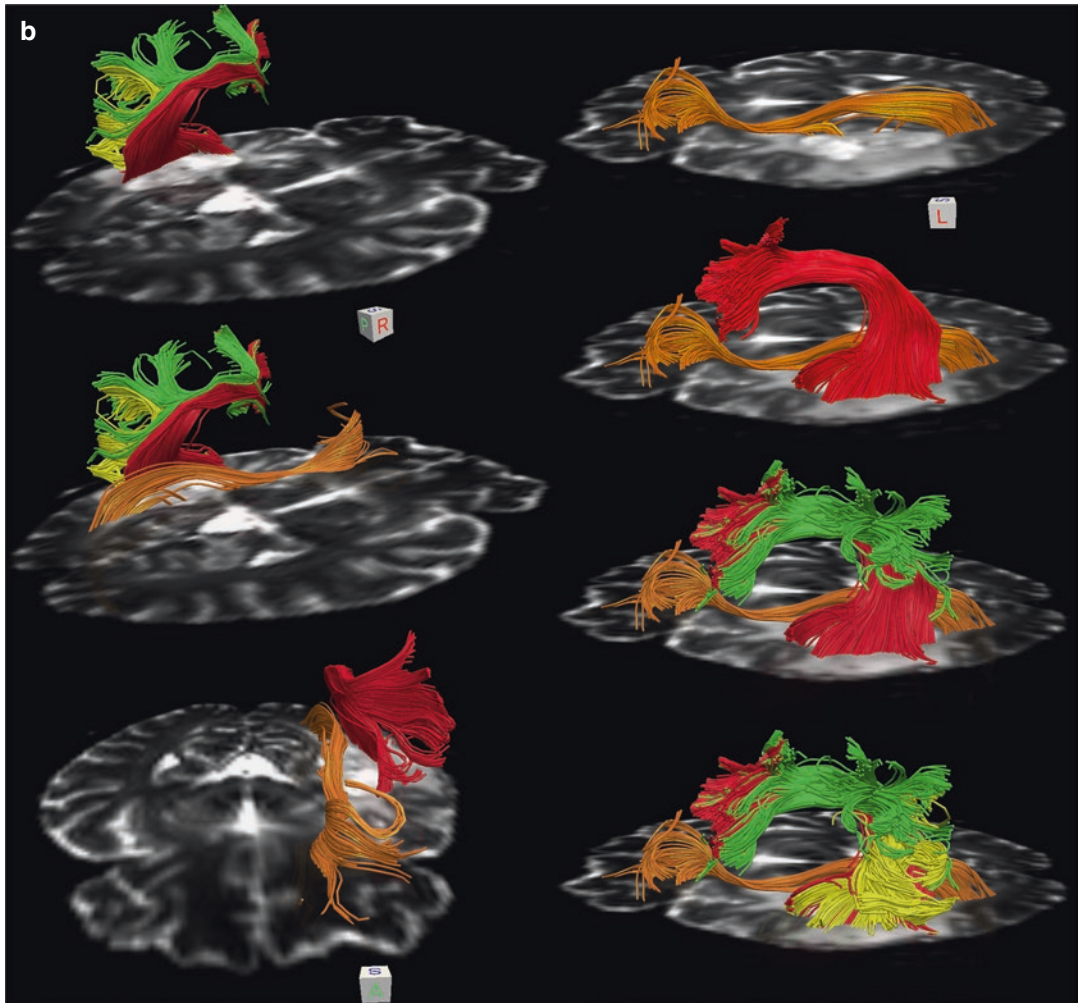

Fig. 12 (continued)

not convinced that combining the two methods in a semi-automatic fashion is worth the effort. fMRI can help identify the seed points of the speech network and to a lesser extent the precentral gyrus when tracking of the CST is requested. We agree with other authors that fMRI is quite helpful to understand the anatomy of sulci and gyri when they are distorted by an infiltrating glioma. When a mass is dislocating the AF or one of its cortical terminations (seed point), the foci of the BOLD response are coherently dislocated (Fig. 14). fMRI is particularly useful to identify the exact anatomy of the IFG and adjacent BA6: despite distortion of the anatomy induced by glioma infiltration a residual cluster of BOLD response is unequivocally located in the ventral precentral sulcus (neurons of the PMv) between these two key anatomy landmarks (Quiñones-Hinojosa et al. 2003; Bizzi et al. 2012).

5.8 Integration in the Operating Room

Nimsky and colleagues were the first to demonstrate that intraoperative DTI was technically feasible in 38 patients with tumor in the proximity of the CST. DEC maps immediately available in the operating theater showed marked and highly variable shifting of the CST caused by surgical

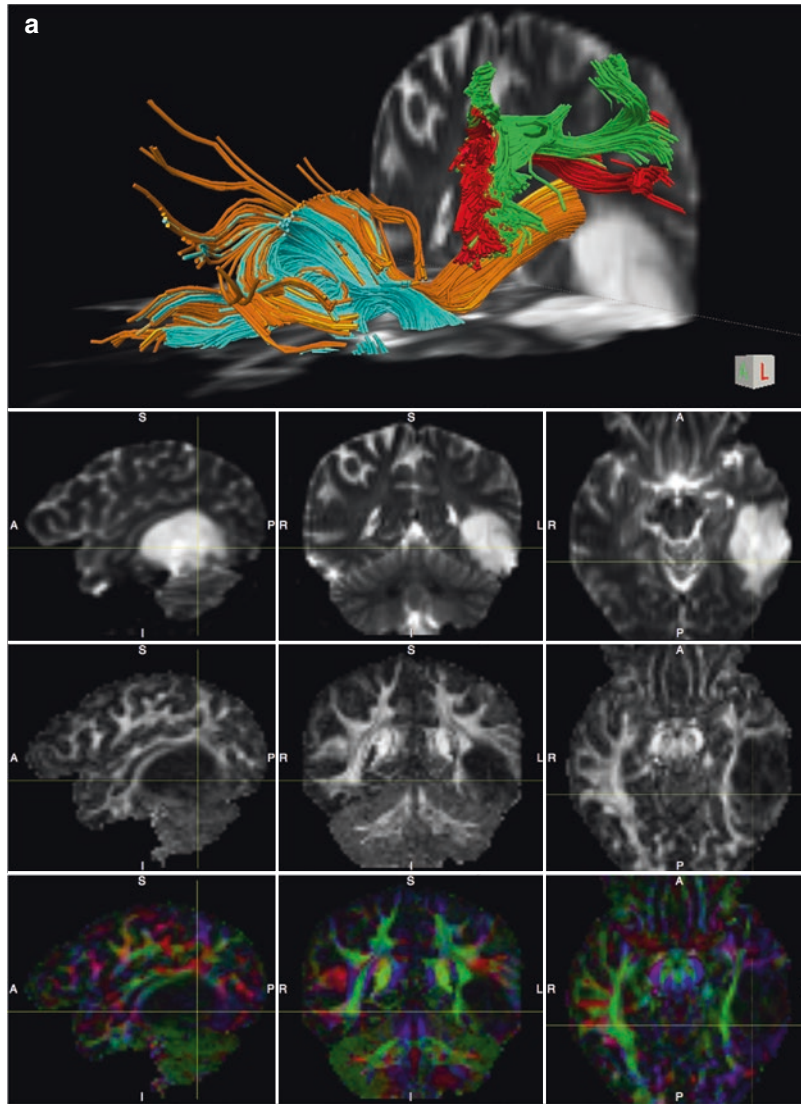

Fig. 13 (**a**) Thirty-one years-old female with a mass expanding in the middle, inferior, and fusiform gyri of the left temporal lobe. Tractography (upper panel) is showing that the main fascicles in the TPFIA can be virtually dissected: the mass is dislocating dorsally the AF-direct (red), medially and superiorly the IFOF (orange) and OR (not shown), medially the ILF (pink). The mass is bright on T2WI (second row) with very low FA (third row). DEC maps (bottom row) are showing that the mass has displayed medially the association tracts but only with tractography it was possible to realize that the IFOF was also displaced dorsally. This information was quite appreciated by the neurosurgeon during presurgical consultation. The functional limits of the resection were confirmed in the operating room with direct subcortical IES. An anaplastic oligodendroglioma WHO-III was removed at surgery. (**b**) Virtual dissection with tractography of the fascicles in the TPFIA. The relationship of five fascicles with the mass (gray) is shown in the upper panel. After "hiding the mass" the medial functional margins of the lesion with the ILF (pink) and IFOF (orange) are illustrated over a FA map in the second panel from above. "Hiding the SLF-III (green)" allows best appreciation of the remarkable dorsal displacement of the temporal arm of the AF-direct (red) in the third panel. "Hiding of the AF-direct" allows appreciation of the ILF and IFOF in the fourth panel. The UF (cyan) is relatively remote from the anterior margin of the lesion. Visualization of eloquent tracts in the proximity of a glioma may have a positive predictive value for postoperative outcome, because it suggests that the fascicle is partially spared by the tumor and that a relatively radical resection can be attempted. Diffusion data were acquired with HARDI (64 gradient directions, $b = 2000$, $2 \times 2 \times 2$ mm^3) and tractography was performed with DTI interpolated streamline algorithm (thresholds FA > 0.1; angle <35°)

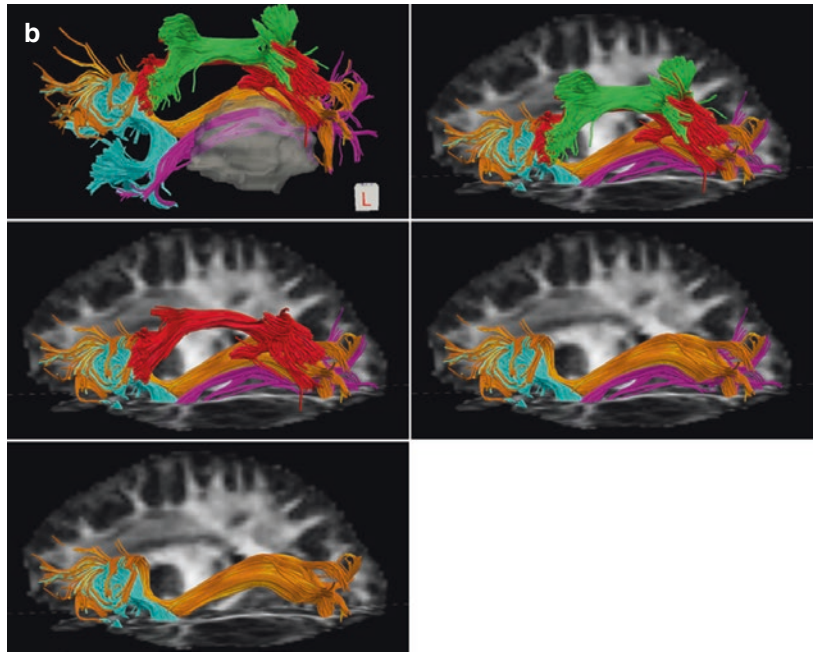

Fig. 13 (continued)

intervention. In the 27 patients who underwent brain tumor resection, CST dislocation ranged from an inward shift of 8 mm to an outward shift of 15 mm (Nimsky et al. 2005).

Another option is fusion of three-dimensional objects of selected tractograms into DICOM post-gadolinium T1WI or T2-FLAIR using a standard neuronavigation system. This method is allowing for intraoperative visualization and localization of the tracts of interest (Nimsky et al. 2007). Display of MR tractograms in the operating room may be useful to determine the relationship of a mass with adjacent fascicles or when the neurosurgeon desires to refresh his anatomical orientation in the operating field, before and after using IES to check the functional limits of a resection on preoperative MRI (Bello et al. 2008).

The long list of important limitations must be well understood and considered when the tractograms are exported to the operating room. Current DTI methods may provide ambiguous results in reconstruction of crossing, kissing, bending, and fanning bundles. MR tractography cannot track the trajectories to their cortical terminations. It is important to be aware that tractography so far is a user-dependent method based on a priori knowledge of the examiner.

The risk of resecting eloquent structures not detected by DTI or HARDI will have to be considered. False negative results may occur especially in areas of T2 signal hyperintensity within a LGG where the trajectories of the tracts appear interrupted due to FA values that are below the recommended 0.10 threshold. The presence of an eloquent tract in the vicinity of the surgical cavity should not be the main reason for stopping the resection prematurely. The finding should be carefully discussed with the surgeon, because an incomplete resection may decrease the impact of surgery on the natural history of the disease. The dangers of using MR tractography in presurgical evaluation of gliomas and intraoperatively has been recently outlined by Duffau (2014). MR tractography does not provide information about the functional status of a fascicle, thus IES should always be used in order to avoid long-term postoperative neurological deficits. IES is the only method able to test WM function in order to create a subcortical functional map that has proven to maximize tumor

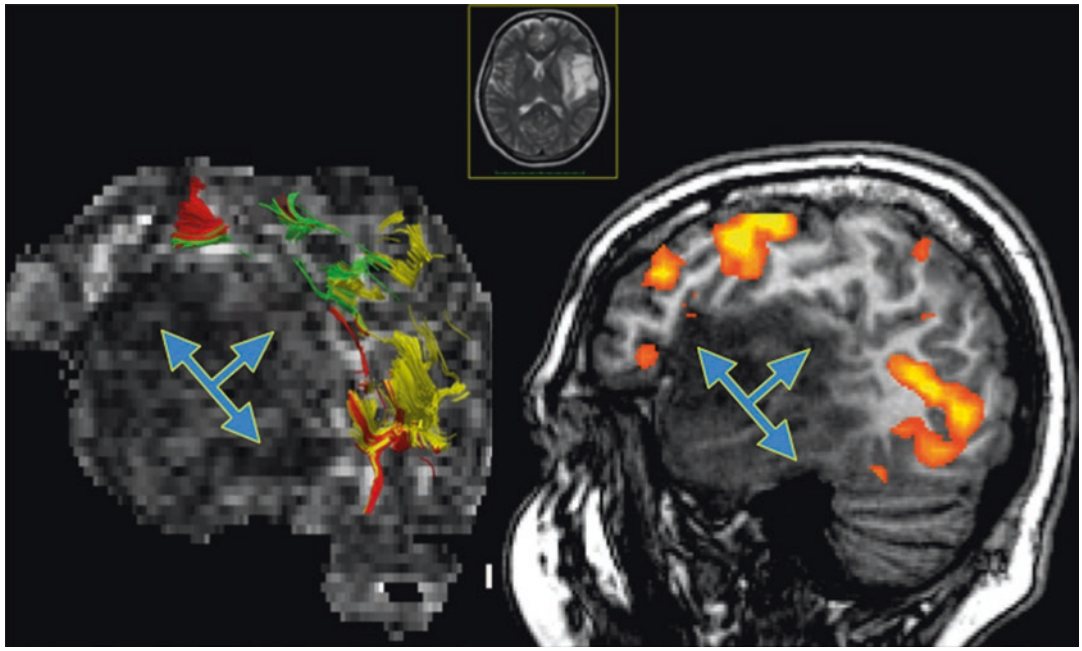

Fig. 14 Forty-one years-old female with a large mass in the left temporal lobe that is hyperintense on T2WI without enhancement after gadolinium injection. Sagittal view of tractography of the left AF (left panel) and fMRI with the verb generation task showing BOLD response in PMv and MTG (right panel). Note that the activation foci on fMRI are coherently dislocated by the mass with the cortical terminations of the three segments of the AF. An oligoastrocitoma WHO-II was removed at surgery. The arrows indicate the direction of AF dislocation. Diffusion data were acquired with HARDI (64 gradient directions, $b = 1000$, $2 \times 2 \times 2$ mm^3) and tractography was performed with DTI interpolated streamline algorithm (thresholds FA > 0.15; angle <45°)

resection and minimize hazards. The main tasks used with subcortical IES in the operating room with related responses, short and long-term deficits are reported in Table 1 for each of the three functional systems discussed in this chapter.

5.9 Impact in Clinical Practice

Presurgical evaluation of patients with glioma has been so far the most successful application of DTI in clinical practice. Other clinical research applications of MR diffusion imaging are in rehabilitation after stroke, multiple sclerosis, mild traumatic brain injury, and degenerative diseases (Alzheimer disease, amyotrophic lateral sclerosis). However in these diseases DTI is mainly used as a clinical research tool and it is not yet ready for prime time patient management.

MR diffusion imaging is the only non-invasive method allowing in vivo detection of the trajectories of main WM fascicles and it can provide information whether a tract is displaced, infiltrated/edematous, or interrupted by a tumor. The accuracy of MR tractography for detecting motor and speech pathways has been validated with IES, with 82–97% concordance across studies (Bello et al. 2008; Berman et al. 2004; Leclercq et al. 2010; Ohue et al. 2012). DTI provides unique anatomic information, whereas IES provides functional feedback about eloquent subcortical connections that, if not safeguarded, may result in permanent neurological deficits. In many medical centers worldwide DTI is frequently requested as an integral part of the presurgical workup of brain tumor patients and the FA/DEC maps or the tractograms of the relevant fascicles are frequently uploaded to a neuronavigational device in the operating room together with morphological and functional MR images. Tractograms of the CST, OR, AF, and IFOF are the most requested by neurosurgeons.

In a unique prospective randomized controlled (Class I) trial on 238 consecutive glioma patients it has been shown that DTI tractography has an impact on outcome after resection of HGG but not of LGG involving the CST (Wu et al. 2007). The authors reported that gross total resection of HGG was more likely with MR tractography guidance rather than without and that new postoperative motor deficits were less frequent. The study showed clear benefits in increasing EOR, median overall survival and 6-month KPS score and it is key evidence supporting the use of DTI-aided resection of gliomas, despite a few limitations. In a retrospective study on 190 patients with LGG in eloquent areas, the EOR and the difference between the T2WI and T1WI volumes were the strongest independent predictors in improving OS as well as delaying progression-free survival and malignant transformation (Ius et al. 2012). The presurgical difference between T2WI and post-contrast T1WI volumes may discriminate glioma growing mechanism along the WM: when proliferation is the major mechanism of tumor expansion the mass has a regular bulky shape with an equivalent volume on T2WI and post-contrast T1WI; when WM infiltration is the predominant mechanism of growth, the mass has a more irregular and complex shape with digitations along the WM that is better detected on T2WI than T1WI (Skrap et al. 2012). In addition, in the same study two groups of patients who underwent tumor resection with a different intraoperative protocol including subcortical IES with or without overlap of fMRI and diffusion tractography on a neuronavigational device were compared. Patients with fMRI/DTI had a median EOR of 90%, while those without had a median EOR of 77%.

Presurgical estimate of the expected surgical outcome both in terms of EOR and functional outcome is of great interest for patient's counseling and clinical decision making. Information provided by DTI tractography may be extremely useful to identify the candidates that could maximally benefit from surgery. It has been recently shown that DTI could be a useful tool to estimate the chance of performing a total resection in patients with gliomas located near eloquent areas (Castellano et al. 2012). In a retrospective tractography study performed in 27 patients with HGG and 46 with LGG, detection of intact fascicles was predictive of a higher probability of total resection. On the contrary, detection of infiltrated or displaced fascicles was predictive of a lower probability of total resection, especially for gliomas with a presurgical volume less than 100 cm^3. Infiltration and even displacement of the CST reduced the chance of achieving a total resection. Moreover, IFOF infiltration in the dominant hemisphere was found predictive of incomplete resection. In particular infiltration of the intermediate third of the IFOF was associated with a very low probability of performing a total resection. On the contrary, no significant correlation was found between infiltration of the SLF/AF and EOR. These results can be explained by considering that the anatomical distribution of the SLF/AF is supposed to be larger than the functional distribution identified by IES, thus a large part of the SLF can be safely resected. The TPFIA is likely another critical area where infiltration or dislocation of the fascicles will likely decrease the chances of a complete resection. Taken together these results emphasize that assessment of WM tracts involvement is an essential part of presurgical evaluation of patients with gliomas in the proximity or within eloquent fascicles and the importance of including HARDI with MR tractography in presurgical imaging protocols.

The value of DTI in performing clinical-anatomical correlations has been shown in a prospective preoperative study on 19 patients with gliomas infiltrating the ventrolateral frontal language areas. Anatomical data provided by DTI tractography was used with the lesion method to identify key structures of the language system responsible for speech deficits. Patients with glioma growing in the left PMv were more likely to presenting with presurgical aphasia than those with glioma infiltrating the IFG, including pars opercularis. However, it was tumor extension to infiltrate or interrupt the AF-direct segment that was associated with preoperative speech deficits, in particular with conduction aphasia (Bizzi et al. 2012).

6 Conclusions

Two decades ago the introduction of DTI changed the way neuroscientists look at WM. Since those first pioneer papers MR diffusion has developed into a sophisticated and complex MR multidisciplinary field with the contribution of physicists, biomedical engineers, mathematicians, cognitive neurologists neuroradiologists, and neurosurgeons. With the development of MR tractography the trajectories of multiple WM fascicles can be identified in vivo in the individual subject and their relationship with a focal lesion can be illustrated and used for presurgical brain mapping. It is now recognized that a detailed understanding of the geometric WM changes induced by a tumor is valuable in order to maximize lesion resection, while avoiding permanent postoperative morbidity. This is particularly true in cases of infiltrating gliomas located within eloquent regions of the brain.

Tractography has gained an undisputed educational reputation for teaching WM architecture. Mapping of WM pathways may improve presurgical planning, surgical targeting with neuronavigational devices and it may reduce intraoperative time. Clinical use of advanced MR imaging tools is growing in importance and exams in patients are being increasingly requested by neurosurgeons worldwide. The role of MR tractography in assisting neurosurgeons to correctly plan subcortical IES and interpret the electrophysiological responses in the operating theater is increasingly recognized by the neurosurgical community.

Although advanced diffusion imaging methods are currently available in most MRI scanners, well beyond the framework of clinical research protocols and academic institutions, they are not yet considered "standard of care." The processes that lead to establishing clinical practice are also quite complex, especially at a time when emphasis on economic difficulties affects health care decisions. Functional MRI and DTI are extremely useful methods that can contribute to improve clinical outcome and to reduce complication rates. As all complex methods they work best when all the members of the team acknowledge their limitations and communicate using a common language.

References

Achard S, Bullmore E (2007) Efficiency and cost of economical brain functional networks. PLoS Comput Biol 3(2):e17. https://doi.org/10.1371/journal.pcbi.0030017

Alexander AL, Hasan K, Kindlmann G, Parker DL, Tsuruda JS (2000) A geometric analysis of diffusion tensor measurements of the human brain. Magn Reson Med 44(2):283–291. http://www.ncbi.nlm.nih.gov/pubmed/10918328

Anwander A, Tittgemeyer M, von Cramon DY, Friederici AD, Knosche TR (2007) Connectivity-based parcellation of Broca's area. Cereb Cortex 17(4):816–825. https://doi.org/10.1093/cercor/bhk034

Assaf Y, Freidlin RZ, Rohde GK, Basser PJ (2004) New modeling and experimental framework to characterize hindered and restricted water diffusion in brain white matter. Magn Reson Med 52(5):965–978. https://doi.org/10.1002/mrm.20274

Assaf Y, Bouznach A, Zomet O et al (2020) Conservation of brain connectivity and wiring across the mammalian class. Nat Neurosci 23:805–808. https://doi.org/10.1038/s41593-020-0641-7

Azevedo FA, Carvalho LR, Grinberg LT, Farfel JM, Ferretti RE, Leite RE, Jacob Filho W, Lent R, Herculano-Houzel S (2009) Equal numbers of neuronal and nonneuronal cells make the human brain an isometrically scaled-up primate brain. J Comp Neurol 513(5):532–541. https://doi.org/10.1002/cne.21974

Bartsch AJ, Geletneky K, Jbabdi S (2013) The temporoparietal fiber intersection area and Wernicke perpendicular fasciculus. Neurosurgery 73(2):E381–E382. https://doi.org/10.1227/01.neu.0000430298.25585.1d

Basser PJ, Mattiello J, LeBihan D (1994) MR diffusion tensor spectroscopy and imaging. Biophys J 66(1):259–267. S0006-3495(94)80775-1 [pii]. https://doi.org/10.1016/S0006-3495(94)80775-1

Basser PJ, Pajevic S, Pierpaoli C, Duda J, Aldroubi A (2000) In vivo fiber tractography using DT-MRI data. Magn Reson Med 44(4):625–632. https://doi.org/10.1002/1522-2594(200010)44:4<625::AID-MRM17>3.0.CO;2-O

Bastin ME, Sinha S, Whittle IR, Wardlaw JM (2002) Measurements of water diffusion and T1 values in peritumoural oedematous brain. Neuroreport 13(10):1335–1340. http://www.ncbi.nlm.nih.gov/pubmed/12151798

Beaulieu C, Does MD, Snyder RE, Allen PS (1996) Changes in water diffusion due to Wallerian degeneration in peripheral nerve. Magn Reson Med 36(4):627–631. http://www.ncbi.nlm.nih.gov/pubmed/8892217

Behrens TEJ, Woolrich MW, Jenkinson M, Johansen-Berg H, Nunes RG, Clare S et al (2003) Characterization and propagation of uncertainty in diffusion-weighted MR imaging. Magn Reson Med 50(5):1077–1088. https://doi.org/10.1002/mrm.10609

Bello L, Acerbi F, Giussani C, Baratta P, Taccone P, Songa V et al (2006) Intraoperative language localization in

multilingual patients with gliomas. Neurosurgery 59(1):115–125. http://www.ncbi.nlm.nih.gov/entrez/query.fcgi?cmd=Retrieve&db=PubMed&dopt=Citation&list_uids=16823307

Bello L, Gallucci M, Fava M, Carrabba G, Giussani C, Acerbi F et al (2007) Intraoperative subcortical language tract mapping guides surgical removal of gliomas involving speech areas. Neurosurgery 60(1):67–80; discussion 80–82. https://doi.org/10.1227/01.NEU.0000249206.58601.DE

Bello L, Gambini A, Castellano A, Carrabba G, Acerbi F, Fava E et al (2008) Motor and language DTI Fiber Tracking combined with intraoperative subcortical mapping for surgical removal of gliomas. NeuroImage 39(1):369–382. S1053-8119(07)00754-9 [pii]. https://doi.org/10.1016/j.neuroimage.2007.08.031

Bello L, Fava E, Carrabba G, Papagno C, Gaini SM (2010) Present day's standards in microsurgery of low-grade gliomas. Adv Tech Stand Neurosurg 35:113–157. http://www.ncbi.nlm.nih.gov/pubmed/20102113

Bello L, Riva M, Fava E, Ferpozzi V, Castellano A, Raneri F, Pessina F, Bizzi A, Falini A, Cerri G (2014) Tailoring neurophysiological strategies with clinical context enhances resection and safety and expands indications in gliomas involving motor pathways. Neuro-Oncology 16(8):1110–1128. https://doi.org/10.1093/neuonc/not327

Berman JI, Berger MS, Mukherjee P, Henry RG (2004) Diffusion-tensor imaging-guided tracking of fibers of the pyramidal tract combined with intraoperative cortical stimulation mapping in patients with gliomas. J Neurosurg 101(1):66–72. https://doi.org/10.3171/jns.2004.101.1.0066

Bizzi A, Nava S, Ferrè F, Castelli G, Aquino D, Ciaraffa F et al (2012) Aphasia induced by gliomas growing in the ventrolateral frontal region: assessment with diffusion MR tractography, functional MR imaging and neuropsychology. Cortex 48(2):255–272. https://doi.org/10.1016/j.cortex.2011.11.015

Bloch O, Han SJ, Cha S, Sun MZ, Aghi MK, McDermott MW et al (2012) Impact of extent of resection for recurrent glioblastoma on overall survival. J Neurosurg 117(6):1032–1038. https://doi.org/10.3171/2012.9.JNS12504

Brat DJ, Aldape K, Colman H, Figrarella-Branger D, Fuller GN, Giannini C, Holland EC, Jenkins RB, Kleinschmidt-DeMasters B, Komori T, Kros JM, Louis DN, McLean C, Perry A, Reifenberger G, Sarkar C, Stupp R, van den Bent MJ, von Deimling A, Weller M (2020) cIMPACT-NOW update 5: recommended grading criteria and terminologies for IDH-mutant astrocytomas. Acta Neuropathol 139(3):603–608. https://doi.org/10.1007/s00401-020-02127-9. Epub 2020 Jan 29

Bucci M, Mandelli ML, Berman JI, Amirbekian B, Nguyen C, Berger MS, Henry RG (2013) Quantifying diffusion MRI tractography of the corticospinal tract in brain tumors with deterministic and probabilistic methods. NeuroImage Clin 3:361–368. https://doi.org/10.1016/j.nicl.2013.08.008

Bullmore E, Sporns O (2012) The economy of brain network organization. Nat Rev Neurosci 13(5):336–349. https://doi.org/10.1038/nrn3214

Buschman TJ, Miller EK (2007) Top-down versus bottom-up control of attention in the prefrontal and posterior parietal cortices. Science (New York, NY) 315(5820):1860–1862. https://doi.org/10.1126/science.1138071

Cajal SR (1995) Histology of the Nervous System of Man and Vertebrates New York: Oxford Univ. Press

Caramazza A, Zurif EB (1976) Dissociation of algorithmic and heuristic processes in language comprehension: evidence from aphasia. Brain Lang 3(4):572–582. https://doi.org/10.1016/0093-934x(76)90048-1

Castellano A, Bello L, Michelozzi C, Gallucci M, Fava E, Iadanza A et al (2012) Role of diffusion tensor magnetic resonance tractography in predicting the extent of resection in glioma surgery. Neuro-Oncology 14(2):192–202. https://doi.org/10.1093/neuonc/nor188

Catani M, Bambini V (2014) A model for Social Communication And Language Evolution and Development (SCALED). Curr Opin Neurobiol 28C:165–171. https://doi.org/10.1016/j.conb.2014.07.018

Catani M, Ffytche DH (2005) The rises and falls of disconnection syndromes. Brain 128(Pt 10):2224–2239. https://doi.org/10.1093/brain/awh622

Catani M, Mesulam M (2008) The arcuate fasciculus and the disconnection theme in language and aphasia: history and current state. Cortex 44(8):953–961. S0010-9452(08)00111-1 [pii]. https://doi.org/10.1016/j.cortex.2008.04.002

Catani M, Thiebaut de Schotten M (2008) A diffusion tensor imaging tractography atlas for virtual in vivo dissections. Cortex 44(8):1105–1132

Catani M, Howard RJ, Pajevic S, Jones DK (2002) Virtual in vivo interactive dissection of white matter fasciculi in the human brain. NeuroImage 17(1):77–94

Catani M, Jones DK, Ffytche DH (2005) Perisylvian language networks of the human brain. Ann Neurol 57(1):8–16

Catani M, Allin MP, Husain M, Pugliese L, Mesulam MM, Murray RM, Jones DK (2007) Symmetries in human brain language pathways correlate with verbal recall. Proc Natl Acad Sci U S A 104(43):17163–17168

Catani M, Dell'Acqua F, Vergani F, Malik F, Hodge H, Roy P et al (2012) Short frontal lobe connections of the human brain. Cortex 48(2):273–291

Catani M, Mesulam MM, Jakobsen E, Malik F, Martersteck A, Wieneke C et al (2013) A novel frontal pathway underlies verbal fluency in primary progressive aphasia. Brain 136(Pt 8):2619–2628. https://doi.org/10.1093/brain/awt163

Caverzasi E, Papinutto N, Amirbekian B, Berger MS, Henry RG (2014) Q-ball of inferior fronto-occipital fasciculus and beyond. PLoS One 9(6):e100274. https://doi.org/10.1371/journal.pone.0100274

Cerri G, Shimazu H, Maier MA, Lemon RN (2003) Facilitation from ventral premotor cortex of primary

motor cortex outputs to macaque hand muscles. J Neurophysiol 90(2):832–842. https://doi.org/10.1152/jn.01026.2002

Chenevert TL, Brunberg JA, Pipe JG (1990) Anisotropic diffusion in human white matter: demonstration with MR techniques in vivo. Radiology 177(2):401–405. https://doi.org/10.1148/radiology.177.2.2217776

Chun MM, Golomb JD, Turk-Browne NB (2011) A taxonomy of external and internal attention. Annu Rev Psychol 62:73–101. https://doi.org/10.1146/annurev.psych.093008.100427

Ciaraffa F, Castelli G, Parati EA, Bartolomeo P, Bizzi A (2012) Visual neglect as a disconnection syndrome? A confirmatory case report. Neurocase. https://doi.org/10.1080/13554794.2012.667130

Claes A, Idema AJ, Wesseling P (2007) Diffuse glioma growth: a guerilla war. Acta Neuropathol 114(5):443–458. https://doi.org/10.1007/s00401-007-0293-7

Conturo TE, Lori NF, Cull TS, Akbudak E, Snyder AZ, Shimony JS et al (1999) Tracking neuronal fiber pathways in the living human brain. Proc Natl Acad Sci U S A 96(18):10422–10427. http://www.ncbi.nlm.nih.gov/entrez/query.fcgi?cmd=Retrieve&db=PubMed&dopt=Citation&list_uids=10468624

Corbetta M, Shulman GL (2002) Control of goal-directed and stimulus-driven attention in the brain. Nat Rev Neurosci 3(3):201–215. https://doi.org/10.1038/nrn755

Crossley NA, Mechelli A, Scott J, Carletti F, Fox PT, McGuire P, Bullmore ET (2014) The hubs of the human connectome are generally implicated in the anatomy of brain disorders. Brain 137(Pt 8):2382–2395. https://doi.org/10.1093/brain/awu132

De Witt Hamer PC, Moritz-Gasser S, Gatignol P, Duffau H (2011) Is the human left middle longitudinal fascicle essential for language? A brain electrostimulation study. Hum Brain Mapp 32(6):962–973. https://doi.org/10.1002/hbm.21082

Dejerine J, Dejerine-Klumpke A (1895) Anatomies des centres nerveux. Rueff et Cie, Paris

Dell'Acqua F, Scifo P, Rizzo G, Catani M, Simmons A, Scotti G, Fazio F (2010) A modified damped Richardson-Lucy algorithm to reduce isotropic background effects in spherical deconvolution. NeuroImage 49(2):1446–1458. https://doi.org/10.1016/j.neuroimage.2009.09.033

Dell'Acqua F, Simmons A, Williams SCR, Catani M (2013) Can spherical deconvolution provide more information than fiber orientations? Hindrance modulated orientational anisotropy, a true-tract specific index to characterize white matter diffusion. Hum Brain Mapp 34(10):2464–2483. https://doi.org/10.1002/hbm.22080

Doran M, Hajnal JV, Van Bruggen N, King MD, Young IR, Bydder GM (1990) Normal and abnormal white matter tracts shown by MR imaging using directional diffusion weighted sequences. J Comput Assist Tomogr 14(6):865–873. http://www.ncbi.nlm.nih.gov/pubmed/2229559

Doricchi F, Tomaiuolo F (2003) The anatomy of neglect without hemianopia: a key role for parietal-frontal disconnection? Neuroreport 14(17):2239–2243. https://doi.org/10.1097/01.wnr.0000091132.75061.64

Dronkers NF (1996) A new brain region for coordinating speech articulation. Nature 384(6605):159–161. https://doi.org/10.1038/384159a0

Ducreux D, Lepeintre J-F, Fillard P, Loureiro C, Tadié M, Lasjaunias P (2006) MR diffusion tensor imaging and fiber tracking in 5 spinal cord astrocytomas. AJNR Am J Neuroradiol 27(1):214–216. http://www.ncbi.nlm.nih.gov/pubmed/16418387

Duffau H (2005) Intraoperative cortico-subcortical stimulations in surgery of low-grade gliomas. Expert Rev Neurother 5(4):473–485. https://doi.org/10.1586/14737175.5.4.473

Duffau H (2014) The dangers of magnetic resonance imaging diffusion tensor tractography in brain surgery. World Neurosurg 81(1):56–58. https://doi.org/10.1016/j.wneu.2013.01.116

Duffau H, Capelle L (2004) Preferential brain locations of low-grade gliomas. Cancer 100(12):2622–2626. https://doi.org/10.1002/cncr.20297

Duffau H, Gatignol P, Mandonnet E, Peruzzi P, Tzourio-Mazoyer N, Capelle L (2005) New insights into the anatomo-functional connectivity of the semantic system: a study using cortico-subcortical electrostimulations. Brain 128(Pt 4):797–810

Duffau H, Gatignol P, Mandonnet E, Capelle L, Taillandier L (2008a) Intraoperative subcortical stimulation mapping of language pathways in a consecutive series of 115 patients with Grade II glioma in the left dominant hemisphere. J Neurosurg 109(September):461–471. https://doi.org/10.3171/JNS/2008/109/9/0461

Duffau H, Leroy M, Gatignol P (2008b) Cortico-subcortical organization of language networks in the right hemisphere: an electrostimulation study in left-handers. Neuropsychologia 46(14):3197–3209. https://doi.org/10.1016/j.neuropsychologia.2008.07.017

Duyn J (2013) MR susceptibility imaging. J Magn Reson 229:198–207. https://doi.org/10.1016/j.jmr.2012.11.013

Ebeling U, von Cramon D (1992) Topography of the uncinate fascicle and adjacent temporal fiber tracts. Acta Neurochir 115(3-4):143–148. http://www.ncbi.nlm.nih.gov/pubmed/1605083

Eckel-Passow JE, Lachance DH, Molinaro AM, Walsh KM, Decker PA, Sicotte H et al (2015) Glioma groups based on 1p/19q, IDH, and TERT promoter mutations in tumors. N Engl J Med 372:2499–2508. https://doi.org/10.1056/NEJMoa1407279

Field AS, Alexander AL, Wu Y-C, Hasan KM, Witwer B, Badie B (2004) Diffusion tensor eigenvector directional color imaging patterns in the evaluation of cerebral white matter tracts altered by tumor. J Magn Reson Imaging 20(4):555–562. https://doi.org/10.1002/jmri.20169

Ford A, McGregor KM, Case K, Crosson B, White KD (2010) Structural connectivity of Broca's area and medial frontal cortex. NeuroImage 52(4):1230–1237. S1053-8119(10)00725-1 [pii]. https://doi.org/10.1016/j.neuroimage.2010.05.018

Forkel SJ, Thiebaut de Schotten M, Dell'Acqua F, Kalra L, Murphy DGM, Williams SCR, Catani M (2014a) Anatomical predictors of aphasia recovery: a tractography study of bilateral perisylvian language networks. Brain 137(Pt 7):2027–2039. https://doi.org/10.1093/brain/awu113

Forkel SJ, Thiebaut de Schotten M, Kawadler JM, Dell'Acqua F, Danek A, Catani M (2014b) The anatomy of fronto-occipital connections from early blunt dissections to contemporary tractography. Cortex 56:73–84. https://doi.org/10.1016/j.cortex.2012.09.005

Fornia L, Puglisi G, Leonetti A, Bello L, Berti A, Cerri G, Garbarini F (2020) Direct electrical stimulation of the premotor cortex shuts down awareness of voluntary actions. Nat Commun 11:705. https://doi.org/10.1038/s41467-020-14517-4

Fridriksson J, Kjartansson O, Morgan PS, Hjaltason H, Magnusdottir S, Bonilha L, Rorden C (2010) Impaired speech repetition and left parietal lobe damage. J Neurosci 30(33):11057–11061. https://doi.org/10.1523/JNEUROSCI.1120-10.2010

Friederici AD (2011) The brain basis of language processing: from structure to function. Physiol Rev 91(4):1357–1392. https://doi.org/10.1152/physrev.00006.2011

Friederici AD (2012) The cortical language circuit: from auditory perception to sentence comprehension. Trends Cogn Sci 16(5):262–268. https://doi.org/10.1016/j.tics.2012.04.001

Ganslandt O, Stadlbauer A, Fahlbusch R, Kamada K, Buslei R, Blumcke I et al (2005) Proton magnetic resonance spectroscopic imaging integrated into image-guided surgery: correlation to standard magnetic resonance imaging and tumor cell density. Neurosurgery 56(2 Suppl):291–298; discussion 291–298. http://www.ncbi.nlm.nih.gov/pubmed/15794826

Gatignol P, Duffau H, Capelle L, Plaza M (2009) Naming performance in two bilinguals with frontal vs. temporal glioma. Neurocase 15(6):466–477. 912523470 [pii]. https://doi.org/10.1080/13554790902950434

Geschwind N (1970) The organization of language and the brain. Science (New York, NY) 170(3961):940–944. http://www.ncbi.nlm.nih.gov/pubmed/5475022

Giese A, Westphal M (1996) Glioma invasion in the central nervous system. Neurosurgery 39(2):235–250; discussion 250–252. http://www.ncbi.nlm.nih.gov/pubmed/8832660

Glasser MF, Smith SM, Marcus DS, Andersson JL, Auerbach EJ, Behrens TE, Coalson TS, Harms MP, Jenkinson M, Moeller S, Robinson EC, Sotiropoulos SN, Xu J, Yacoub E, Ugurbil K, Van Essen DC (2016) The Human Connectome Project's neuroimaging approach. Nat Neurosci 19(9):1175–1187. https://doi.org/10.1038/nn.4361

Gorno-Tempini ML, Price CJ, Josephs O, Vandenberghe R, Cappa SF, Kapur N et al (1998) The neural systems sustaining face and proper-name processing. Brain 121(Pt 11):2103–2118. http://www.ncbi.nlm.nih.gov/pubmed/9827770

Greenblatt SH (1973) Alexia without agraphia or hemianopsia. Anatomical analysis of an autopsied case. Brain 96(2):307–316

Herbet G, Moritz-Gasser S, Lemaitre A-L, Almairac F, Duffau H (2019) Functional compensation of the left inferior longitudinal fasciculus for picture naming. Cogn Neuropsychol 36(3–4):140–157. https://doi.org/10.1080/02643294.2018.1477749

Hickok G, Poeppel D (2007) The cortical organization of speech processing. Nat Rev Neurosci 8(5):393–402. nrn2113 [pii]. https://doi.org/10.1038/nrn2113

Homola GA, Jbabdi S, Beckmann CF, Bartsch AJ (2012) A brain network processing the age of faces. PLoS One 7(11):e49451. https://doi.org/10.1371/journal.pone.0049451

Ius T, Isola M, Budai R, Pauletto G, Tomasino B, Fadiga L, Skrap M (2012) Low-grade glioma surgery in eloquent areas: volumetric analysis of extent of resection and its impact on overall survival. A single-institution experience in 190 patients: clinical article. J Neurosurg 117(6):1039–1052. https://doi.org/10.3171/2012.8.JNS12393

Jellison BJ, Field AS, Medow J, Lazar M, Salamat MS, Alexander AL (2004) Diffusion tensor imaging of cerebral white matter: a pictorial review of physics, fiber tract anatomy, and tumor imaging patterns. AJNR Am J Neuroradiol 25(3):356–369. http://www.ncbi.nlm.nih.gov/entrez/query.fcgi?cmd=Retrieve&db=PubMed&dopt=Citation&list_uids=15037456

Jenkinson M, Beckmann CF, Behrens TEJ, Woolrich MW, Smith SM (2012) FSL. NeuroImage 62(2):782–790. https://doi.org/10.1016/j.neuroimage.2011.09.015

Jeurissen B, Leemans A, Tournier J-D, Jones DK, Sijbers J (2013) Investigating the prevalence of complex fiber configurations in white matter tissue with diffusion magnetic resonance imaging. Hum Brain Mapp 34(11):2747–2766. https://doi.org/10.1002/hbm.22099

Jones DK (2008) Studying connections in the living human brain with diffusion MRI. Cortex 44(8):936–952. S0010-9452(08)00110-X [pii]. https://doi.org/10.1016/j.cortex.2008.05.002

Keles GE, Berger MS (2004) Advances in neurosurgical technique in the current management of brain tumors. Semin Oncol 31(5):659–665. http://www.ncbi.nlm.nih.gov/pubmed/15497119

Kinoshita M, de Champfleur NM, Deverdun J, Moritz-Gasser S, Herbet G, Duffau H (2014) Role of fronto-striatal tract and frontal aslant tract in movement and speech: an axonal mapping study. Brain Struct Funct. https://doi.org/10.1007/s00429-014-0863-0

Krainik A, Lehéricy S, Duffau H, Capelle L, Chainay H, Cornu P et al (2003) Postoperative speech disorder after medial frontal surgery: role of the supplementary motor area. Neurology 60(4):587–594. http://www.ncbi.nlm.nih.gov/pubmed/12601097

Kumar M, Gupta RK, Nath K, Rathore RKS, Bayu G, Trivedi R et al (2008) Can we differentiate true white matter fibers from pseudofibers inside a brain abscess cavity using geometrical diffusion tensor imaging

metrics? NMR Biomed 21(6):581–588. https://doi.org/10.1002/nbm.1228

Lawes IN, Barrick TR, Murugam V, Spierings N, Evans DR, Song M, Clark CA (2008) Atlas-based segmentation of white matter tracts of the human brain using diffusion tensor tractography and comparison with classical dissection. NeuroImage 39(1): 62–79

Laws ER (2001) Resection of low-grade gliomas. J Neurosurg 95(5):731–732. https://doi.org/10.3171/jns.2001.95.5.0731

Laws ER, Parney IF, Huang W, Anderson F, Morris AM, Asher A et al (2003) Survival following surgery and prognostic factors for recently diagnosed malignant glioma: data from the Glioma Outcomes Project. J Neurosurg 99(3):467–473. https://doi.org/10.3171/jns.2003.99.3.0467

Leclercq D, Duffau H, Delmaire C, Capelle L, Gatignol P, Ducros M et al (2010) Comparison of diffusion tensor imaging tractography of language tracts and intraoperative subcortical stimulations. J Neurosurg 112(3):503–511. https://doi.org/10.3171/2009.8.JNS09558

Leemans A, Jeurissen B, Sijbers J, Jones DK (2009) ExploreDTI: a graphical toolbox for processing, analyzing and visualizing diffusion MR data. ISMRM Annu Meeting Proc 17:3537

Lehéricy S, Ducros M, Krainik A, Francois C, Van de Moortele P-F, Ugurbil K, Kim D-S (2004) 3-D diffusion tensor axonal tracking shows distinct SMA and pre-SMA projections to the human striatum. Cereb Cortex 14(12):1302–1309. https://doi.org/10.1093/cercor/bhh091

Lemon RN (2008) Descending pathways in motor control. Annu Rev Neurosci 31:195–218. https://doi.org/10.1146/annurev.neuro.31.060407.125547

Lemon RN, Griffiths J (2005) Comparing the function of the corticospinal system in different species: organizational differences for motor specialization? Muscle Nerve 32(3):261–279. https://doi.org/10.1002/mus.20333

Louis DN, Ohgaki H, Wiestler OD, Cavenee WK et al (2007) WHO classification of tumors of the central nervous system. IARC Press, Lyon, France

Louis DN, Perry A, Reifenberger G, von Deimling A, Figarella-Branger D, Cavenee WK et al (2016) The 2016 World Health Organization Classification of tumors of the central nervous system: a summary. Acta Neuropathol 131:803–820. https://doi.org/10.1007/s00401-016-1545-1

Ludwig E, Klingler J (1956) Atlas cerebri humani. Little, Brown and Company, Boston, MA

Makris N, Pandya DN (2009) The extreme capsule in humans and rethinking of the language circuitry. Brain Struct Funct 213(3):343–358. https://doi.org/10.1007/s00429-008-0199-8

Makris N, Kennedy DN, McInerney S, Sorensen AG, Wang R, Caviness VS, Pandya DN (2005) Segmentation of subcomponents within the superior longitudinal fascicle in humans: a quantitative, in vivo, DT-MRI study. Cereb Cortex 15(6):854–869. https://doi.org/10.1093/cercor/bhh186

Makris N, Papadimitriou GM, Kaiser JR, Sorg S, Kennedy DN, Pandya DN (2009) Delineation of the middle longitudinal fascicle in humans: a quantitative, in vivo, DT-MRI study. Cereb Cortex 19(4):777–785. bhn124 [pii]. https://doi.org/10.1093/cercor/bhn124

Maldonado IL, Moritz-Gasser S, de Champfleur NM, Bertram L, Moulinié G, Duffau H (2011a) Surgery for gliomas involving the left inferior parietal lobule: new insights into the functional anatomy provided by stimulation mapping in awake patients. J Neurosurg 115(4):770–779. https://doi.org/10.3171/2011.5.JNS112

Maldonado IL, Moritz-Gasser S, Duffau H (2011b) Does the left superior longitudinal fascicle subserve language semantics? A brain electrostimulation study. Brain Struct Funct 216(3):263–274. https://doi.org/10.1007/s00429-011-0309-x

Mandelli ML, Berger MS, Bucci M, Berman JI, Amirbekian B, Henry RG (2014) Quantifying accuracy and precision of diffusion MR tractography of the corticospinal tract in brain tumors. J Neurosurg 121(2):349–358. https://doi.org/10.3171/2014.4.JNS131160

Mandonnet E, Jbabdi S, Taillandier L, Galanaud D, Benali H, Capelle L, Duffau H (2007a) Preoperative estimation of residual volume for WHO grade II glioma resected with intraoperative functional mapping. Neuro-Oncology 9(1):63–69. https://doi.org/10.1215/15228517-2006-015

Mandonnet E, Nouet A, Gatignol P, Capelle L, Duffau H (2007b) Does the left inferior longitudinal fasciculus play a role in language? A brain stimulation study. Brain 130(Pt 3):623–629

Mandonnet E, Gatignol P, Duffau H (2009) Evidence for an occipito-temporal tract underlying visual recognition in picture naming. Clin Neurol Neurosurg 111(7):601–605. https://doi.org/10.1016/j.clineuro.2009.03.007

Martino J, Brogna C, Robles SG, Vergani F, Duffau H (2010) Anatomic dissection of the inferior fronto-occipital fasciculus revisited in the lights of brain stimulation data. Cortex 46(5):691–699. https://doi.org/10.1016/j.cortex.2009.07.015

Martino J, De Witt Hamer PC, Vergani F, Brogna C, de Lucas EM, Vázquez-Barquero A et al (2011) Cortex-sparing fiber dissection: an improved method for the study of white matter anatomy in the human brain. J Anat 219(4):531–541. https://doi.org/10.1111/j.1469-7580.2011.01414.x

Martino J, da Silva-Freitas R, Caballero H, Marco de Lucas E, García-Porrero JA, Vázquez-Barquero A (2013) Fiber dissection and diffusion tensor imaging tractography study of the temporoparietal fiber intersection area. Neurosurgery 72(1 Suppl Operative):87–97; discussion 97–8. https://doi.org/10.1227/NEU.0b013e318274294b

Mawrin C (2005) Molecular genetic alterations in gliomatosis cerebri: what can we learn about the origin

and course of the disease? Acta Neuropathol 110(6): 527–536. https://doi.org/10.1007/s00401-005-1083-8

Menjot de Champfleur N, Lima Maldonado I, Moritz-Gasser S, Machi P, Le Bars E, Bonafé A, Duffau H (2013) Middle longitudinal fasciculus delineation within language pathways: a diffusion tensor imaging study in human. Eur J Radiol 82(1):151–157. https://doi.org/10.1016/j.ejrad.2012.05.034

Meynert TH (1887) In: Sachs BT (ed) A clinical treatise on diseases of the fore-brain based upon a study of its structure, functions, and nutrition. G.P. Putman's Sons, New York

Miraillé C (1896) De laphasie sensorielle. G. Steinheil, Paris. http://gallica.bnf.fr/ark:/12148/bpt6k5711953h. Accessed 2 Jan 2021

Mori S, Crain BJ, Chacko VP, van Zijl PC (1999) Three-dimensional tracking of axonal projections in the brain by magnetic resonance imaging. Ann Neurol 45(2):265–269. http://www.ncbi.nlm.nih.gov/entrez/query.fcgi?cmd=Retrieve&db=PubMed&dopt=Citation&list_uids=9989633

Müller-Oehring EM, Kasten E, Poggel DA, Schulte T, Strasburger H, Sabel BA (2003) Neglect and hemianopia superimposed. J Clin Exp Neuropsychol 25(8):1154–1168. https://doi.org/10.1076/jcen.25.8.1154.16727

Naeser MA, Palumbo CL, Helm-Estabrooks N, Stiassny-Eder D, Albert ML (1989) Severe nonfluency in aphasia. Role of the medial subcallosal fasciculus and other white matter pathways in recovery of spontaneous speech. Brain 112(Pt 1):1–38. http://www.ncbi.nlm.nih.gov/pubmed/2917272

Nimsky C, Ganslandt O, Hastreiter P, Wang R, Benner T, Sorensen AG, Fahlbusch R (2005) Intraoperative diffusion-tensor MR imaging: shifting of white matter tracts during neurosurgical procedures—initial experience. Radiology 234(1):218–225

Nimsky C, Ganslandt O, Fahlbusch R (2007) Implementation of fiber tract navigation. Neurosurgery 58(1 Suppl):306–318

Ohue S, Kohno S, Inoue A, Yamashita D, Harada H, Kumon Y et al (2012) Accuracy of diffusion tensor magnetic resonance imaging-based tractography for surgery of gliomas near the pyramidal tract: a significant correlation between subcortical electrical stimulation and postoperative tractography. Neurosurgery 70(2):283–93; discussion 294. https://doi.org/10.1227/NEU.0b013e31823020e6

Oishi K, Zilles K, Amunts K, Faria A, Jiang H, Li X et al (2008) Human brain white matter atlas: identification and assignment of common anatomical structures in superficial white matter. NeuroImage 43(3):447–457

Owen JP, Li YO, Ziv E, Strominger Z, Gold J, Bukhpun P, Wakahiro M, Friedman EJ, Sherr EH, Mukherjee P (2013) The structural connectome of the human brain in agenesis of the corpus callosum. NeuroImage 70:340–355. https://doi.org/10.1016/j.neuroimage.2012.12.031

Pajevic S, Pierpaoli C (1999) Color schemes to represent the orientation of anisotropic tissues from diffusion tensor data: application to white matter fiber tract mapping in the human brain. Magn Reson Med 42(3):526–540. http://www.ncbi.nlm.nih.gov/pubmed/10467297

Pallud J, Blonski M, Mandonnet E, Audureau E, Fontaine D, Sanai N et al (2013) Velocity of tumor spontaneous expansion predicts long-term outcomes for diffuse low-grade gliomas. Neuro-Oncology 15(5):595–606. https://doi.org/10.1093/neuonc/nos331

Papadogiorgaki M, Koliou P, Kotsiakis X, Zervakis ME (2013) Mathematical modelling of spatio-temporal glioma evolution. Theor Biol Med Model 10:47. https://doi.org/10.1186/1742-4682-10-47

Papagno C, Miracapillo C, Casarotti A, Romero Lauro LJ, Castellano A, Falini A et al (2010) What is the role of the uncinate fasciculus? Surgical removal and proper name retrieval. Brain. awq283 [pii]. https://doi.org/10.1093/brain/awq283

Papagno C, Casarotti A, Comi A, Pisoni A, Lucchelli F, Bizzi A, Riva M, Bello L (2016) Long-term proper name anomia after removal of the uncinate fasciculus. Brain Struct Funct 221(1):687–694. https://doi.org/10.1007/s00429-014-0920-8. Epub 2014 Oct 28

Penfield W, Rasmussen T (1950) The cerebral cortex of man: a clinical study of localization of function. Macmillan, New York

Petrella JR, Shah LM, Harris KM, Friedman AH, George TM, Sampson JH et al (2006) Preoperative functional MR imaging localization of language and motor areas: effect on therapeutic decision making in patients with potentially resectable brain tumors. Radiology 240(3):793–802. https://doi.org/10.1148/radiol.2403051153

Petrides M, Pandya DN (1984) Projections to the frontal cortex from the posterior parietal region in the rhesus monkey. J Comp Neurol 228(1):105–116. https://doi.org/10.1002/cne.902280110

Petrides M, Pandya DN (1988) Association fiber pathways to the frontal cortex from the superior temporal region in the rhesus monkey. J Comp Neurol 273:52–66

Pierpaoli C, Jezzard P, Basser PJ, Barnett A, Di Chiro G (1996) Diffusion tensor MR imaging of the human brain. Radiology 201(3):637–648. http://www.ncbi.nlm.nih.gov/entrez/query.fcgi?cmd=Retrieve&db=PubMed&dopt=Citation&list_uids=8939209

Pierpaoli C, Walker L, Irfanoglu MO, Barnett A, Basser P, Chang L-C et al (2010) TORTOISE: an integrated software package for processing of diffusion MRI data. ISMRM Annu Meeting Proc 18:1597

Plaza M, Gatignol P, Leroy M, Duffau H (2009) Speaking without Broca's area after tumor resection. Neurocase 15(4):294–310. 909314371 [pii]. https://doi.org/10.1080/13554790902729473

Posner MI (1980) Orienting of attention. Q J Exp Psychol 32(1):3–25. http://www.ncbi.nlm.nih.gov/pubmed/7367577

Price CJ (2010) The anatomy of language: a review of 100 fMRI studies published in 2009. Ann N Y

Acad Sci 1191:62–88. NYAS5444 [pii]. https://doi.org/10.1111/j.1749-6632.2010.05444.x

Price SJ, Jena R, Burnet NG, Hutchinson PJ, Dean AF, Peña A et al (2006) Improved delineation of glioma margins and regions of infiltration with the use of diffusion tensor imaging: an image-guided biopsy study. AJNR Am J Neuroradiol 27(9):1969–1974. http://www.ncbi.nlm.nih.gov/pubmed/17032877

Puglisi G, Howells H, Sciortino T, Leonetti A, Rossi M, Conti Nibali M, Gabriel Gay L, Fornia L, Bellacicca A, Viganò L, Simone L, Catani M, Cerri G, Bello L (2019) Frontal pathways in cognitive control: direct evidence from intraoperative stimulation and diffusion tractography. Brain 142(8):2451–2465. https://doi.org/10.1093/brain/awz178

Pujol J, Deus J, Losilla JM, Capdevila A (1999) Cerebral lateralization of language in normal left-handed people studied by functional MRI. Neurology 52(5):1038–1043. http://www.ncbi.nlm.nih.gov/pubmed/10102425

Quiñones-Hinojosa A, Ojemann SG, Sanai N, Dillon WP, Berger MS (2003) Preoperative correlation of intraoperative cortical mapping with magnetic resonance imaging landmarks to predict localization of the Broca area. J Neurosurg 99(2):311–318

Rathelot J-A, Strick PL (2006) Muscle representation in the macaque motor cortex: an anatomical perspective. Proc Natl Acad Sci U S A 103(21):8257–8262. https://doi.org/10.1073/pnas.0602933103

Rathelot J-A, Strick PL (2009) Subdivisions of primary motor cortex based on cortico-motoneuronal cells. Proc Natl Acad Sci U S A 106(3):918–923. https://doi.org/10.1073/pnas.0808362106

Robles SG, Gatignol P, Lehéricy S, Duffau H (2008) Long-term brain plasticity allowing a multistage surgical approach to World Health Organization Grade II gliomas in eloquent areas. J Neurosurg 109(4):615–624

Rohde GK, Barnett AS, Basser PJ, Marenco S, Pierpaoli C (2004) Comprehensive approach for correction of motion and distortion in diffusion-weighted MRI. Magn Reson Med 51(1):103–114. https://doi.org/10.1002/mrm.10677

Rolheiser T, Stamatakis EA, Tyler LK (2011) Dynamic processing in the human language system: synergy between the arcuate fascicle and extreme capsule. J Neurosci 31(47):16949–16957. https://doi.org/10.1523/JNEUROSCI.2725-11.2011

Sanai N, Mirzadeh Z, Berger MS (2008) Functional outcome after language mapping for glioma resection. N Engl J Med 358:18–27

Sanai N, Martino J, Berger MS (2012) Morbidity profile following aggressive resection of parietal lobe gliomas. J Neurosurg 116(6):1182–1186. https://doi.org/10.3171/2012.2.JNS111228

Sati P, van Gelderen P, Silva AC, Reich DS, Merkle H, de Zwart JA, Duyn JH (2013) Micro-compartment specific T2* relaxation in the brain. NeuroImage 77:268–278. https://doi.org/10.1016/j.neuroimage.2013.03.005

Saur D, Kreher BW, Schnell S, Kummerer D, Kellmeyer P, Vry MS et al (2008) Ventral and dorsal pathways for language. Proc Natl Acad Sci U S A 105(46):18035–18040. 0805234105 [pii]. https://doi.org/10.1073/pnas.0805234105

Saur D, Schelter B, Schnell S, Kratochvil D, Kupper H, Kellmeyer P et al (2010) Combining functional and anatomical connectivity reveals brain networks for auditory language comprehension. NeuroImage 49(4):3187–3197. S1053-8119(09)01193-8 [pii]. https://doi.org/10.1016/j.neuroimage.2009.11.009

Schmahmann JD, Pandya DN (2006) Fiber pathways of the brain. Oxford University Press, Oxford

Schmahmann JD, Pandya DN, Wang R, Dai G, D'Arceuil HE, de Crespigny AJ, Wedeen VJ (2007) Association fibre pathways of the brain: parallel observations from diffusion spectrum imaging and autoradiography. Brain 130(Pt 3):630–653. https://doi.org/10.1093/brain/awl359

Schonberg T, Pianka P, Hendler T, Pasternak O, Assaf Y (2006) Characterization of displaced white matter by brain tumors using combined DTI and fMRI. NeuroImage 30(4):1100–1111. https://doi.org/10.1016/j.neuroimage.2005.11.015

Seunarine KK, Alexander DC (2009) Multiple fibers: beyond the diffusion tensor. In: Johansen-Berg H, Behrens TE (eds) Diffusion MRI: from quantitative measurement to in vivo neuroanatomy. Elsevier, Oxford, UK, pp 55–72

Skrap M, Mondani M, Tomasino B, Weis L, Budai R, Pauletto G et al (2012) Surgery of insular nonenhancing gliomas: volumetric analysis of tumoral resection, clinical outcome, and survival in a consecutive series of 66 cases. Neurosurgery 70(5):1081–1093.; discussion 1093–1094. https://doi.org/10.1227/NEU.0b013e31823f5be5

Smith JS, Chang EF, Lamborn KR, Chang SM, Prados MD, Cha S et al (2008) Role of extent of resection in the long-term outcome of low-grade hemispheric gliomas. J Clin Oncol 26(8):1338–1345. https://doi.org/10.1200/JCO.2007.13.9337

Smits M, Vernooij MW, Wielopolski PA, Vincent AJPE, Houston GC, van der Lugt A (2007) Incorporating functional MR imaging into diffusion tensor tractography in the preoperative assessment of the corticospinal tract in patients with brain tumors. AJNR Am J Neuroradiol 28(7):1354–1361. https://doi.org/10.3174/ajnr.A0538

Sporns O (2014) Contributions and challenges for network models in cognitive neuroscience. Nat Neurosci 17(5):652–660. https://doi.org/10.1038/nn.3690

Stummer W, Reulen H-J, Meinel T, Pichlmeier U, Schumacher W, Tonn J-C et al (2008) Extent of resection and survival in glioblastoma multiforme: identification of and adjustment for bias. Neurosurgery 62(3):564–576.; discussion 564–576. https://doi.org/10.1227/01.neu.0000317304.31579.17

Stummer W, Tonn J-C, Mehdorn HM, Nestler U, Franz K, Goetz C et al (2011) Counterbalancing risks and gains from extended resections in malignant glioma surgery: a supplemental analysis from the randomized 5-aminolevulinic acid glioma resection study.

Clinical article. J Neurosurg 114(3):613–623. https://doi.org/10.3171/2010.3.JNS097

Stupp R, Hegi ME (2013) Brain cancer in 2012: molecular characterization leads the way. Nat Rev Clin Oncol 10(2):69–70. https://doi.org/10.1038/nrclinonc.2012.240

Stupp R, Mason WP, van den Bent MJ, Weller M, Fisher B, Taphoorn MJB et al (2005) Radiotherapy plus concomitant and adjuvant temozolomide for glioblastoma. N Engl J Med 352(10):987–996. https://doi.org/10.1056/NEJMoa043330

Sturm D, Witt H, Hovestadt V, Khuong-Quang D-A, Jones DTW, Konermann C et al (2012) Hotspot mutations in H3F3A and IDH1 define distinct epigenetic and biological subgroups of glioblastoma. Cancer Cell 22(4):425–437. https://doi.org/10.1016/j.ccr.2012.08.024

Thiebaut de Schotten M, Urbanski M, Duffau H, Volle E, Levy R, Dubois B, Bartolomeo P (2005) Direct evidence for a parietal-frontal pathway subserving spatial awareness in humans. Science 309:2226

Thiebaut de Schotten M, Kinkingnéhun S, Delmaire C, Lehéricy S, Duffau H, Thivard L et al (2008) Visualization of disconnection syndromes in humans. Cortex 44(8):1097–1103. https://doi.org/10.1016/j.cortex.2008.02.003

Thiebaut de Schotten M, Dell'Acqua F, Forkel SJ, Simmons A, Vergani F, Murphy DGM, Catani M (2011a) A lateralized brain network for visuospatial attention. Nat Neurosci 14(10):1245–1246. https://doi.org/10.1038/nn.2905

Thiebaut de Schotten M, Ffytche DH, Bizzi A, Dell'Acqua F, Allin M, Walshe M et al (2011b) Atlasing location, asymmetry and inter-subject variability of white matter tracts in the human brain with MR diffusion tractography. NeuroImage 54(1):49–59. https://doi.org/10.1016/j.neuroimage.2010.07.055

Thiebaut de Schotten M, Dell'Acqua F, Valabregue R, Catani M (2012) Monkey to human comparative anatomy of the frontal lobe association tracts. Cortex 48(1):82–96. https://doi.org/10.1016/j.cortex.2011.10.001

Thiebaut de Schotten M, Tomaiuolo F, Aiello M, Merola S, Silvetti M, Lecce F et al (2014) Damage to white matter pathways in subacute and chronic spatial neglect: a group study and 2 single-case studies with complete virtual "in vivo" tractography dissection. Cereb Cortex 24(3):691–706. https://doi.org/10.1093/cercor/bhs351

Thomas L, Di Stefano AL, Ducray F (2013) Predictive biomarkers in adult gliomas: the present and the future. Curr Opin Oncol 25(6):689–694. https://doi.org/10.1097/CCO.0000000000000002

Tournier J-D, Calamante F, Gadian DG, Connelly A (2004) Direct estimation of the fiber orientation density function from diffusion-weighted MRI data using spherical deconvolution. NeuroImage 23(3):1176–1185. https://doi.org/10.1016/j.neuroimage.2004.07.037

Tuch DS (2004) Q-ball imaging. Magn Reson Med 52(6):1358–1372. https://doi.org/10.1002/mrm.20279

Tyler LK, Marslen-Wilson WD, Randall B, Wright P, Devereux BJ, Zhuang J et al (2011) Left inferior frontal cortex and syntax: function, structure and behaviour in patients with left hemisphere damage. Brain 134(Pt 2):415–431. https://doi.org/10.1093/brain/awq369

Vallar G, Bello L, Bricolo E, Castellano A, Casarotti A, Falini A et al (2014) Cerebral correlates of visuospatial neglect: a direct cerebral stimulation study. Hum Brain Mapp 35(4):1334–1350. https://doi.org/10.1002/hbm.22257

Van den Heuvel MP, Sporns O (2011) Rich-club organization of the human connectome. J Neurosci 31(44):15775–15786. https://doi.org/10.1523/JNEUROSCI.3539-11.2011

Van den Heuvel MP, Sporns O (2013) Network hubs in the human brain. Trends Cogn Sci 17(12):683–696. https://doi.org/10.1016/j.tics.2013.09.012

Vassal F, Schneider F, Sontheimer A, Lemaire J-J, Nuti C (2013) Intraoperative visualisation of language fascicles by diffusion tensor imaging-based tractography in glioma surgery. Acta Neurochir 155(3):437–448. https://doi.org/10.1007/s00701-012-1580-1

Vergani F, Lacerda L, Martino J, Attems J, Morris C, Mitchell P et al (2014) White matter connections of the supplementary motor area in humans. J Neurol Neurosurg Psychiatry. https://doi.org/10.1136/jnnp-2013-307492

Vidorreta JG, Garcia R, Moritz-Gasser S, Duffau H (2011) Double dissociation between syntactic gender and picture naming processing: a brain stimulation mapping study. Hum Brain Mapp 32(3):331–340. https://doi.org/10.1002/hbm.21026

Vuorinen V, Hinkka S, Färkkilä M, Jääskeläinen J (2003) Debulking or biopsy of malignant glioma in elderly people - a randomised study. Acta Neurochir 145(1):5–10. https://doi.org/10.1007/s00701-002-1030-6

Wang S, Kim S, Chawla S, Wolf RL, Zhang W-G, O'Rourke DM et al (2009) Differentiation between glioblastomas and solitary brain metastases using diffusion tensor imaging. NeuroImage 44(3):653–660. https://doi.org/10.1016/j.neuroimage.2008.09.027

Wedeen VJ, Wang RP, Schmahmann JD, Benner T, Tseng WYI, Dai G et al (2008) Diffusion spectrum magnetic resonance imaging (DSI) tractography of crossing fibers. NeuroImage 41(4):1267–1277. https://doi.org/10.1016/j.neuroimage.2008.03.036

Wedeen VJ, Rosene DL, Wang R, Dai G, Mortazavi F, Hagmann P et al (2012) The geometric structure of the brain fiber pathways. Science 335(6076):1628–1634. https://doi.org/10.1126/science.1215280

Weller M, Stupp R, Hegi ME, van den Bent M, Tonn JC, Sanson M et al (2012) Personalized care in neuro-oncology coming of age: why we need MGMT and 1p/19q testing for malignant glioma patients in clinical practice. Neuro-Oncology 14(Suppl 4):iv100–iv108. https://doi.org/10.1093/neuonc/nos206

Wu J-S, Zhou L-F, Tang W-J, Mao Y, Hu J, Song Y-Y et al (2007) Clinical evaluation and follow-up outcome of diffusion tensor imaging-based functional

neuronavigation: a prospective, controlled study in patients with gliomas involving pyramidal tracts. Neurosurgery 61(5):935–948.; discussion 948–949. https://doi.org/10.1227/01.neu.0000303189.80049.ab

Yakovlev PI, Locke S (1961) Corticocortical connections of the anterior cingulate gyrus; te cingulum and subcallosal bundle. Trans Am Neurol Assoc 86:252–256. http://www.ncbi.nlm.nih.gov/pubmed/14008718

Yamada K, Sakai K, Hoogenraad FGC, Holthuizen R, Akazawa K, Ito H et al (2007) Multitensor tractography enables better depiction of motor pathways: initial clinical experience using diffusion-weighted MR imaging with standard b-value. AJNR Am J Neuroradiol 28(9):1668–1673. https://doi.org/10.3174/ajnr.A0640

Yordanova YN, Moritz-Gasser S, Duffau H (2011) Awake surgery for WHO Grade II gliomas within "noneloquent" areas in the left dominant hemisphere: toward a "supratotal" resection. Clinical article. J Neurosurg 115(2):232–239. https://doi.org/10.3171/2011.3.JNS101333

Zamecnik J (2005) The extracellular space and matrix of gliomas. Acta Neuropathol 110(5):435–442. https://doi.org/10.1007/s00401-005-1078-5

Zhang H, Schneider T, Wheeler-Kingshott CA, Alexander DC (2012) NODDI: practical in vivo neurite orientation dispersion and density imaging of the human brain. NeuroImage 61(4):1000–1016. https://doi.org/10.1016/j.neuroimage.2012.03.072